Université de Montréal

Novel M(II) β-diketiminate Complexes for the Polymerization of Lactide

par
Todd Whitehorne

Département de Chimie
Faculté des Arts et des Sciences

Thèse présentée à la Faculté des études supérieures et postdoctorales en vue de l'obtention du grade de Ph.D. en chimie

Août 2013

Abstract

Diketimine ligands bearing *N*-benzyl, *N*-9-anthrylmethyl and *N*-mesitylmethyl substituents (*nacnac*^{Bn}H, *nacnac*^{An}H, and *nacnac*^{Mes}H) were prepared from condensation of amine with either acetyl acetone or its ethylene glycol monoketal. Chlorination of the 3-position was achieved using N-chlorosuccinimide, yielding Cl*nacnac*^{Bn}H and Cl*nacnac*^{An}H. The 3-position was also substituted by succinimido by lithiation of *nacnac*^{Bn}H followed by reaction with N-chlorosuccinimide (3-succinimido-*nacnac*^{Bn}H). N-aryl ligands *nacnac*^{ipp}H and *nacnac*^{Naph}H (ipp = 2-isopropylphenyl, Naph = 1-naphthyl) were prepared from literature. The ligands were reacted with Zn(TMSA)$_2$ (TMSA = N(SiMe$_3$)$_2$) to yield *nacnac*^{An}Zn(TMSA) and Cl*nacnac*^{Bn}Zn(TMSA). Protonation with isopropanol gave *nacnac*^{An}ZnO*i*Pr and Cl*nacnac*^{Bn}ZnO*i*Pr. Reaction of the diketimines with Mg(TMSA)$_2$ afforded *nacnac*^{An}Mg(TMSA), *nacnac*^{Mes}Mg(TMSA), Cl*nacnac*^{Bn}Mg(TMSA) and Cl*nacnac*^{An}Mg(TMSA). Subsequent protonation with *tert*-butanol produced *nacnac*^{Mes}MgO*t*Bu and Cl*nacnac*^{Bn}MgO*t*Bu, but only decomposition was observed with *N*-anthrylmethyl substituents. Reaction of the diketimines with Cu(O*i*Pr)$_2$ yielded the heteroleptic [*nacnac*^{Bn}Cu(μ-O*i*Pr)]$_2$ and [3-Cl-*nacnac*^{Bn}Cu(μ-O*i*Pr)]$_2$ when using sterically undemanding ligands. When sterically more demanding diketimines were used, stabilization of the heteroleptic complex by dimerization was not possible, resulting in the formation of the homoleptic complexes Cu(*nacnac*^{ipp})$_2$ and Cu(*nacnac*^{Naph})$_2$ by ligand exchange. Homoleptic complexes were also prepared with *N*-benzyl ligands, i. e. Cu(*nacnac*^{Bn})$_2$ and Cu(3-succinimido-*nacnac*^{Bn})$_2$. Even bulkier ligands such as *nacnac*^{An}H, *nacnac*^{Mes}H or *N*-methylbenzyl substituents failed to react with Cu(O*i*Pr)$_2$. Most complexes were characterized by single crystal X-ray diffraction. TMSA complexes and homoleptic complexes were monomeric, alkoxide complexes were dimeric in the solid state. All alkoxide complexes, as well as *nacnac*^{An}Mg(TMSA)/BnOH and Cl*nacnac*^{An}Mg(TMSA)/BnOH were moderately to highly active in *rac*-lactide polymerization (90% conversion in 30 sec to 3 h). *nacnac*^{An}ZnO*i*Pr produced highly heterotactic polymer (P_r = 0.90), Cl*nacnac*^{Bn}MgO*t*Bu/BnOH produced slightly isotactic polymer at –30 °C (P_r = 0.43), all other catalysts produced atactic polymers with a slight heterotactic bias (P_r = 0.48 – 0.55). Heteroleptic complexes [*nacnac*^{Bn}Cu(μ-O*i*Pr)]$_2$ and [3-Cl-*nacnac*^{Bn}Cu(μ-O*i*Pr)]$_2$ are very highly active *rac*-lactide

polymerization catalysts, with complete monomer conversion at ambient temperature in solution in 0.5 – 5 min. [*nacnac*^{Bn}Cu(μ-O*i*Pr)]$_2$ specifically polymerized in the presence or absence of isopropanol as a chain-transfer reagent with very high activity (k_2 = 32 $M^{-1}\cdot s^{-1}$), in methylene chloride. While in acetonitrile, THF, dichloromethane and toluene has a k_{obs} = 2.4(1), 5.3(5), 3.6-4.4 and 10(1) min^{-1}, respectively. [*nacnac*^{Bn}Cu(μ-O*i*Pr)]$_2$ yields narrow polydispersities and no evidence of side reactions such as transesterification, epimerization or catalyst decomposition. The homoleptic complexes in the presence of free alcohol, seem to be in equilibrium with small amounts of the respective heteroleptic complex, which are sufficient to complete polymerization in less than 60 min at room temperature. All Cu catalysts show high control of polymerization with polydispersities of 1.1 and below. The obtained polymers were essentially atactic, with a slight heterotactic bias at ambient temperature and at –17 °C. [*nacnac*^{Bn}Cu(μ-O*i*Pr)]$_2$ polymerizes β-butyrolactone (BL), ε-caprolactone (CL) and δ-valerolactone (VL) with rate constants of k_{obs} = 3.0(1)·10^{-2}, 1.2–2.7·10^{-2}, and 0.11(1) min^{-1}, respectively. Homopolymers showed narrow polydispersities of appr. 1.1. Sequential addition polymerizations showed evidence for transesterification (not seen in homopolymerizations) if BL or CL are introduced after a lactide block.

Keywords: Zinc, Magnesium, Copper, β-diketimine, polymerization, *rac*-lactide, lactide, beta-butyrolactone, epsilon-caprolactone, delta-valerolactone.

Résumé

Des ligands diketimines porteurs de substituants *N*-benzyl, *N*-9-anthrylmethyl et *N*-mesitylmethyl (*nacnac*^{Bn}H, *nacnac*^{An}H, and *nacnac*^{Mes}H) ont été synthétisés par condensation d'une amine et d'acétyl acétone ou son monoacétal d'éthylène glycol. La chlorination de la position 3 a été effectuée à l'aide de N-chlorosuccinimide conduisant à la formation des ligands Cl*nacnac*^{Bn}H et Cl*nacnac*^{An}H. Cette même position 3 a également été substituée par un groupement succinimide par lithiation du *nacnac*^{Bn}H, suivi de la réaction avec le N-chlorosuccinimide (3-succinimido-*nacnac*^{Bn}H). Les ligands N-aryl *nacnac*^{ipp}H et *nacnac*^{Naph}H (ipp = 2-isopropylphenyl, Naph = 1-naphthyl) ont été préparés selon les procédures reportées dans la littérature.

La réaction de ces ligands avec Zn(TMSA)$_2$ (TMSA = N(SiMe$_3$)$_2$) conduit à la formation des complexes *nacnac*^{An}Zn(TMSA) et Cl*nacnac*^{Bn}Zn(TMSA). La protonation avec l'isopropanol permet l'obtention des complexes *nacnac*^{An}ZnO*i*Pr et Cl*nacnac*^{Bn}ZnO*i*Pr.

La réaction avec Mg(TMSA)$_2$ permet quant à elle la formation des complexes *nacnac*^{An}Mg(TMSA), *nacnac*^{Mes}Mg(TMSA), Cl*nacnac*^{Bn}Mg(TMSA) et Cl*nacnac*^{An}Mg(TMSA). La protonation subséquente à l'aide du *tert*-butanol permet l'obtention du *nacnac*^{Mes}MgO*t*Bu et du Cl*nacnac*^{Bn}MgO*t*Bu, alors que l'on observe uniquement une décomposition avec les ligands possédant des substituants *N*-anthrylmethyl.

La réaction de ces diketimines avec Cu(O*i*Pr)$_2$ conduit aux dimères hétéroleptiques [*nacnac*^{Bn}Cu(μ-O*i*Pr)]$_2$ et [3-Cl-*nacnac*^{Bn}Cu(μ-O*i*Pr)]$_2$ lors de l'usage des ligands stériquement peu encombrés. Lors de l'utilisation de ligands plus encombrés, la stabilisation du complexe hétéroleptique par dimérisation n'est plus possible, conduisant, par un échange de ligand, à la formation des complexes homoleptiques Cu(*nacnac*^{ipp})$_2$ et Cu(*nacnac*^{Naph})$_2$. Les complexes homoleptiques Cu(*nacnac*^{Bn})$_2$ et Cu(3-succinimido-*nacnac*^{Bn})$_2$ ont été obtenus à partir des ligands *N*-benzyl. Les ligands encore plus encombrés tels que *nacnac*^{An}H, *nacnac*^{Mes}H ou ceux comportant des substituants *N*-methylbenzyl ne présentent alors plus de réactivité avec le Cu(O*i*Pr)$_2$.

La plupart des complexes ont été caractérisés par Diffraction des Rayons X. Les complexes homoleptiques ainsi que ceux de TMSA sont monomériques, alors que ceux formés à partir d'alkoxides se présentent

sous forme de dimères à l'état solide. Tous les complexes d'alkoxides ainsi que les *nacnac*^{An}Mg(TMSA)/BnOH et Cl*nacnac*^{An}Mg(TMSA)/BnOH présentent une réactivité modérée à haute en matière de polymérisation du rac-lactide (90% de conversion en 30 secondes à 3 heures). Le *nacnac*^{An}ZnO*i*Pr permet la synthèse d'un polymère hautement hétérotactique (P_r = 0.90) quand le Cl*nacnac*^{Bn}MgO*t*Bu/BnOH génère un polymère isotactique à -30°C (P_r = 0.43). Tous les autres catalyseurs produisent des polymères atactiques avec une légère tendance hétérotactique (P_r = 0.48 – 0.55). Les complexes hétéroleptiques [*nacnac*^{Bn}Cu(μ-O*i*Pr)]$_2$ et [3-Cl-*nacnac*^{Bn}Cu(μ-O*i*Pr)]$_2$ se révèlent être de très bons catalyseurs pour la polymérisation du rac-lactide présentant une conversion complète du monomère à température ambiante, en solution, en 0,5 à 5 minutes. Le [*nacnac*^{Bn}Cu(μ-O*i*Pr)]$_2$ est actif en présence ou absence d'isopropanol, agissant comme agent de transfert de chaine à haute activité (k_2 = 32 $M^{-1}\cdot s^{-1}$) dans le dichlorométhane. Dans l'acétonitrile, le THF, le dichloromethane et le toluène, [*nacnac*^{Bn}Cu(μ-O*i*Pr)]$_2$ conduit à une étroite polydispersité, possédant respectivement des k_{obs} = 2.4(1), 5.3(5), 3.6-4.4 and 10(1) min^{-1}. Aucune réaction parasite, telle qu'une trans-esterification, une épimerisation ou une décomposition du catalyseur, n'a été observée. Les complexes homoleptiques en présence d'alcool libre semblent présenter un équilibre avec une petite quantité de leurs équivalents hétéroleptiques, permettant une polymérisation complète, en moins de 60 min, à température ambiante. Tous les catalyseurs de cuivre présentent un haut contrôle de la polymérisation avec une polydispersité égale ou inférieure à 1.1. Les polymères obtenus sont essentiellement atactiques, avec une légère tendance à l'hétérotacticité à température ambiante et -17°C. Le [*nacnac*^{Bn}Cu(μ-O*i*Pr)]$_2$ polymérise également la β-butyrolactone (BL), l'ε-caprolactone (CL) et la δ-valerolactone (VL) avec des constantes respectivement égales à k_{obs} = 3.0(1)$\cdot 10^{-2}$, 1.2–2.7$\cdot 10^{-2}$, et 0.11(1) min^{-1}. Les homopolymères présentent une étroite polydispersité d'approximativement 1.1. Les polymérisations par addition séquentielle ont mis en évidence une trans-estérification (non observée dans les homopolymérisations) si BL ou CL sont introduits après un bloc lactide.

Mot-Clé : Zinc, Magnesium, Cuivre, β-diketimine, polymérisation, rac-lactide, beta-butyrolactone, epsilon-caprolactone, delta-valerolactone.

Table of Contents

List of Figures

List of Tables

List of Schemes

List of Abbreviations

An.....9-anthryl methyl
Ar.....aryl
Bn.....benzyl
BnOH.....benzyl alcohol
CCVC.....Centre en Chimie verte et catalyse
dipp.....1,3 diisopropyl phenyl
Et.....ethyl
GPC.....gel permeation chromatography
Hnacnac.....β-diketimine
ipp.....2-isopropylphenyl
*i*Pr.....isopropyl
Me.....methyl
Mes.....mesityl methyl
Naph.....Naphthyl
NSERC.....National Science and Engineering Research Council
NMR.....nuclear magnetic resonance
Ph.....phenyl
PLA.....Polylactic acid
rac.....racemic
ROP.....Ring Opening Polymerization
*t*Bu.....tert-butyl
TMSA.....bis trimethylsilylamide
TsOH.....para toluenesulphonic acid
OTf.....triflate
N^N.....pyrazolylmethyl-pyradine

Acknowledgements

I would like to begin by thanking my supervisor, Prof. Frank Schaper for his helpful guidance in my research and constant attention to detail that he instilled upon me to become the chemical researcher I am today. Thanks also for the hours of time it took to work through all of those problematic crystal structures.

I would like to thank the support staff of U de M, who took the time to train me on the university's wealth of instruments. These include Francine Bélanger, Michel Simard and Thiery Maris for their help and training in the field of crystallography. Pierre Ménard-Tremblay who taught me how to use the GPC. Cedrique Malveau who helped me through the early stages of homonuclear decoupled proton NMR and Elena Nadezhina for her careful elemental analysis of all my compounds.

I have had the pleasure of having many students work with me throughout my project, of whom I've formed long lasting relationships. Thanks to Fred, Paul, Ibrahim, Maria, Marine, Elodie, Johannes, Simon, Arek, Thomas, Lylia, and Pargol.

Most importantly, thanks Mom and Dad.

1. Introduction

1.1 Lactide

Polylactic acid (PLA) has received much attention in the past as a specialty polymer for medical application such as implants, sutures and even slow drug delivery.[1] The fact that PLA is biologically benign, biodegradable, and formed from a renewable resource, lactic acid, makes it an excellent candidate as a material for disposable food and drink packaging.[2]

Lactic acid is obtained from D-glucose produced from starches and sugars. Bacterial fermentation of D-glucose produces optically pure L-lactic acid.[3] PLA can be formed directly from lactic acid via condensation polymerization. However, this method results in low molecular weight polymer (MW < 5000) as the competing hydrolysis reaction depolymerizes the polymer. These low molecular weight polymers are then depolymerized to form lactide, the dimeric anhydride of lactic acid.[4]

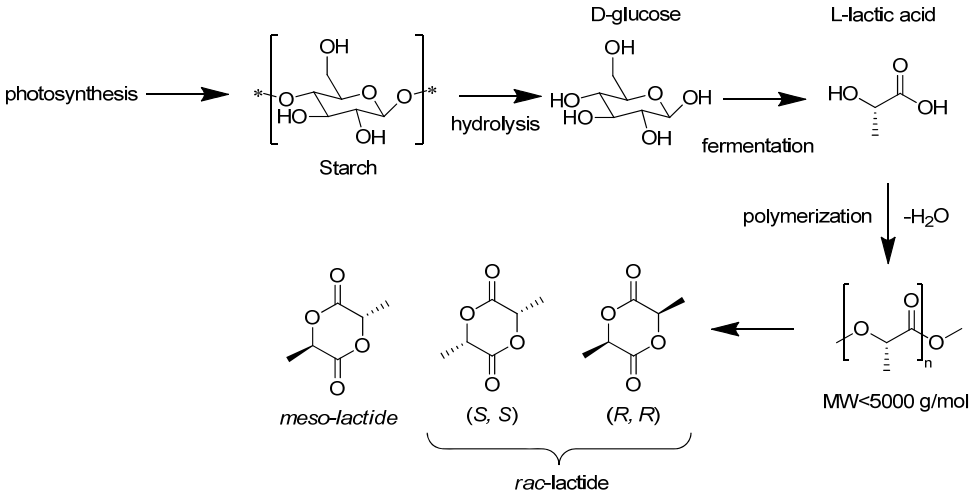

Figure 1.1- Synthesis of lactide and isomeric forms

The depolymerisation and cyclization processes result in partial racemization of the chiral sites, and as lactide has two sites per molecule, yielding its three isomeric forms. The *meso*, *RR*, and *SS* isomers thus have to be purified to produce optically pure monomer. As the monomers have varied chirality so too does the resultant polymer have varied tacticity with differing physical polymer properties.

1.2 Polymerization of Lactide

High molecular weight polymers are now accessible through ring-opening polymerization of lactide with metal complexes containing an activator group, typically a metal alkoxide functionality. Polymerization then follows a coordination-insertion mechanism (Figure 1.2).[5]

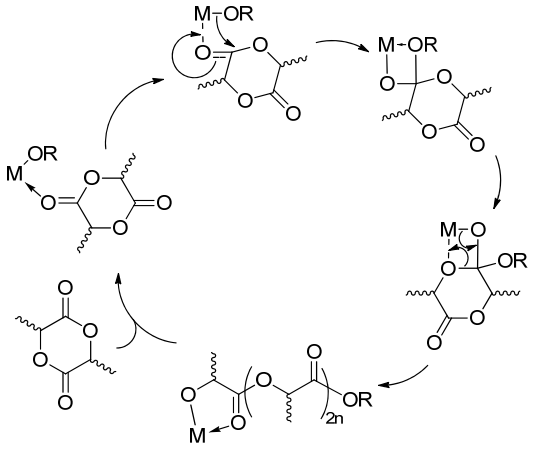

Figure 1.2 - Coordination-insertion mechanism of lactide polymerization using metal catalysts.

Other polymerization mechanisms, including the activated monomer mechanism, organic catalysts for ROP, both of which offer little possibility for polymerization control and will not be discussed in this document.

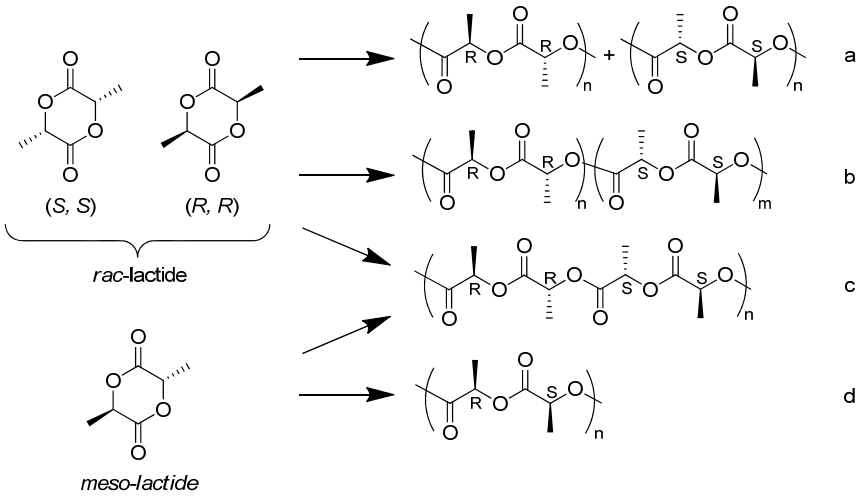

Figure 1.3 - Typical PLA microstructures: a) Racemic mixture of isotactic chains. b) Isotactic stereoblock. c) Heterotactic. d) Syndiotactic.

1.3 Selective Polymerization

The cost of petrochemical feedstocks for the production of polyolefins continues to increase. This, combined with new technologies in lactide production make PLA a front running candidate for future bulk polymers. One method that would aid in decreasing the cost required for purification of bulk lactide would be a catalyst which could selectively polymerize a racemic mixture (*SS* and *RR* isomers) into isotactic polymers or isotactic block copolymers.

Selective polymerization can be achieved by two major mechanistic pathways. The chain-end-control mechanism requires that the chirality of the last inserted unit determines the chirality of the next unit to be inserted. The other major mechanism is catalytic-site control, where the catalyst architecture determines the chirality of the next inserted unit, independent of the chirality of the previously inserted unit. The advantage of catalytic site control is that random stereo error in monomer insertion will not propagate throughout the polymer chain, while the inverse is true in the chain-end-control mechanism.

When a sterically unemcumbered catalyst is used, such as a homoleptic metal alkoxide, *rac*-lactide is polymerized typically via a chain-end-control mechanism, yielding polymers with a heterotactic preference.[8] This is also true when polymerizing *meso*-lactide; the chirality of the chain end favours the insertion of the alternate unit yielding chains with a syndiotactic preference.[9] The effect of the chain end can be amplified by increasing the steric bulk at the metal centre, as was shown in the seminal work by Coates *et al.*[10] wherein the use of a 2,6 diisopropylphenyl (dipp) β-diketimine provided adequate bulk at the Zn(II) catalytic site to amplify the effect of the chain end control mechanism (Figure 1.4).

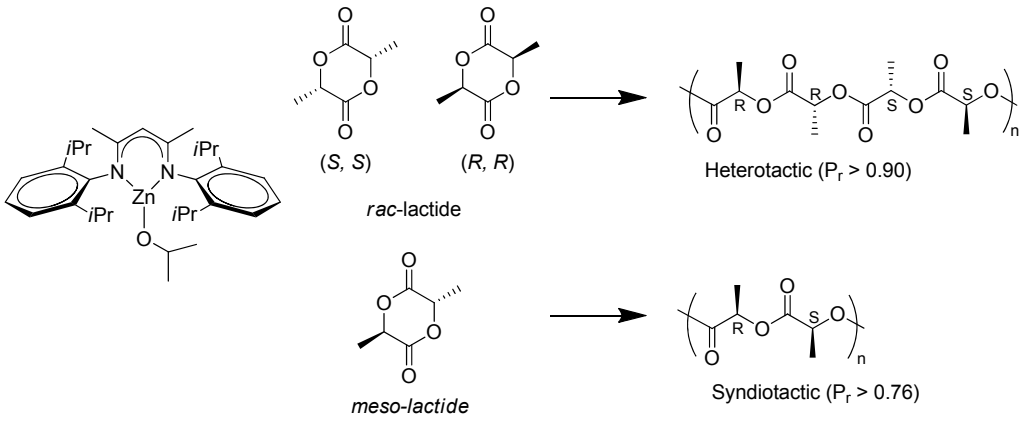

Figure 1.4 - Example of chain end control amplification using sterically demanding catalysts.[10]

Enantioselectivity to produce isotactic PLA from *rac*-lactide is also possible. To do so typically a racemic mixture of chiral catalysts are used in an effort to maximize the catalytic site control mechanism, but this is inherently difficult as the chirality of the chain end is oftentimes fighting the selectivity of the catalyst.

1.4 Side Reactions of Polymerization

Aluminum complexes have been shown to be highly stereoselective for the polymerization of *rac*-lactide as the racemic catalyst shown in Figure 1.5.[11] This example proceeds via catalytic site control mechanism as the two catalyst enantiomers polymerize their respective lactide enantiomers. However, these complexes suffer from low activity, as well as a tendency for side reactions such as transesterification and epimerization.

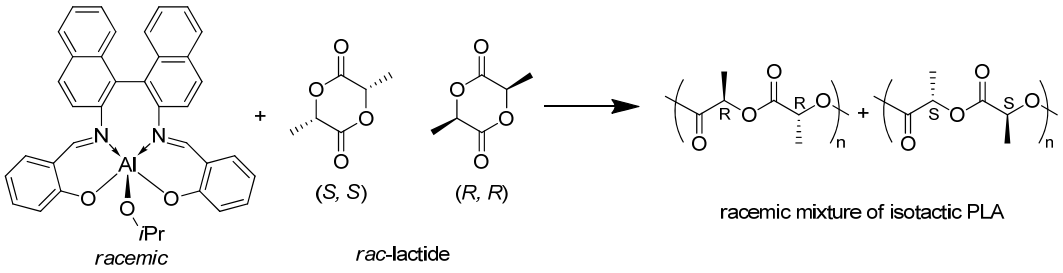

Figure 1.5 – Al(III) chiral catalysts for the formation of isotactic stereoblock compolymers[11]

Transesterification in ring opening polymerization (ROP) of lactide is mediated by the catalytic site, and results in broadening of molecular weights, as well as in the formation of *rr* triads in the case of polymerization of *rac*-lactide. The formation of *rr* triads can be attributed to intramolecular transesterification by the repolymerization of formed cyclic esters, or by intermolecular transesterification by the splitting/recombination of chains. (Figure 1.6).

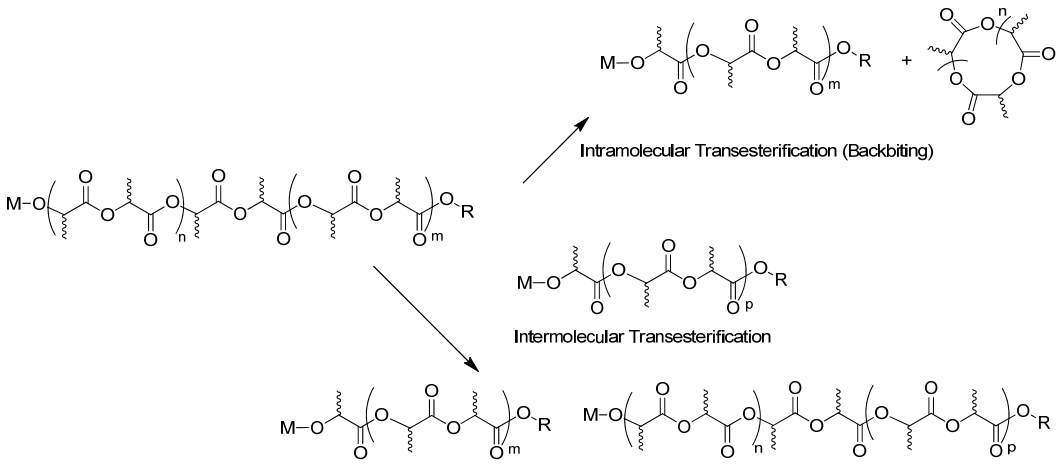

Figure 1.6 –Catalyst mediated transesterification pathways

Epimerization can also occur during polymerization, since the catalyst contains a basic alkoxide and since the chiral site has a relatively acidic proton. In the case of *rac*-lactide polymerization, epimerization can produce *r* diads resulting in the otherwise impossible *rr* triads, but does not result in increased polydispersities. Epimerization can be tested for by polymerization of pure *RR* or *SS* monomer, since transesterification in polymerizations of *R,R* or *S,S*-lactide would not yield *r* diads.

1.5 Living and Immortal Polymerization

Living polymerization in homogeneous catalysis is a process by which one polymer chain is growing per catalyst centre in the absence of chain transfer or termination. That is, the growing polymer chain remains bound to the catalytic centre as propagation occurs (Figure 1.7(a)), while also remaining active upon consumption of reactant, able to polymerize added monomer (b). Living polymerization thus requires a quenching step to remove polymer from catalyst and to render the catalyst inert (c).

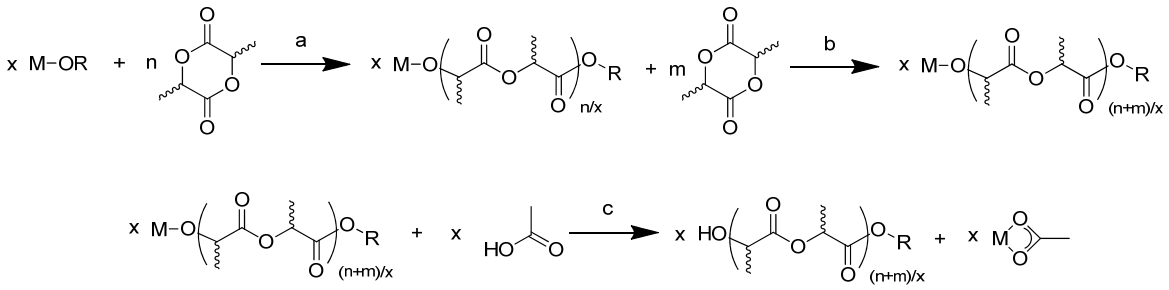

Figure 1.7 – Living polymerization.

A practical application of living polymerization is the multi-addition preparation of block copolymers, as the catalyst remains active when monomer is completely consumed. Living

polymerization produces narrow polydispersities due to the rate of chain initiation being much greater than the rate of chain propagation which ultimately results in a tunability with respect to polymer molecular weight. It's important to note that the living ROP of lactide and other cyclic lactones is an equilibrium process (Figure 1.8), and that polymerizations often do not reach 100% conversion.[12] The polymerization has been shown to be pushed to completion by addition of a different cyclic ester.[13]

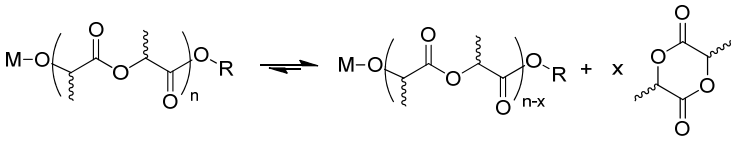

Figure 1.8 – ROP equilibrium.

Living polymerization is a requirement of immortal polymerization. The process of immortal polymerization requires a chain transfer agent, in the case of cyclic ester polymerization, this is usually an alcohol (Figure 1.9).[14]

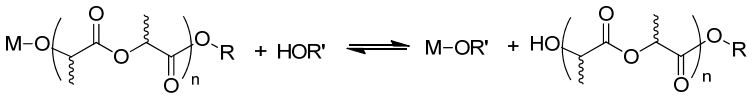

Figure 1.9 – Immortal polymerization equilibrium.

If the catalyst is sufficiently stable to the presence of alcohol (chain transfer agent), the fast interchange of alcohol and catalyst will allow for multiple polymer chains to grow per catalytic centre. The forward reaction (Figure 1.9) is a chain transfer reaction, which usually results in dead chains, but in this case the reverse reaction can also take place. Provided the exchange reaction is much faster than polymer growth, the polydispersity of the resultant polymer will remain low.[15] The polymerization then behaves much like living polymerization (Figure 1.7) as seen below in Figure 1.10, which also requires quenching (not shown).

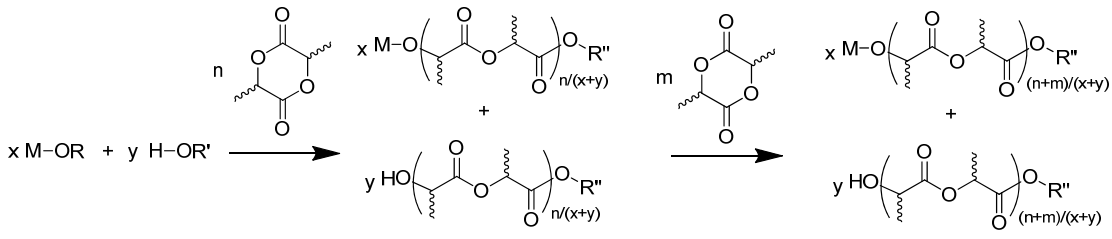

Figure 1.10 – Immortal polymerization.

The practical application of an immortal catalyst is the reduction of catalyst loading, which has obvious economic advantages. Possibly even more important, if the catalytic centre is biologically inactive, decreased loadings may allow for a wider application, including food products. The use of immortal catalysts may thus prove to decrease cost of PLA even further.

1.6 Copolymers

Aforementioned, living polymerization catalysts allow for the convenient preparation of copolymers. For the scope of this work, and in the interest of brevity, only bipolymers will be discussed.

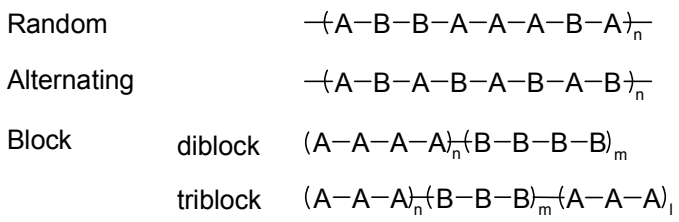

Figure 1.11 – Types of bipolymers**.**

Commonly employed is the use of a macroinitiator which is a macromolecule used to initiate the polymerization. This results in diblock copolymers or in the case of diblock macroinitiators, triblock copolymers. There are two additional pathways for the synthesis of diblock copolymers. The first being the conventional polymerization of a mixture of monomers, where one is preferentially polymerized until depleted, then the subsequent polymerization of the second. The second pathway is sequential polymerization, wherein a homopolymerization forms the first block, followed by addition of the second monomer, resulting in a block copolymer. All methods have their benefits; the macroinitiator method for example has been shown to be often faster as there is no monomer competition at the reactive site,[16] as well as minimizes the random polymer length between two blocks.[17] The two-monomer method is dependent on catalyst, temperature, respective monomer concentrations, and the monomers themselves and has been shown by Florczak *et al*. as a viable pathway towards random and block copolymers of lactide and capralactone, though significant random polymerization was seen between blocks.[18] This makes the macroinitiator method the better choice for block copolymers and the conventional method the preferred pathway towards random or alternating polymers, in general.[19]

With respect to lactide/cyclic ester copolymerization, many monomers have been used (Figure 1.12), but by far the most utilized is that of ε-caprolactone, and glycolides.[20] Epoxides such as cyclohexane oxide, propylene oxide and ethylene oxide have also seen prominent use[21]. Intriguing is the expanding literature base of terpolymers of CO_2 with epoxides, while incorporating lactide or other cyclic esters seen in Figure 1.12.

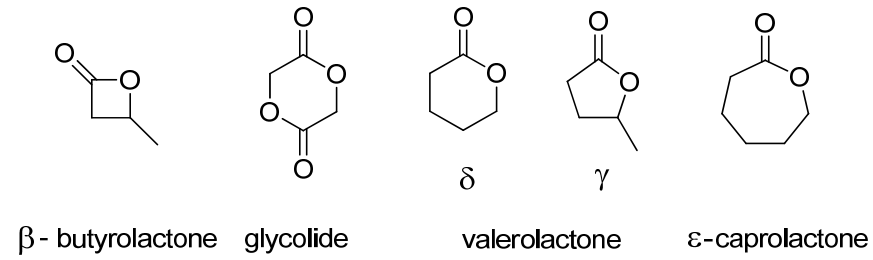

Figure 1.12 - Cyclic esters used with lactide for copolymerization in literature

An often targeted application of copolymerization of lactide is in an effort to increase PLA's half-life in vivo (2 weeks)[22], as well as decrease PLA hydrophilicity[23] for the purposes of drug delivery. Nomura *et al.* found that using an Al(III) homosalen complex random polymerization could be achieved[19] with polycaprolactone (PCL), which is more hydrophobic than PLA and has a longer half-life in vivo (1 year).[22]

1.7 Previous work

Previous work done in our group sought to remedy the problems discussed previously. Zn(II) and Mg(II) metal tetrahedral catalytic centres were chosen as catalytic centres due to their bio-inactivity, low cost, and limited epimerization/transesterification. N-alkyl based β-diketiminate (*nacnac*) were used as ligands. The premise is that when the catalyst is in the anti-conformation they provide a chiral coordination environment. This might lead to isotactic PLA provided the rate of polymerization is much greater than the rate of isomerization. A possible drawback is that, depending on the N-substituent, the syn conformation may be more stable and result in atactic polymer.

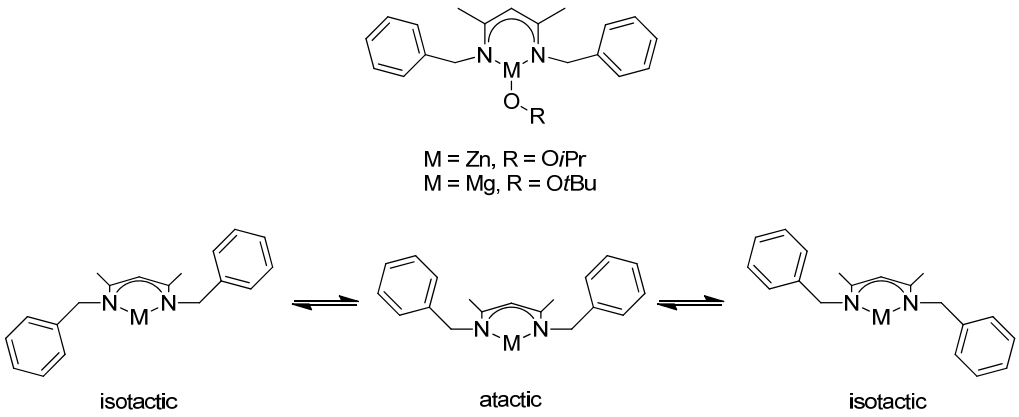

Figure 1.13 – Previously reported catalyst basic architecture.

These design features attempt to create a catalyst that is selective, highly active, bio-inactive, and most of all inexpensive. It was found that high activity could be achieved for both Zn(II) and Mg(II).[23] [24] In the case of Mg(II), a slight isotactic preference was observed (P_r = 0.46).

1.8 Current state of the science

The quantity of ring opening polymerization catalysts available for discussion in this section is extremely vast. This might not only be due to the fact that biodegradable and renewable polymers would have economic and ecological implications. The lack of understanding of catalyst structure/reactivity polymerization trends, in comparison to other systems such as α-olefin polymerization catalysts, results from the complexity of the coordination insertion pathway, possible side reactions such as transesterification, back biting and even chain exchange. The reversibility and inherent equilibrium of the polymerization process, and the existence of two similar transition states of similar energy for both insertion and ring opening at least in the case of tetrahedral coordination environments.[25] The complexity of this subject alludes to the multitude of work being done in the field, a knowledge base that is too vast to easily summarize. However there are many published reviews on the subject, none of them comprehensive but of merit. For instance in 2011 Lin *et al.* released a relatively comprehensive review on metal initiators for lactide and glycolide ring opening polymerization, including copolymerization.[26] Similar to the Lin review, the Bourissou *et al.* review[27] covers metal initiators of lactide and glycolide polymerization, but is less comprehensive. The review by Christophe Thomas in 2009[28] leans towards the

production of novel polymers using multiple lactone initiators, but gives the most concise introduction to the state of the art, in terms of catalyst, available in literature.

With respect to this work, the review by Hayes *et al.*[29] has the most applicability, as it deals specifically with the state of Zn, Ca and Mg catalysts for lactide polymerization, as well as Dove's review in 2010[30] of the current (at the time) state of stereocontrolled ring opening polymerization of lactide.

Significant work done since these reviews include some highly selective Indium complexes coming out of the Mehrkhodavandi group,[31] wherein highly active chiral octahedral In(III) salen complexes that are dimeric in the solid phase (Figure 1.14 a) were utilized. It was found that from racemic catalyst mixtures, P_r values of 0.23 could be achieved when polymerizing *rac*-lactide with consistent polydispersities of ~1.5. These catalysts were not used under immortal conditions, and no mention was made of their stability towards alcohol. Polymerizations were considered fast as when utilizing a 2 mM catalyst concentration, 200 equivalents of *rac*-lactide was polymerized in 30 min at room temperature.

Bakewell *et al.* have also recorded high isoselectivity[32] ($P_r = 0.16$) when polymerizing *rac*-lactide when utilizing yttrium phosphasalen initiators, and also when tuning their ligand slightly to induce the heteroselective polymerization of *rac*-lactide with $P_r = 0.90$. This addition to the selective polymerization of *rac*-lactide is made more impressive by the fact that the polydispersities never exceed 1.10 for the most selective of the catalysts. The catalysis of some of these systems were found to benefit by the addition of alcohol to the polymerization reaction in order to facilitate initiation, however no mention of polymerization under immortal conditions was mentioned. This would be an exciting addition to their research as already a resistivity to decomposition has been shown.

Horeglad *et al.* recently synthesized a relatively simple dialkyl Ga(III) complex with a methoxy activator group, capped by an N-heterocyclic carbene.[33] This catalyst would not only polymerize to completion (97% in 30 min at -20 ^oC) but also exhibited excellent stereoselectivity when polymerizing *rac*-lactide, yielding polymers consistently with $P_r = 0.22$. The downfall of their catalyst is that it is highly sensitive to impurities in both lactide and solvent. The polymerizations themselves had high catalyst concentrations, though not stated within the documented, when calculated from supporting information

found to be 32 mM, with monomer loadings typically of 50 equivalents of monomer. When reaching monomer loadings of 320 equivalents, time for polymerization completion drastically increases, from 30 min to 16 hrs. This is most likely due to the inherent viscosity of the polymer mixture and inaccessibility to the catalytic centre at high conversion, though was not commented on by the authors. No mention of catalyst stability towards the addition of alcohol was made, but these are sensitive systems.

Until recently, the most isoselective Mg(II) centres have come out of the Schaper group while maintaining high activity.[23] New work done by Song *et al.*[34] utilizes salan-like multidentate aminophenolate ligands were able to achieve P_r values of 0.30 the lowest as yet recorded for Mg after 10 min utilizing 5 mM catalyst in toluene. The negative aspect of the catalysts being that they produce highly polydisperse polymers with PDI values in the range of 1.46 to 2.10 for polymerizations of P_r = 0.39-0.30. Attempts to utilize this system in immortal catalysis failed due to their decomposition in the presence of excess alcohol. Song's addition to the literature represents to our knowledge the only representation of isotactic preference in the polymerization of *rac*-lactide by Zn(II), Mg(II) or Cu(II) catalysts.

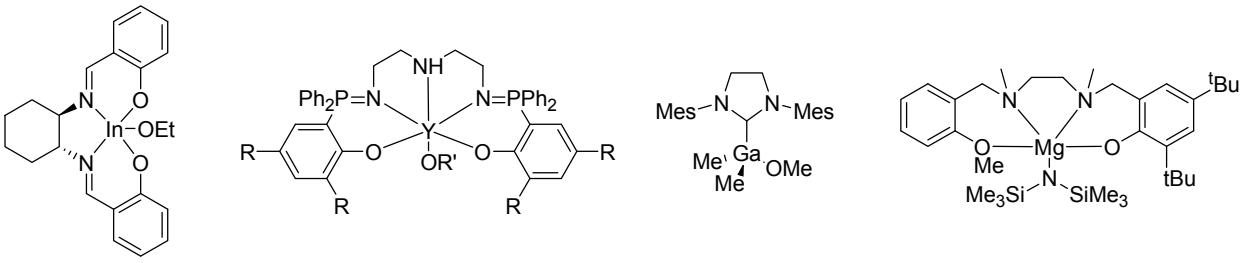

Figure 1.14 – Recent advances in isoselective *rac*-lactide polymerization catalysts

The catalysts in Figure 1.14 represent some of the most isoselective catalysts in the polymerization or *rac*-lactide. The motivation for catalyst design is obvious for: a), the use of a chiral ligand may impart it's chirality on the growing polymer chain via an entiomorphic site control mechanism, which was clearly successful. Whereas catalysts b-d show no chirality yet induce selectivity. To the authors merit in the case of b), they even state "no chiral auxiliaries/ligands are needed for the stereocontrol. The combination of such high rates with high *iso*-selectivities is very unusual." In the case of c), one could imagine that by abstraction of a methyl group for another alkyl would enter into a case of mirror image chirality which

could induce entiomorphic site control, however this is not the case. The authors offered no structural reason for their isotactic induction, nor did the solid state structure offer any obvious insight. Catalyst d), is at least asymmetric and could theoretically polymerize preferentially one lactide isomer over the other. However multiple *rrr* tetrads in the ^{13}C NMR indicated that the polymer was periodically crossing over to selectively insert the alternate monomer. A frustrating aspect of this chemistry is the inability to predict the enantioselectivity of a catalyst. Oftentimes a well designed catalyst will lead to poor selectivity, while a catalyst not necessarily designed for selective polymerization may have excellent performance. In the rare case as in the Mehrkhodavandi work, good catalyst design results in the desired results.

Trends in isospecificity with respect to metal centre are difficult to generalize as the ligand seems to be the dominating design aspect, at least in Figure 1.14 excluding c). Five coordinate M(III) complexes have shown the best selective performance as seen by a) and b) but as far back as the work by Spassky on Al(III) five coordinate complexes, this has been the case.[35] With respect to this work, it has been shown several times that moving from Zn(II) to Mg(II) while maintaining the same ligand framework results in enhanced activity.[29] This may be a result of the increased ionic nature of bonding in Mg(II), allowing for increased ligand flexibility in a given transition state, this has not been proven.

In comparison to catalyst selectivity, catalyst activity is an area with considerably more rationale. Independent of ligand framework, it stands to reason that via a coordination insertion pathway with a Lewis base, the most Lewis acidic metal centre will be the most active.[29] That generalization however may only hold true for the most active of catalysts across metal centres as seen in Table 1.1. However there are a multitude of factors that determine catalyst activity. In accumulating data upon active catalysts, it becomes quickly apparent that the manner in which authors report their activity results is not uniform and often qualitative. For example, authors may state the temperature of polymerization, the ratio of catalyst to monomer, but not the concentration of these reactants. Oftentimes the concentration of reactants must be calculated independently by the reader to calculate k_1 and more assumptions have to be made for a value of k_2, the second order catalyst concentration independent rate law (see Table 1.1) in order to put the results in perspective.[33] A recent review by Arbaoui and Redshaw[36] tackled the activity

issue of activity of metal catalysts for the polymerization of ε-caprolactone by tabulating known catalysts and ranking them with respect to metal centre, ligand framework, and qualitative activity in order to discern general trends. The catalysts were ranked on a scale of activity from "inactive" to "exceptional". The trends in general were found to favor activity in the rare earth elements of which the third oxidation state was more active than the second, congruent with arguments of Lewis acidity. Transition metal complexes range in activities, but the most active come from nitrogen donating ligands such as amidinates, β-diketiminates, and hetero-scorpionate ligands.

Table 1.1 Highest activities in lactide polymerization at ambient temperature for different metal catalysts

	k_2 ($M^{-1}s^{-1}$)	PDI	P_r	entry
Cu(II)	$7.7x10^{-4}$	1.5	-	a[32]
Ca(II)	2[a]	1.2-1.4	0.50	b[33]
Mg(II)	60[b]	1.6	0.43	c[34]
Zn(II)	2.2	1.4	-	d[35]
Y(III)	80[a]	1.1-1.2	0.90	e[36]

Conditions: room temperature (except for Cu(II): 70°C), solution polymerization. [a] Estimated from k_1, assuming a 2nd order rate law. [b] Estimated from time and conversion, assuming a 2nd order rate law.

Table 1.1 shows representative examples of highly active catalysts with different metal centers, while a) in Table 1.1 (Figure 1.15) represents the most active Cu catalyst, it is also representative of a poor catalyst design for insertion polymerization. Though homoleptic complexes offer an ease of synthesis and stability they have the drawback of having to break chelation for the coordination-insertion pathway of lactone polymerization to take place. This combined with a coordinatively saturated centre results in catalysts that required elevated temperatures and extended periods of time for polymerization, ultimately resulting in transesterification, high polydispersity index, and unpredictable molecular weight (*vide infra*). The solution to this issue is the use of heteroleptic systems, incorporating an alkoxide as an

initiator in the case of a) heteroleptic systems were most likely inaccessible by their synthetic route. The catalysts b-d in Figure 1.15, represents the state of the art in terms of polymerization rate with respect to metal. As can be seen, Schiff base ligands have been used extensively in polymerization catalysts. In the case of c) HO*i*Pr was added to the polymerization mixture, essentially generating the desired alkoxide catalyst *in situ.* Another design aspect that has been incorporated is the addition of flexible ligand frameworks with Lewis basic sites that can weakly coordinatively saturate the catalytic site but can easily dissociate in solution or the presence of cyclic esters, allowing for an unencumbered reactive site.

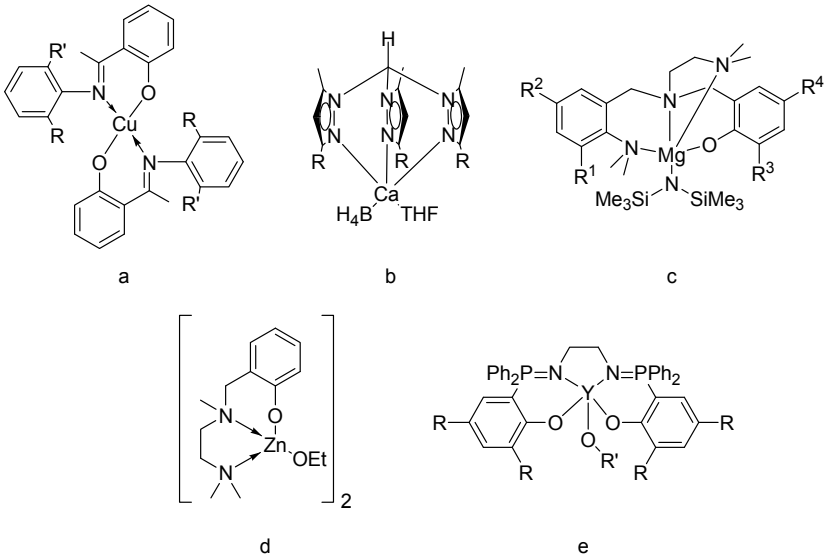

Figure 1.15 – Catalysts that appear in Table 1.1.

1.9 Catalyst Design

The catalyst design aspect of this work was based on utilizing N-alkyl and aryl β-diketimines to create C_2 symmetric catalysts for the selective polymerization of racemic lactide. With this primary guideline, some secondary catalyst requirements were employed:

1) Ease of synthesis – for the purposes of creating a mass produced catalyst.
2) Inexpensive – Since the main practical application of polyesters formed from the ROP of cyclic lactones is as a biodegradable alternative to traditional food and beverage packaging, the cost must remain low.

3) Biologically inactive – It's important to use non-toxic centres (ex. Mg, Zn), as the catalytic metal will remain in the polymer post polymerization, as their primary use is in the packaging of consumables.
4) Resistant to decomposition in the presence of alcohol – If for some reason the designed catalyst requires a multistep ligand pathway (1,2), or an expensive metal centre (2) or a slightly toxic centre, these costs can be offset by decreasing catalyst loadings by having an immortal polymerization catalyst, where stability towards alcohols is a requirement.
5) Clean initiation– Complete, simultaneous catalyst initiation ensures that the polydispersity of the target polymer is narrow. This can be achieved by utilizing alcohol groups which are prone to fast initiation by cyclic esters as they may be sterically and electronically accessible (ex. $^{-}$OiPr, $^{-}$OBn). The use of coordinatively unsaturated metal centres is equally beneficial provided oligomerization is minimal in solution. This allows for facile monomer coordination without requiring catalyst dissociation or reorganization prior to polymerization.
6) High rate of polymerization- Transesterification and epimerization can compete in systems requiring long polymerization times and/or high temperatures. If the polymerization rate can be increased to such a point as to minimize these side reactions, then the catalysts can be quenched upon polymerization completion and prior to significant polymer degradation.

1.10 Objectives/Overview

Reflecting upon previous success with Mg(II) N-alkyl diketiminate complexes[34] the work herein is divided into two parts. The design and implementation of novel N-alkyl diketimine ligands, to be used with Mg(II) centres for the purposes of the selective polymerization of *rac*-lactide. These ligands will be carried over into the second portion of this work, the exploration of square planar Cu(II) complexes for the polymerization of *rac*-lactide.

Chapter 2 will discuss the synthesis of new N-alkyl β-diketimine ligands, their application to Zn(II) and Mg(II) metal centres, and the implementation of these complexes in the polymerization of *rac*-lactide.

Chapters 3 and 4 explores homoleptic, and heteroleptic complexes of these new ligands with a square planar Cu(II) centre and their application to polymerization of *rac*-lactide.

In Chapter 5 Cu(II) complexes will be explored in their application for homopolymerization and copolymerization of *rac*-lactide, ε-caprolactone, β-butyrolactone and δ-valerolactone.

1.11 References

1. Domenek, S.; Courgneau, C.; Ducruet, V., *Biopolymers*, **2011**, 183-223.
2. Leibfarth, F. A.; Moreno, N.; Hawker, A. P.; Shand, J. D., *J. Polym. Sci., Part A: Polym. Chem.* **2012,** *50*, 4814-4822.
3. McKenzie, A., *J. Chem. Soc., Trans.* **1905,** *87*, 1373-1383.
4. Hirao, K.; Masutani, K.; Ohara, H., *J. Chem. Eng. Jpn.* **2009,** *42*, 687-690.
5. Dubois, P.; Jacobs, C.; Jerome, R.; Teyssie, P., *Macromolecules* **1991,** *24*, 2266-2270.
6. Kubisa, P., *Makromol Chem-M Symp* **1988,** *13-14*, 203-210.
7. Dove, A. P., *ACS Macro Letters* **2012,** *1*, 1409-1412.
8. Dove, A. P.; Gibson, V. C.; Marshall, E. L.; Rzepa, H. S.; White, A. J. P.; Williams, D. J., *J. Am. Chem. Soc.* **2006,** *128*, 9834-9843.
9. Boor, J.; Youngman, E. A., *J. Polym. Sci., Part A: Polym. Chem.* **1966,** *4*, 1861-1884.
10. Chamberlain, B. M.; Cheng, M.; Moore, D. R.; Ovitt, T. M.; Lobkovsky, E. B.; Coates, G. W., *J. Am. Chem. Soc.* **2001,** *123*, 3229-3238.
11. Spassky, N.; Wisniewski, M.; Pluta, C.; Le Borgne, A., *Macromol. Chem. Phys.* **1996,** *197*, 2627-2637.
12. Save, M.; Schappacher, M.; Soum, A., *Macromol. Chem. Phys.* **2002,** *203*, 889-899.
13. Simic, V.; Pensec, S.; Spassky, N., *Macromolecular Symposia* **2000,** *153*, 109-121.
14. Liu, Y.-C.; Ko, B.-T.; Lin, C.-C., *Macromolecules* **2001,** *34*, 6196-6201.
15. Inoue, S., *J. Polym. Sci., Part A: Polym. Chem.* **2000,** *38*, 2861-2871.
16. Wei, Z., Liu, L., Qu, C., Qi, M,. *Polymer* **2009**, *50*, 1423–1429
17. Pappalardo, D., Annunziata, L., Pellecchia, C., *Macromolecules* **2009**, *42*, 6056–6062
18. Marcin Florczak and Andrzej Duda, *Angew. Chem. Int. Ed.* **2008**, *47*, 9088 –9091
19. Nomura, N., Akita, A., Ishii, R., Mizuno, M., *J. Am. Chem. Soc.* **2010**, *6*, 132
20. Dechy-Cabaret, O., Martin-Vaca, B., Bourissou, D., *Chem. Rev*. **2004,** 104, 6147-6176
21. Stridsberg, K., Albertsson, A., *J. Polym. Sci., Part A: Polym. Chem.*, **2000**, *38*, 1774–1784
22. Shen, Y.; Zhu, K. J.; Shen, Z.; Yao, K.-M. *J. Polym. Sci., Part A: Polym. Chem.* **1996**, *34*, 1799.
23. Drouin, F.; Whitehorne, T. J. J.; Schaper, F., *Dalton Trans.* **2011,** *40*, 1396-1400.
24. Drouin, F. D. R.; Oguadinma, P. O.; Whitehorne, T. J. J.; Prud'homme, R. E.; Schaper, F., *Organometallics* **2010,** *29*, 2139-2147.
25. Marshall, E. L.; Gibson, V. C.; Rzepa, H. S. *J. Am. Chem. Soc.* **2005**, *127*, 6048.
26. Dutta, S., Hung, W., Huang, B., Lin, C., *Adv Polym Sci* **2012**, *245*, 219–284
27. Dechy-Cabaret, O., Martin-Vaca, B., Bourissou, D., *Chem. Rev.* **2004,** 104, 6147-6176
28. Thomas, C.M. *Chem. Soc. Rev.*, **2010**, *39*, 165–173
29. Wheaton, C. A., Hayes, P. J., Ireland, B. J., *Dalton Trans.*, **2009**, 4832–4846
30. Stanforda, M. J., Dove, A. P., *Chem. Soc. Rev*., **2010**,*39*, 486-494
31. Aluthge, D.C., Patricka, B.O., Mehrkhodavandi,P., *Chem. Commun.*, **2013**,*49*, 4295-4297
32. Bakewell, C., Cao, T., Long, N., Le Goff, X. F., Auffrant, A., Williams, C. K., *J. Am. Chem. Soc.* **2012**, *134*, 20577−20580
33. Horeglad, P., Szczepaniak,G., Drankab, M., Zacharab, J., *Chem. Commun.*, 2012,*48*, 1171-1173

34. Song, S., Ma, H., Yang, Y., *Dalton Trans.*, **2013**, *42*, 14200
35. (a) Spassky, N.; Wisniewski, M.; Pluta, C.; Le Borgne, A. *Macromol. Chem. Phys.* **1996**, *197*, 2627. (b) Zhong, Z.; Dijkstra, P. J.; Feijen, J. *Angew. Chem., Int. Ed.* **2002**, *41*, 4510. (c) Nomura, N.; Ishii, R.; Akakura, M.; Aoi, K. *J. Am. Chem. Soc.* **2002**, *124*, 5938. (d) Hormnirun, P.; Marshall, E. L.; Gibson, V. C.; White, A. J. P.; Williams, D. J. *J. Am. Chem. Soc.* **2004**, *126*, 2688. (e) Chisholm, M. H.; Patmore, N. J.; Zhou, Z. *Chem. Commun. (Cambridge, U. K.)* **2005**, 127. (f) Chisholm, M. H.; Gallucci, J. C.; Quisenberry, K. T.; Zhou, Z. *Inorg. Chem.* **2008**, *47*, 2613.
36. Arbaouia, A., Redshaw, C., *Polym. Chem.*, **2010**,*1*, 801-826
37. Bhunora, S., Mugo, J., Bhaw-Luximon, A., Mapolie, S., Van Wyk, J., Darkwa, J., Nordlander, E., *Appl. Organomet. Chem.*, **2011**, *25*, 133
38. Cushion, M. G., Mountford, P. *Chem. Commun. (Cambridge, U. K.)*, **2011**, *47*, 2276.
39. Wang, L., Ma, H., *Macromolecules*, **2010**, *43*, 6535.
40. Williams, C. K., Breyfogle, L. E., Choi, S. K. Nam, W., Young, V. G., Hillmyer, M. A., Tolman, W. B., *J. Am. Chem. Soc.*, **2003**, *125*, 11350.
41. Cao, T., Buchard, A., Le Goff, X. F., Auffrant, A., Williams, C. K., *Inorg. Chem.*, **201**2, *51*, 2157.

2. Impact of steric and electronic variations in diketiminate Mg and Zn complexes on lactide polymerization

*Todd J. J. Whitehorne, Boris Vabre, Frank Schaper**

Département de chimie, Université de Montréal, 2900 Boul. E.-Montpetit, Montréal, QC, H3T 1J4, Canada

Abstract

Diketimine ligands bearing *N*-benzyl, *N*-9-anthrylmethyl and *N*-mesitylmethyl substituents (*nacnac*^{Bn}H, *nacnac*^{An}H, and *nacnac*^{Mes}H) were prepared from condensation of the amine with either acetyl acetone or its ethylene glycol monoketal. Chlorination with *N*-chlorosuccinimide in the 3-position yielded Cl*nacnac*^{Bn}H and Cl*nacnac*^{An}H. The ligands were reacted with Zn(TMSA)$_2$ (TMSA = N(SiMe$_3$)$_2$) to yield *nacnac*^{An}Zn(TMSA) and Cl*nacnac*^{Bn}Zn(TMSA). Protonation with isopropanol afforded *nacnac*^{An}ZnO*i*Pr and Cl*nacnac*^{Bn}ZnO*i*Pr. Reaction of the diketimines with Mg(TMSA)$_2$ afforded *nacnac*^{An}Mg(TMSA), *nacnac*^{Mes}Mg(TMSA), Cl*nacnac*^{Bn}Mg(TMSA) and Cl*nacnac*^{An}Mg(TMSA). Subsequent protonation with *tert*-butanol produced *nacnac*^{Mes}MgO*t*Bu and Cl*nacnac*^{Bn}MgO*t*Bu, but only decomposition was observed with *N*-anthrylmethyl substituents. Most complexes were characterized by X-ray diffraction studies. TMSA complexes were monomeric, alkoxide complexes dimeric in the solid state. All alkoxide complexes, as well as *nacnac*^{An}Mg(TMSA)/BnOH and Cl*nacnac*^{An}Mg(TMSA)/BnOH were moderately to highly active in *rac*-lactide polymerization (90% conversion in 30 sec to 3 h). *nacnac*^{An}ZnO*i*Pr produced highly heterotactic polymer (P_r = 0.90), Cl*nacnac*^{Bn}MgO*t*Bu/BnOH produced slightly isotactic polymer at –30 °C (P_r = 0.43), all other catalysts produced atactic polymers with a slight heterotactic bias (P_r = 0.48 – 0.55).

Introduction

Biodegradable polymers,[1] i. e. polymers which degrade completely into CO_2 and water in the environment, are gaining importance or at least interest due to concerns about the impact of macroscopic plastic debris and microplastics on wildlife,[2] in particular in the marine environment.[3] Polyesters are attractive targets for biodegradable polymers, since the ester bond can be cleaved by hydrolysis. Of these, polylactic acid (PLA), which is currently used in medical applications and produced on an industrial scale for packing applications, offers the additional advantage that the monomer is obtained from a renewable feedstock.[1c, 4] PLA is obtained industrially from Sn-catalyzed polymerization of lactide, the dimeric anhydride of lactic acid. Catalyst development for the coordination-insertion polymerization of lactide has become a highly investigated research area due to the challenge of polymerizing lactide with high isotacticity and high activity.[4a, 5] Compared to α-olefin polymerization, for example, general structure-reactivity/selectivity relationships for the polymerization of lactide and other cyclic esters are mostly lacking. We investigated in recent years the influence of general catalyst geometry on catalyst performance using structurally similar *N*-alkyl diketiminates (*nacnac*^{R}) as spectator ligands. Octahedral zirconium bisdiketiminate complexes, (±)-C_6H_{10}-(*nacnac*^{R})$_2$Zr(OEt)$_2$ (Scheme 2.1), showed by far the highest activity obtained with group 4 metal catalysts, but did not provide selectivity and were unsatisfactory catalysts due to transesterification side reactions and catalyst decomposition.[6] Square-planar copper diketiminate complexes, {*nacnac*^{R}$_2$Cu(μ-O*i*Pr)}$_2$ (Scheme 2.1), also showed extremely high activities, which were orders of magnitude above other Cu(II) catalysts, but showed no stereoselectivity.[7] Contrary to the octahedral Zr catalyst, the Cu catalyst was highly stable, able to produce block-copolymers, did not undergo transesterification reactions or chain-transfer even in the absence of monomer, and was suitable for immortal polymerization conditions. Zn and Mg catalysts, **2.1**-**2.3** (Scheme 2.1), having the same *N*-alkyl diketimine ligands in a tetrahedral coordination geometry, displayed only moderate activity in comparison to other complexes with the same central metal.[8] While the Zn catalysts provided heterotactic polymer, Mg catalyst **2.3** showed a slight preference for isotactic

monomer enchainment at low temperatures. The source of the preference for isotactic enchainment is not clear at the moment, but a ligand-mediated chain-end control mechanism was proposed based on the available data.[8a]

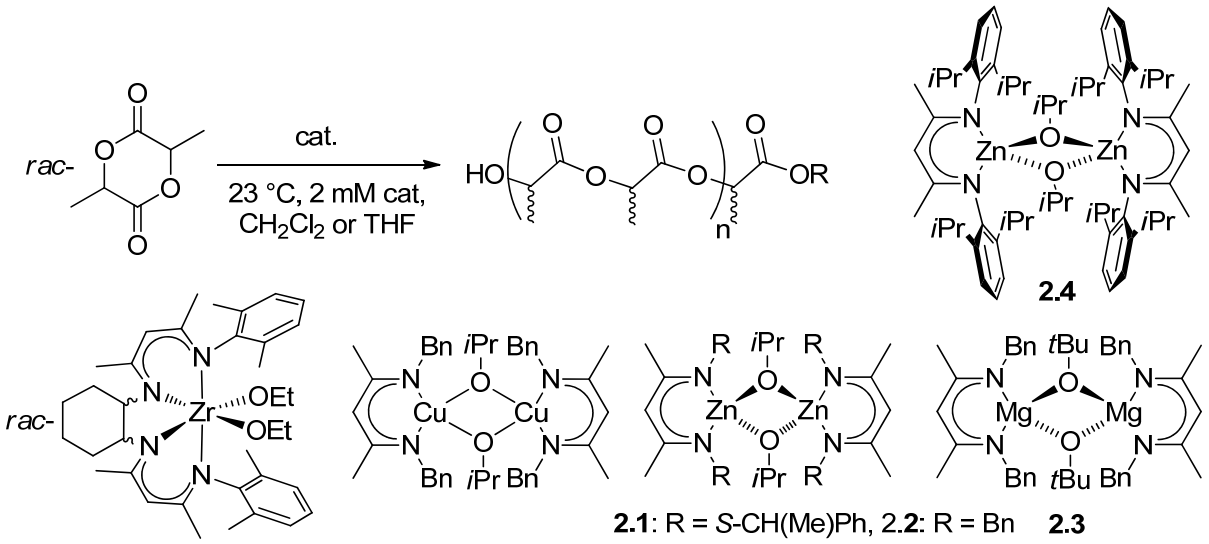

Scheme 2.1

Zinc[8b, 9] and magnesium[8a, 9b-i, 10] diketiminate complexes have been widely used in lactide polymerization, starting with the seminal work of Coates using *nacnac*^{dipp}ZnO*i*Pr,[11] **2.4**, (dipp = diisopropylphenyl).[9a, 9b] In all cases, monomer insertion occurred either unselectively or with heterotactic preference, following a chain-end control mechanism. The latter can be very efficient, provided that the ligand is sufficiently bulky, and P_r-values of >90% were be obtained with several catalysts (P_r = probability of alternating enantiomer insertion). Non-symmetric, mono-substituted *N*-aryl diketiminate ligands have been used in several cases to yield C_2- or C_1-symmetric Mg or Zn diketiminate complexes.[9e-g, 9o-q] However, catalyst geometry did not impact on stereoselectivity and the catalysts continued to show only heterotactic preference, if any, for monomer insertion in the polymerization of *rac*-lactide.[9e-g, 9o, 9p] Magnesium complex **2.3** thus represents so far the only example of a diketiminate catalyst with an isotactic preference. To gain a better understanding of the structural factors governing selectivity in lactide polymerization, we investigated slight variations in the substitution pattern of *N*-alkyl diketiminate Zn and Mg complexes similar to **2.3**, while maintaining the primary alkyl (CH_2R) substituent on *N* which enables the formation of chiral rotamers, suspected to be responsible for the isotactic preference.

Results and Discussion

Zinc complexes. Initial variations of the ligand substitution pattern concentrated on increasing the steric bulk of the *N*-benzyl substituent by replacement with *N*-anthrylmethyl (**2.5a**, Scheme 2.2). The condensation of anthrylmethylamine with acetyl acetone, a route successfully employed for other *N*-alkyl diketimines,[12] yielded only the monocondensation product (Scheme 2.2), regardless of reaction conditions (1-2 equiv HCl, TsOH or a mixture of both). Condensation in ethanolic HCl at reflux[13] likewise failed to provide **2.5a**. Reaction of acetyl acetone ethylene glycol monoketal (Scheme 2.2) with two equiv of amine in the absence of solvent[14] finally yielded **2.5a** in 62% yield (see Figure 2.1)for the crystal structure of **2.5a**).

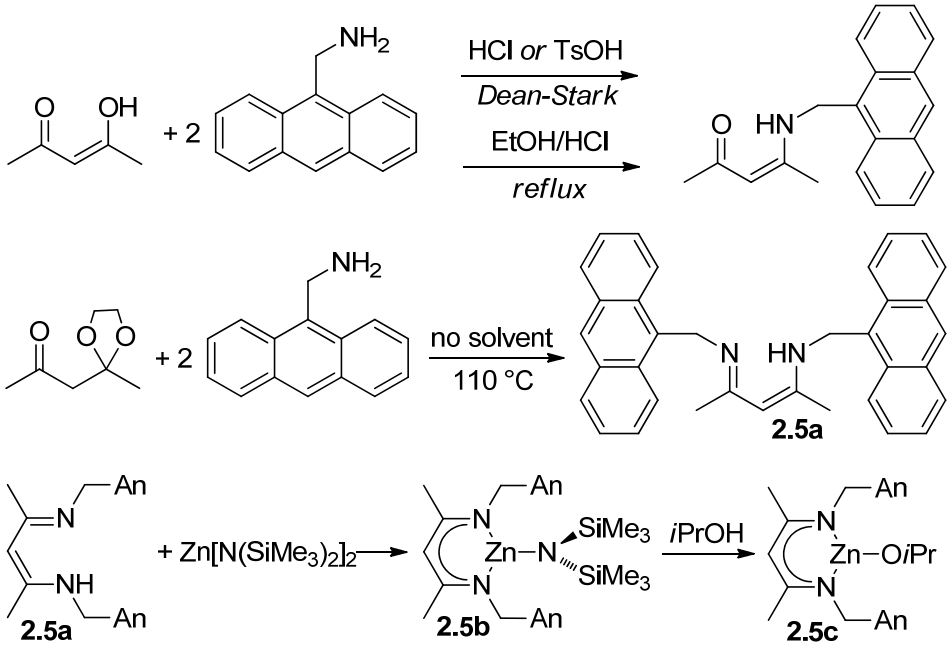

Scheme 2.2

Reaction of **2.5a** with $Zn[N(SiMe_3)_2]_2$ cleanly yielded the respective Zn amide complex, **2.5b** (Scheme 2.2). Further protonation with isopropanol afforded *nacnac*^{An}ZnO*i*Pr, **2.5c**. As typically observed for *nacnac*ZnN$(SiMe_3)_2$ complexes, **2.5b** crystallized as a monomeric complex with a trigonal-planar geometry around the Zn atom and a perpendicular orientation of the amide ligand versus the ligand mean plane (Figure 1). Bond distances and angles in **2.5b** are in the range typically observed for *nacnac*ZnN$(SiMe_3)_2$ (Table S1).[8b, 9f, 9g, 15] Alkoxide complex **2.5c** crystallized as an alkoxide bridged dimer (Fig 2.2), as do all other similar complexes with the exception of monomeric *nacnac*^{dipp}ZnO*t*Bu.[9d]

The zinc atom is found in a distorted tetrahedral coordination geometry. Bond distances and angles are comparable to other alkoxide bridged zinc diketiminates (Table S1),[8b, 9a, 9b, 9q, 15a, 16] but on the lower end of the range observed for Zn-N distances and the higher end for the N-Zn-N angle, indicating rather low steric pressure from the ligand despite the annulated aromatic ring. The orientation of the anthryl moieties in **2.5c** are in agreement with π-stacking interactions: the anthryl moieties are nearly coplanar (angle between mean planes: 7°), with a slight offset placing a carbon atom in the middle of the aromatic rings and distances of 3.3 – 3.7 Å.

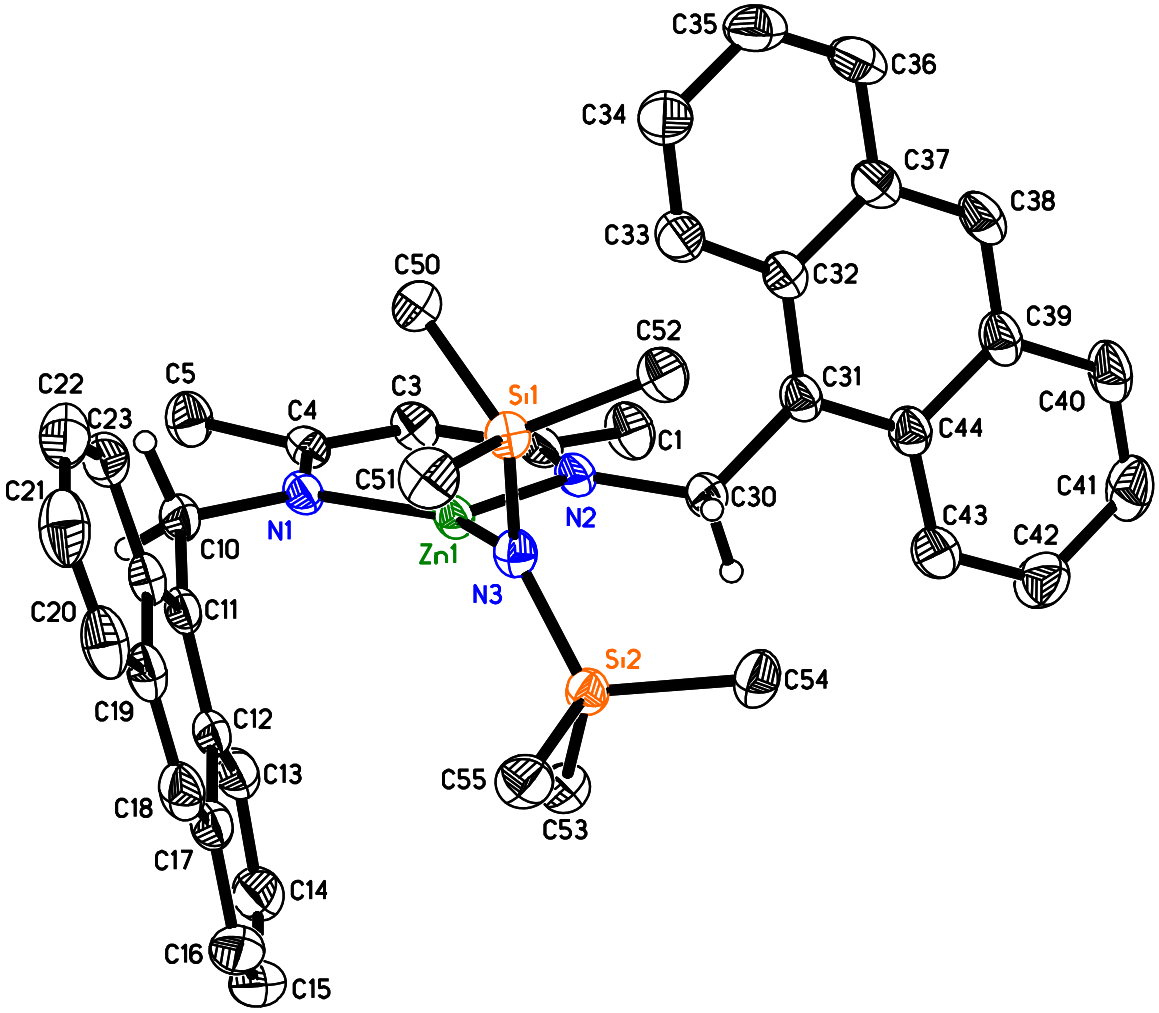

Figure 2.1 X-ray structure of **2.5b**. Most hydrogen atoms, the second independent molecule of comparable geometry and co-crystallized solvent were omitted for clarity. Thermal ellipsoids are drawn at 50% probability. Bond distances/Å: Zn1-N1: 1.935(1) & Zn2-N5: 1.935(1), Zn1-N2: 1.986(1) & Zn2-

N4: 1.992(1), Zn1-N3: 1.897(1) & Zn2-N6: 1.902(1). Bond angles/deg: N1-Zn1-N2: 100.11(6) & N4-Zn2-N5: 99.60(6), N1-Zn1-N3: 142.41(6) & N5-Zn2-N6: 144.00(6), N2-Zn1-N3: 117.30(6) & N4-Zn2-N6: 116.33(6).

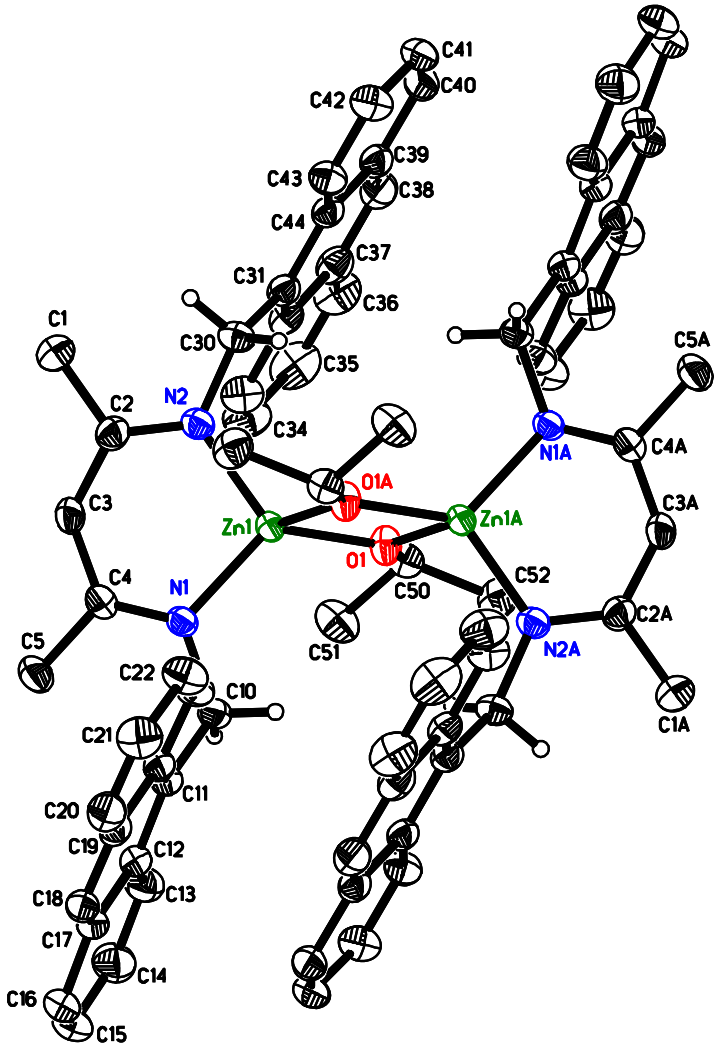

Figure 2.2 X-ray structure of **2.5c**. Most hydrogen atoms and co-crystallized solvent omitted for clarity. Thermal ellipsoids are drawn at 50% probability. The molecule has crystallographic inversion symmetry. Bond distances/Å: Zn1-N1: 1.973(2), Zn1-N2: 1.959(2), Zn1-O1: 1.975(2), Zn1-O1A: 1.977(2), Zn1-Zn1A: 2.9816(6). Bond angles/deg: N1-Zn1-N2: 100.66(8), O1-Zn1-O1A: 81.99(7), N1-Zn1-O1: 117.75(8), N2-Zn1-O1: 121.21(8), N1-Zn1-O1A: 126.24(8), N2-Zn1-O1: 110.22(8), Zn1-O1-Zn1A: 98.01(7).

Complex **2.5c** proved to be moderately active and a controlled catalyst for the solution polymerization of *rac*-lactide (Table 2.1, Fig S2.2). After a short induction period, the reaction was first-order in lactide concentration with an apparent rate constant of k_{app} = $1.2 \cdot 10^{-2}$ – $1.6 \cdot 10^{-2}$ min^{-1} at 2 mM catalyst

concentration. The activity is very similar to the rate constants observed for the respective *N*-benzyl complex **2.1** (k_{app} = 2·10^{-2} - 4·10^{-2} min^{-1}) and *N*-methylbenzyl complex **2.2** (k_{app} = 1·10^{-2} - 2·10^{-2} min^{-1})[8b] and only slightly lower than *nacnac*^{dipp}ZnO*i*Pr, **2.4** (k_{app} = 5·10^{-2} min^{-1}).[9b] The obtained polymer is highly heterotactic, with P_r values around 90% (Table 2.1, P_r). Complex **2.5c** thus shows an even higher heterotactic preference then the corresponding benzyl complex **2.2**. A closer look at the crystal structures of **2.5b** and **2.5c** offers a tentative explanation for the lack of catalytic-site control. In **2.5b**, one anthrylmethyl substituent is oriented nearly symmetrically with regard to the ligand mean plane (Fig 2.1), the other is turned with the anthryl moiety towards the backbone of the ligand. The latter orientation is also observed for one of the *N*-substituents in dimeric **2.5c** (Fig 2.2). In both orientations, complex geometry becomes essentially *C*s-symmetric and no catalytic site control by a putative C_2-symmetric rotamer is observed. Polymer molecular weight control with **2.5c** was rather poor and polymer molecular weights significantly higher than expected were obtained. Neither a notable induction period, nor catalyst decomposition was observed, in agreement with overall narrow polydispersities. Prolonged reaction times after completion of polymerization increased the P_r value as well as the discrepancy between expected and obtained polymer molecular weight (c. f. #1 vs. #2). This might indicate transesterification side-reactions as possible source for the lack of polymer molecular weight control (see supp. information).[8b] In the presence of one equiv of benzyl alcohol the expected molecular weight for two chains per metal centre is obtained with narrow polydispersities (Table 2.1, #3), indicating some stability of **2.5c** under immortal polymerization conditions.

Table 2.1 *rac*-Lactide polymerization with Zn complexes

#	Catalyst	[Zn] : lactide (: BnOH)	Conversion / time	Final conversion	P_r	M_n ·mol/g	Chains per Zn	M_w/M_n
1	**2.5c**	1:300	40% / 30 min	93% / 3 h	0.88	66 500	0.6	1.14
2	**2.5c**	1:300	33% / 30 min	95% / 6 h	0.93	118 000	0.3	1.16
3	**2.5c**	1:300:1	19% / 30 min	87% / 3 h	0.87	14 900	2.3	1.04
4	**2.6c**	1:300	80% / 3h	80%	0.59	n. d.		

Conditions: CH_2Cl_2, ambient temperature (23 °C), 2 mM [Zn]. Conversion determined from ^{1}H NMR. P_r determined from decoupled ^{1}H NMR by $P_r = 2 \cdot I_1/(I_1+I_2)$, with I_1 = 5.20 – 5.25 ppm (*rmr, mmr/rmm*),

I_2 = 5.13 – 5.20 ppm (*mmr/rmm, mmm, mrm*). M_w and M_n determined by size exclusion chromatography vs. polystyrene standards, with an MH correction factor of 0.58. Number of chains per catalyst determined from (conversion·$m_{lactide}/n_{Zn}+M_{iPrOH}$)/$M_n$.

To investigate electronic effects on catalyst performance, we prepared diketimine **2.6a** with a chlorine substituent in the 3-position of the ligand backbone by reaction of the parent diketimine with *N*-chlorosuccinimide (Scheme 2.3). Reaction with $Zn[N(SiMe_3)_2]_2$ yielded the amide complex **2.6b** as an oil, which was reacted, without further purification, with isopropanol to yield alkoxide complex **2.6c**. Polymerization of *rac*-lactide with **2.6c** (Table 2.1, #4) showed an activity comparable to that of its non-chlorinated analogue **2.2** and a P_r value of 0.59, only slightly reduced compared to **2.2** (0.65 – 0.71).[8b]

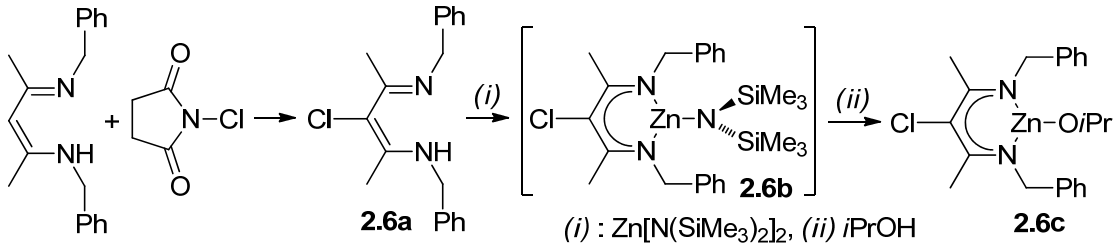

Scheme 2.3

Magnesium complexes. Since magnesium complex **2.3** was the first diketiminate complex with an isotactic preference for monomer insertion, it was of interest to see how slight variations of the substitution pattern influenced stereoselectivity in lactide polymerization. Reaction of $Mg[N(SiMe_3)_2]_2$ with **2.5a** yielded the respective amide complex **2.5d** (Scheme 2.4). As other diketiminate metal amides, **2.5d** is monomeric in the solid state (Fig 2.3). In comparison to the corresponding Zn amide **2.5b** (Fig 2.1), the more ionic bonds in the Mg complex allow a stronger deviation from trigonal-planar geometry and the Mg atom is bent by 29° out of the plane of the diketiminate ligand. This deviation is higher than in the corresponding *N*-aryl complex *nacnac*$^{dipp}MgN(SiMe_3)_2$,[17] where this deviation is only 16°. The difference can be ascribed to the higher flexibility of *N*-alkyl diketiminates, which allow an easier out-of-plane bending of the metal atom.[18] Other geometrical parameters in **2.5d** are comparable to those of *nacnac*$^{dipp}MgN(SiMe_3)_2$ (Table S2).

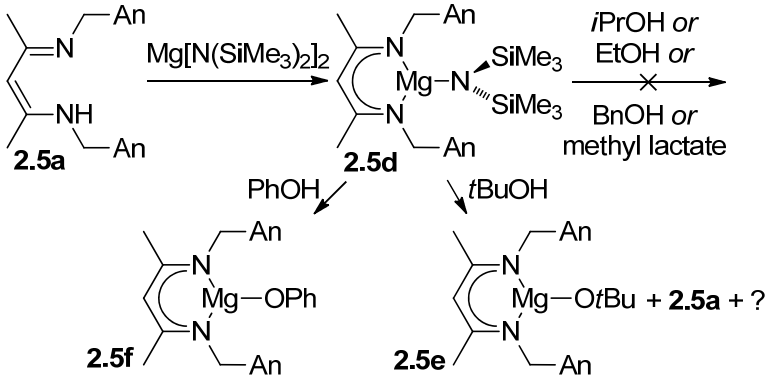

Scheme 2.4

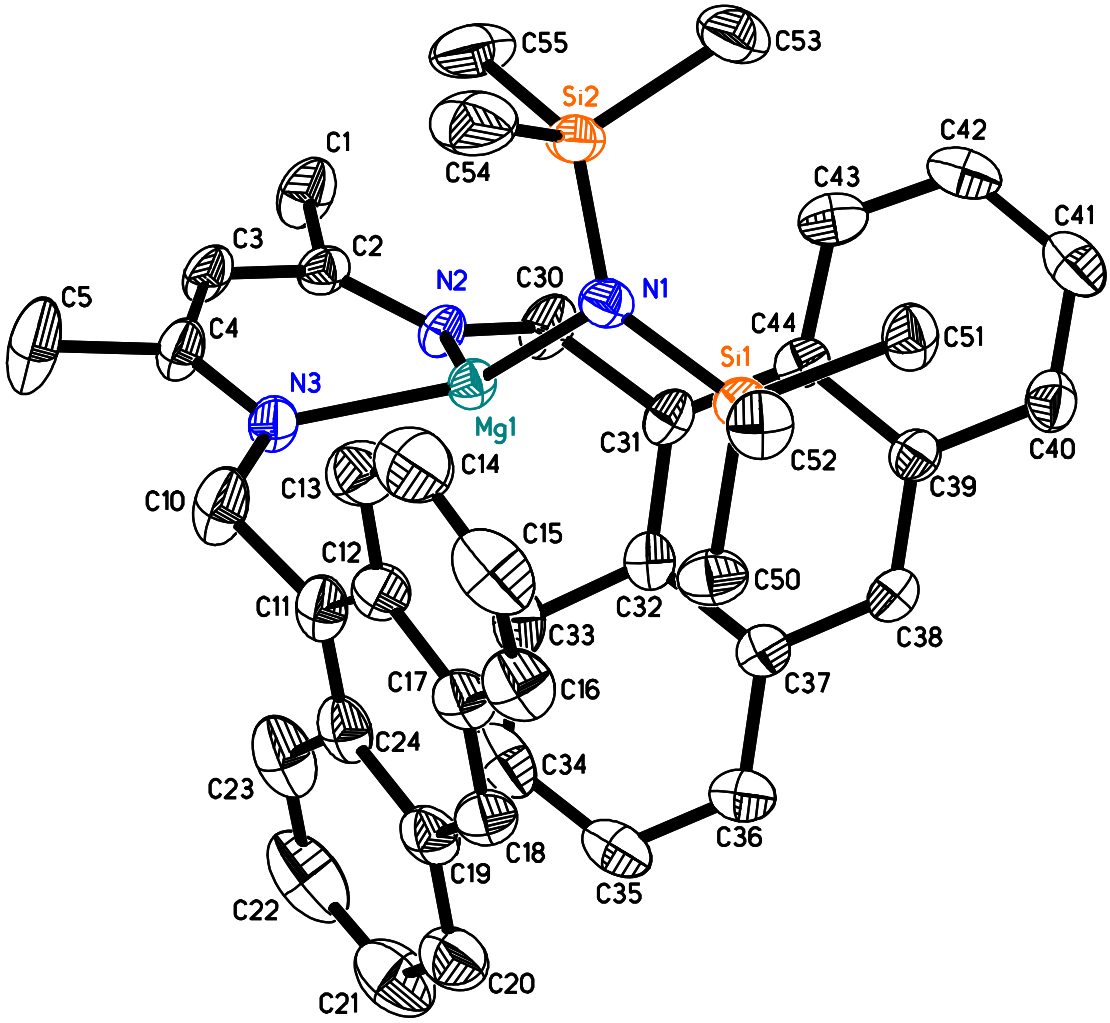

Figure 2.3 X-ray structure of **2.5d**. Hydrogen atoms and co-crystallized solvent omitted for clarity. Thermal ellipsoids are drawn at 50% probability. Mg1-N2: 2.026(2) Å, Mg1-N3: 2.029(2) Å, Mg1-N1: 1.972(2) Å, N2-Mg1-N3: 96.80(8)°, N1-Mg1-N2: 126.55(8)°, N1-Mg1-N3: 125.34(9)°.

Attempts to introduce an alkoxide substituent by reaction of **2.5d** with isopropanol led to decomposition. In the case of **2.3**, similar problems had been circumvented by employing *tert*-butanol,[8a]

but the reaction proved less controlled with **2.5d**: When an C_6D_6 solution of **2.5d** was titrated with *tert*-butanol, resonances assigned to the target complex **2.5e** were obtained upon addition of 0.25 equiv of *tert*-butanol (Scheme 2.4, Fig S2.3). Further addition of alcohol, however, led to the presence of increasing amounts of the ligand **2.5a** and unknown by-products. (The expected by-product, homoleptic (*nacnac*^{An})$_2$Mg, seems not to be present in the mixture. Likewise, we were unable to prepare the homoleptic complex by reaction of magnesium amide with two equiv of **2.5a**.) Although *tert*-butoxide complex **2.5e** was the major species present, we were unable to obtain a pure product despite extensive recrystallization experiments. Reaction of **2.5d** with several other alcohols, such as ethanol, benzyl alcohol, methyl lactate, or phenol, likewise failed to yield an isolatable pure product. In the case of phenol, single crystals of the phenolate complex **2.5f** suitable for X-ray diffraction were obtained (Fig 2.4), but only in quantities insufficient for further characterization. Bond distances and angles in **2.5f** are comparable to other [*nacnac*Mg(μ-OR)]$_2$ complexes (Table S3).[8a, 9b, 9g, 19] The structure of **2.5f** illustrates the high flexibility of *N*-alkyl diketiminate ligands: all the anthryl orientations described for **2.5b** and **2.5c** are realized in **2.5f**. Two anthryl groups are arranged in a π-stacking orientation and display the forward orientation of the anthryl moiety targeted for effective stereocontrol, the other two do not show suitable orientations for enforcing C_2-symmetry: one anthryl group is nearly perpendicular to the mean ligand plane, the other one is rotated towards the ligand backbone.

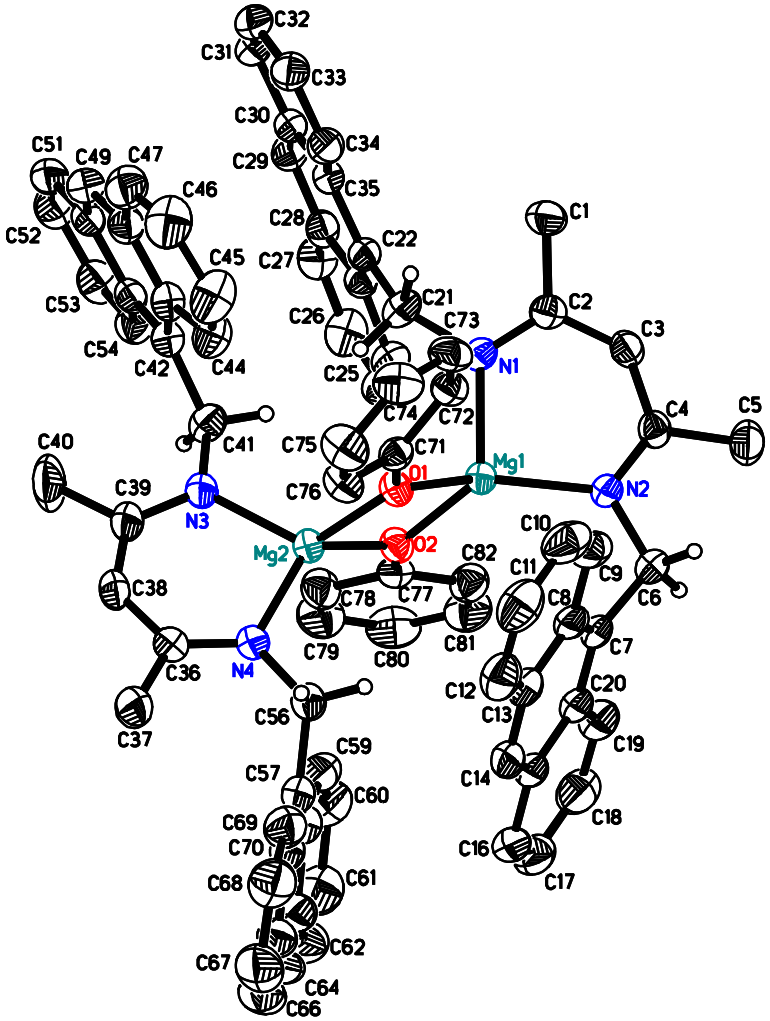

Figure 2.4 X-ray structure of **2.5f**. Most hydrogen atoms and co-crystallized solvent omitted for clarity. Thermal ellipsoids are drawn at 50% probability. Bond distances/Å: Mg1-N1: 2.0559(15), Mg1-N2: 2.0406(15), Mg2-N3: 2.0281(16), Mg2-N4: 2.0172(16), Mg1-O1: 1.9862(13), Mg1-O2: 1.9940(13), Mg2-O1: 1.9700(13), Mg2-O2: 1.9845(13), Mg1-Mg2: 3.0122(8). Bond angles/deg: N1-Mg1-N2: 94.88(6), N3-Mg2-N4: 95.67(6), O1-Mg1-O2: 80.65(5), O1-Mg2-O2: 81.29(5).

In the absence of an isolated alkoxide complex, the amide complex **2.5d** was employed for *rac*-lactide polymerizations. Surprisingly, **5d** proved to be highly active (Table 2.2, #1; Fig S2.4), slightly faster than complex **2.3** with *N*-benzyl substituents. None of the polymerizations performed reached completion, indicating instability of the catalyst under polymerization conditions. As with **2.3**, polymerization at room temperature yielded an atactic polymer. A notable induction period (Fig S2.4), a low number of polymer chains per catalyst centre and high polydispersities above 1.8 indicate slow initiation of polymerization.

Addition of one equiv benzyl alcohol to polymerizations with **2.5d** removed the induction period and polymerization was complete in less than one minute (Table 2.2, #2-#8; Fig S2.5+S2.6; c.f.: *nacnac*^{dipp}MgOR, 97% in 2 min[9b]), rendering **2.5d** a highly active catalyst with k_{obs} = 2.8(3) min^{-1} at 2 mM catalyst concentration. If two equiv BnOH were used (Table 2.2, #5; Fig S2.5) or at an increased lactide:Mg ratio of 900:1 (Table 2.2, #8; Fig S2.6), catalyst decomposition prevented complete polymerization. In all cases, the obtained polymer was atactic and, contrary to **2.3**, polymerization at reduced temperatures did not affect stereoselectivity (Table 2.2, #9). Polydispersities varied between 1.2 and 1.7, smaller than for polymerizations without additional alcohol, but nevertheless indicative of poor polymer weight control. In addition, obtained polymer weights were now much lower than expected with 1.5 to 3.9 polymer chains produced per metal centre. Participation of $(Me_3Si)_2NH$ as a chain-transfer agent seems unlikely, given its low acidity and slow insertion rates. Consequently, no notable presence of polymer bound $N(SiMe_3)_2$ was detected in ^{1}H NMR spectra of polymers obtained with **2.5d**/BnOH. Variations in the catalyst:monomer ratio (1:100 – 1:900; #3, #6-#8) did not correlate with the number of polymer chains obtained per catalyst, thus excluding impurities in the monomer acting as chain-transfer agents. Increasing amounts of benzyl alcohol (0.7 – 2 equiv; #2-#5), led to lower polydispersities, in agreement with its activating effect on initiation, but they still remained above 1.15. Higher amounts of alcohol increased, as expected, the number of chains per catalyst centre, but the obtained polymer molecular weight remained lower than expected in all cases. GPC traces did not indicate the presence of a low-molecular-weight fraction that would be indicative of intramolecular transesterifications to yield cyclic oligomers. However, the P_r value varied slightly more (P_r = 0.48 – 0.52) than the usual experimental error and correlates – somewhat noisily – with the discrepancy of expected and obtained molecular weight, i. e. the number of chains per catalyst centre produced (Fig S2.7). Since a likely cause for variations in P_r are transesterification reactions (the appearance of rr-triads causes an artificial reduction of P_r, if calculated as described in Table 2.2), the observed discrepancy in expected and obtained molecular weight might be attributed to transesterification (see supp. inform.).

Table 2.2 *rac*-Lactide polymerization with Mg catalysts

#	Catalyst	[Mg] : lactide (: BnOH)	Conversion / time	Final conversion	P_r	M_n · mol/g	Chains per Mg	M_w/M_n
1	**2.5d**	1:100	20 – 30% / 1 min [a]	60% – 65% [a]	0.51 – 0.52	15 100 – 15 700	0.6	1.79 – 1.87
2	**2.5d**	1:300:0.7	80% / 30 sec	95%	0.52	24 800	1.6	1.65
3	**2.5d**	1:300:1	75 - 95% / 30 sec [a]	> 95%	0.49	15 500 – 16 300	2.5 – 2.7	1.39 – 1.60
4	**2.5d**	1:300:1.3	95% / 30 sec	95%	0.49	13 300	3.1	1.49
5	**2.5d**	1:300:2	50% / 30 sec	70%	0.48	7900	3.9	1.15
6	**2.5d**	1:100:1	90% / 30 sec	95%	0.51	9500	1.4	1.29
7	**2.5d**	1:600:1	95% / 30 sec	> 95%	0.49	27 200	3.1	1.60
8	**2.5d**	1:900:1	60% / 30 sec	65%	0.50	36 800	2.2	1.45
9	**2.5d**, –30 °C	1:100:1		85% / 40 min	0.52	n. d.		
10	**2.7e**	1:300	70% / 5 min	80%	0.53	45 400	0.8	1.62
11	**2.7e**, –30 °C	1:300		92% / 17 h	0.55	55 500	0.7	1.98
12	**2.6e**	1:300	70 – 80% / 10 min [a]	75 – 90% [a]	0.54	23 300 – 39 000	0.8 – 1.6	1.34 – 1.71
13	**2.6e**	1:300:1	15 - 95% / 10 min [a]	30 – 95% [a]	0.46 – 0.50	16 600 – 27 800	0.7 – 2.1	1.04 – 1.20
14	**2.6e**, –30 °C	1:300:1		90-99% / 50 min [a]	0.43	31 900 – 37 900	1.1 – 1.2	1.08 – 1.11
15	**2.8d**	1:300:1	30% / 1 min	40%	0.48	n. d.		

Conditions: CH_2Cl_2, ambient temperature, 2 mM catalyst concentration. Final conversion without a given time is the maximum conversion, when the conversion/time plot plateaued. See supp. information for approximate rate constants. P_r determined from decoupled ^{1}H NMR by $P_r = 2 \cdot I_1/(I_1+I_2)$, with I_1 = 5.20 – 5.25 ppm (*rmr, mmr/rmm*), I_2 = 5.13 – 5.20 ppm (*mmr/rmm, mmm, mrm*). M_n and M_w determined by size exclusion chromatography vs. polystyrene standards, with an MH correction factor of 0.58. Number of chains per Mg centre determined from (conversion$\cdot m_{lactide}/n_{Mg}+M_{iPrOH})/M_n$. [a] Minimum and maximum values of multiple experiments.

Given the high amount of π-stacking observed in the X-ray structures of **2.5c** and **2.5f**, which might stabilize the undesired *meso*-rotamer, we investigated ligand **2.7a**, which is sterically similar to **2.5a**, but should show a reduced tendency for π-π-interactions. Ligand **2.7a** was obtained similarly to **2.5a**, but the presence of molecular sieves was essential to obtain yields above 20% (Scheme 2.5). Reaction with $Mg[N(SiMe_3)_2]_2$ yielded the amide complex **2.7d**. The crystal structure of amide complex **2.7d** is nearly identical to that of **2.5d** (Fig 2.5, Table S2) with the only difference being that the near C_s-symmetry in **2.5d** was observed as crystallographic C_s-symmetry in **2.7d**. Complex **2.7d** reacted with *tert*-butanol to yield **2.7e**. Alternatively, direct addition of *tert*-butanol to the crude reaction mixture containing **2.7d** in a one-pot, two-step reaction yielded **2.7e** in comparable yields. The crystal structure of **2.7e** shows a higher than usual bending of the Mg atom out of the mean plane of the diketiminate ligand and a likewise higher distortion from tetrahedral symmetry, which are both indicative of the steric strain introduced by the mesitylmethyl substituent, but otherwise geometric parameters are comparable to **2.5f**, **2.6e** and other dimeric $\{nacnacMg(\mu\text{-}OR)\}_2$ complexes (Fig 2.6, Table S3).[8a, 9b, 9g, 19] Satisfyingly, the π-stacking interactions observed in **2.5f** are absent in **2.7e**.

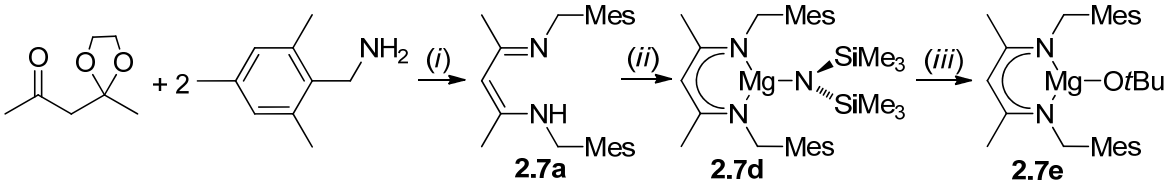

Mes = 2,4,6-trimethylphenyl. *(i)* : no solvent, Δ, mol. sieves, (*ii*): $Mg[N(SiMe_3)_2]_2$, *(iii)* *t*BuOH

Scheme 2.5

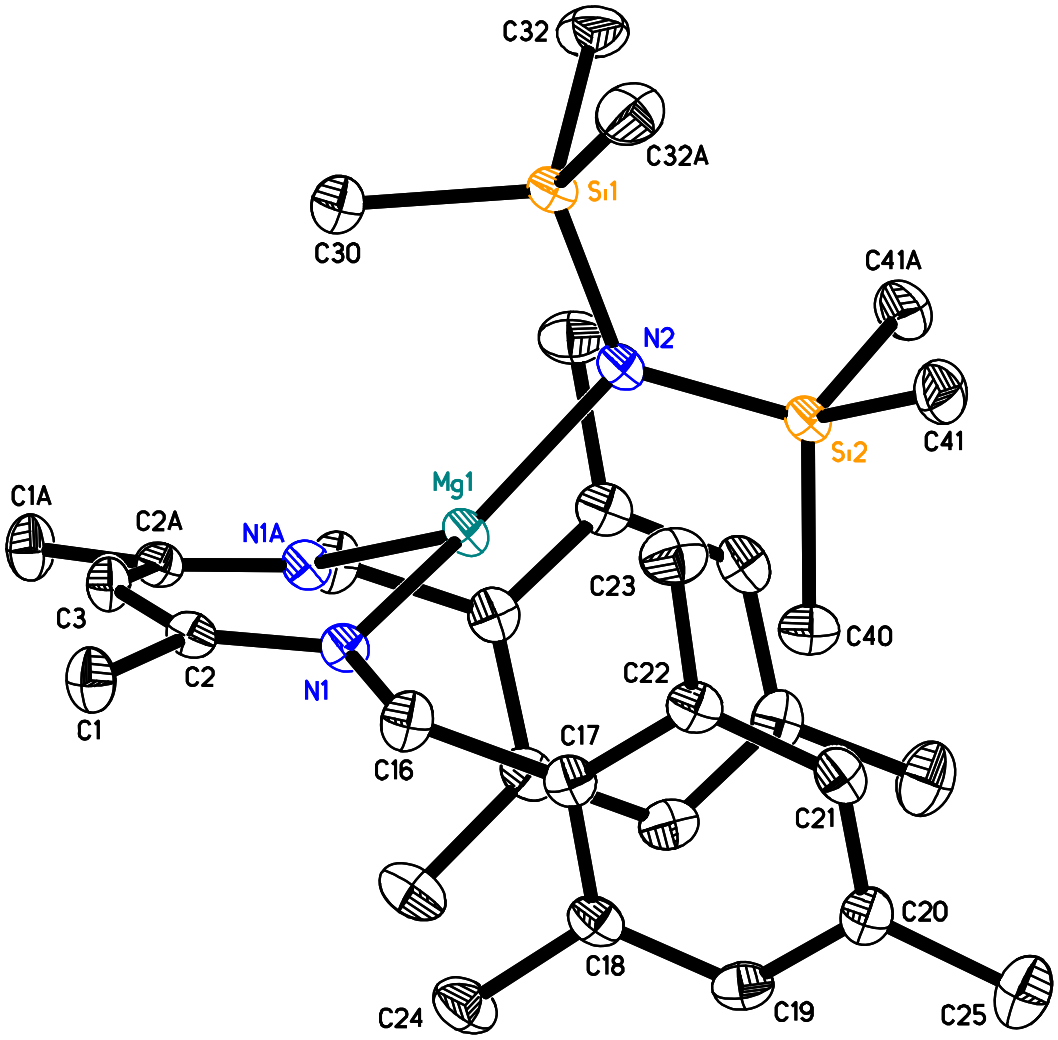

Figure 2.5 X-ray structure of **2.7d**. Hydrogen atoms omitted for clarity. Thermal ellipsoids are drawn at 50% probability. Mg1-N1: 2.036(1) Å, Mg1-N2: 1.975(2) Å, N1-Mg1-N1A: 95.28(6)°, N1-Mg1-N2: 129.39(3)°.

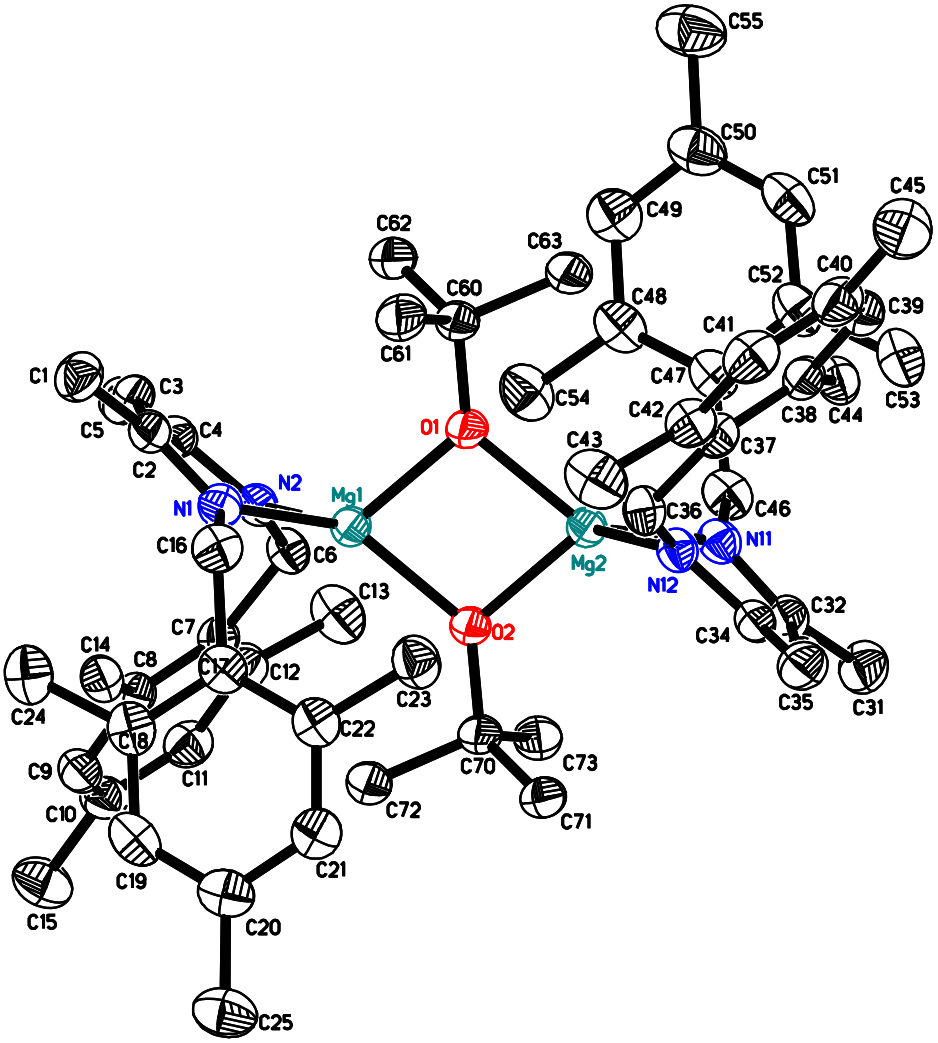

Figure 2.6 X-ray structure of **2.7e**. Hydrogen atoms and co-crystallized solvent omitted for clarity. Thermal ellipsoids are drawn at 50% probability. Bond distances/Å: Mg1-N1: 2.0718(18), Mg1-N2: 2.0468(17), Mg2-N11: 2.0660(18), Mg2-N12: 2.0465(17), Mg1-O1: 1.9752(15), Mg1-O2: 1.9612(14), Mg2-O1: 1.9583(14), Mg2-O2: 1.9841(14), Mg1-Mg2: 2.9711(9). Bond angles/deg: N1-Mg1-N2: 90.61(7), N11-Mg2-N12: 90.97(7), O1-Mg1-O2: 82.17(6), O1-Mg2-O2: 82.01(6).

Performance of **2.7e** in lactide polymerization was disappointing (Table 2.2, #10-#11). Activities are lower than those of **2.5d**/BnOH, but are still significantly higher than those observed for **2.3**.[8a] *Ortho*-substitution of the *N*-benzyl substituent thus increased activity in **2.7e** as well as **2.5d**. However, catalyst decomposition led to incomplete monomer consumption at room temperature and polydispersities were above 1.6 at room temperature and at –30 °C, despite a very minor induction period (Fig S2.8). In addition, the catalyst showed no preference for isotactic monomer insertion even at low temperatures.

Magnesium complexes with β-chloro-diketiminate ligands. The effect of ligand chlorination was studied using β-chloro-diketimines **2.6a** and **2.8a** (Scheme 2.6). Reaction of $Mg[N(SiMe_3)_2]_2$ with **2.6a** yielded mixtures of $Mg[N(SiMe_3)_2]_2$, the heteroleptic amide complex **2.6d** and the homoleptic bisdiketiminate complex **2.6f**. To corroborate assignment, **2.6f** was prepared independently and characterized by X-ray diffraction (Fig 2.7). Comparison of **2.6f** with the corresponding homoleptic complex lacking the chlorine substituent, *nacnac*$^{Bn}{}_2$Mg,[8a] allows the delineation of the structural impact of introducing a substituent on the C_β atom of the diketiminate ligand (Table 2.3). Both structures show a distorted tetrahedral geometry, with similar orientations of the benzyl substituents. Electronic influences are rather small, leading to a minor contraction of the Mg-N bond lengths in **2.6f** (0.1 Å, Table 2.3). More notable is the steric impact of the chlorine substituent. By way of the methyl groups at the ligand backbone (widening of the C_β-C_α-C_{Me} angles by 3 – 4°, Table 2.3), substitution at C_β pushes the *N*-substituents closer to the front of the complex (reduction of C_N-C_β-C_N by 4° and of N-C_β-N by 2°). Other geometric data is consistent with a minor increase of steric pressure in **2.6f** (Table 2.3), in particular the slight reduction of the distances between Mg and the *N*-substituents.

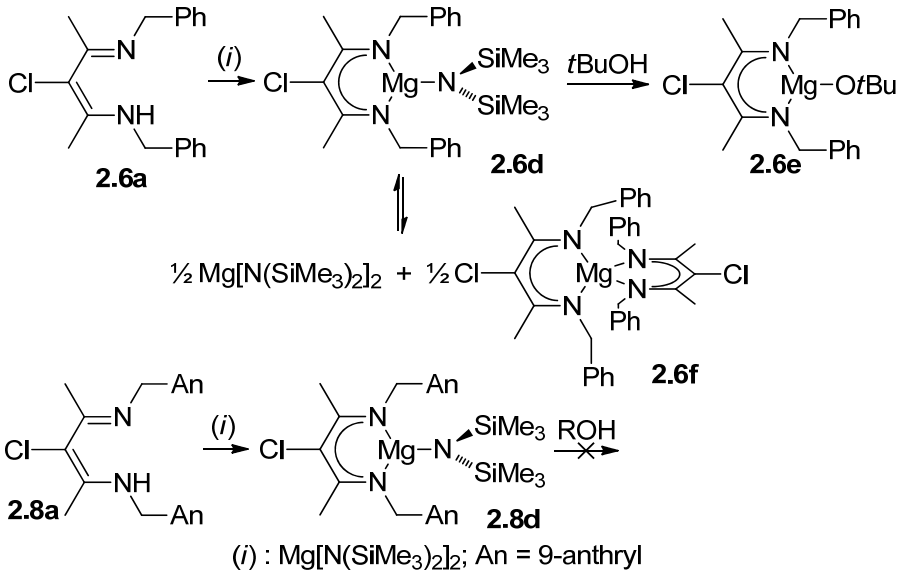

Scheme 2.6

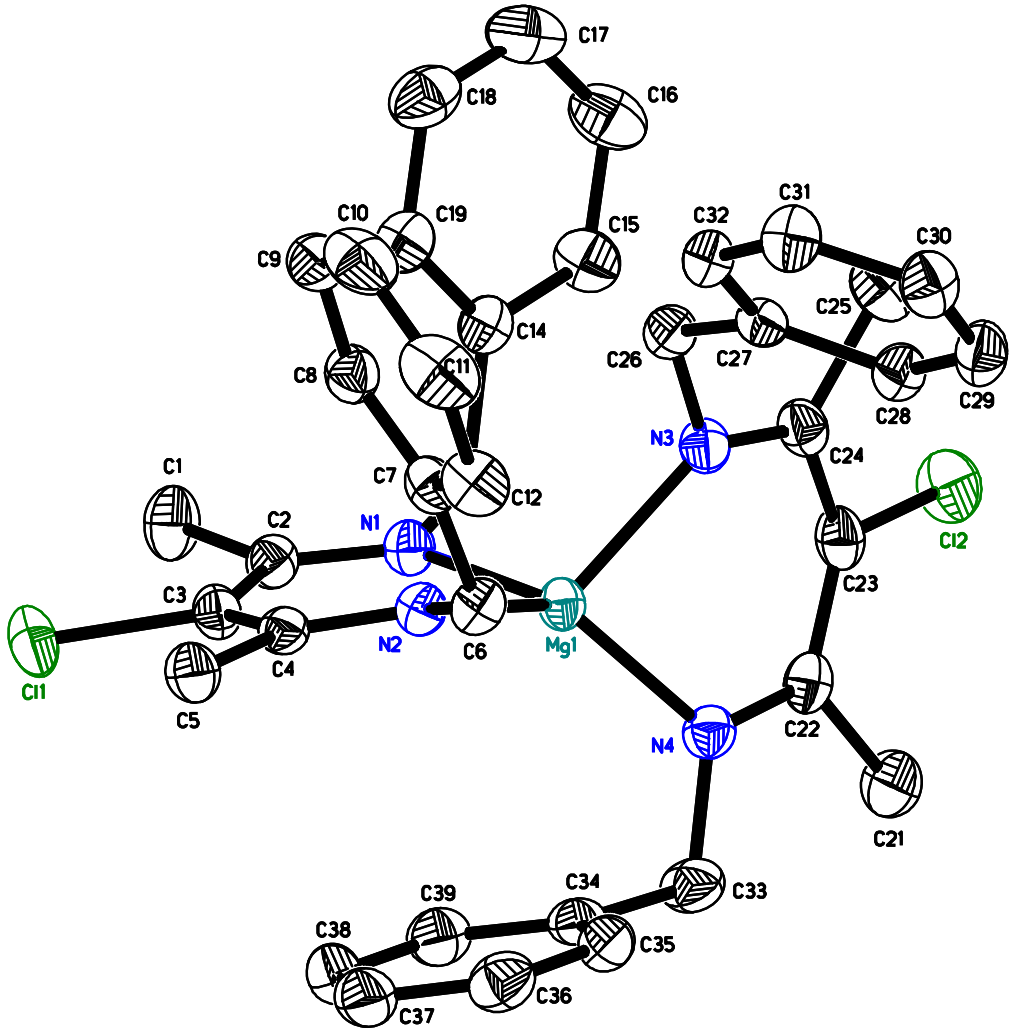

Figure 2.7 X-ray structure of **2.6f**. Hydrogen atoms omitted for clarity. Thermal ellipsoids are drawn at 50% probability. Mg1-N1: 2.023(1) Å, Mg1-N2: 2.024(1) Å, Mg1-N3: 2.038(1) Å, Mg1-N4: 2.045(1) Å, N1-Mg1-N2: 90.39(5)°, N3-Mg1-N4: 89.93(5)°.

Table 2.3 Geometric impact of a chlorine substituent at the diketiminate C_β atom

	2.6f	**2.8f**	(*nacnac*^{Bn})$_2$Mg [8a]	**2.6e**	**2.3** [8a]
Mg-N	2.03(1) Å	2.07(1) Å	2.04(1) Å	2.037(2) Å	2.041(3)
Mg-C_N	2.98(6) Å	3.05(5) Å	3.02(2) Å	2.95 Å	3.01 – 3.06 Å
C_β-C_α-C_{Me}	118° – 119°	117° – 119°	114° – 116°	118°	115°
N-Mg-N	90°	88°	94°	92°	94°
C_N-C_β-C_N	95° – 96°	97° – 98°	100°	97°	99°
N-C_β-N	74°	73° – 74°	76°	75°	76°

Errors are standard deviations of the average of equivalent bond lengths or angles, not experimental uncertainties. C_N: benzylic carbon atom; C_β: central carbon atom of the ligand backbone; C_{Me}: diketiminate methyl group

Although heteroleptic **2.6d** could not be isolated from the obtained product mixtures, use of excess Mg[N(SiMe$_3$)$_2$]$_2$ favoured its formation sufficiently for NMR characterization. The alkoxide complex **2.6e** was obtained by addition of *tert*-butanol to a 1:1 mixture of **2.6a** and Mg[N(SiMe$_3$)$_2$]$_2$. The crystal structure of **2.6e** shows the expected dimeric structure with the Mg atom in a tetrahedral environment (Fig 2.8). Contrary to its non-chlorinated analog **2.3**,[8a] the *meso*-rotamer is observed in the solid state, with both *N*-benzyl substituents on the same side of the ligand plane. The *syn*-orientation of the benzyl substituents results in a smaller distortion of the tetrahedral coordination geometry around Mg than in **2.3**, where the benzyl groups are found in the *anti*-orientation of the *C*$_2$-symmetric rotamer (angle of the MgN$_2$ and MgO$_2$ mean planes: **2.6e**: 87°, **2.3**: 80°). In other aspects, **2.6e** is very similar to **2.3**, with the same minor steric impact of the chlorine substituent as discussed for **2.6f** (Table 2.3).

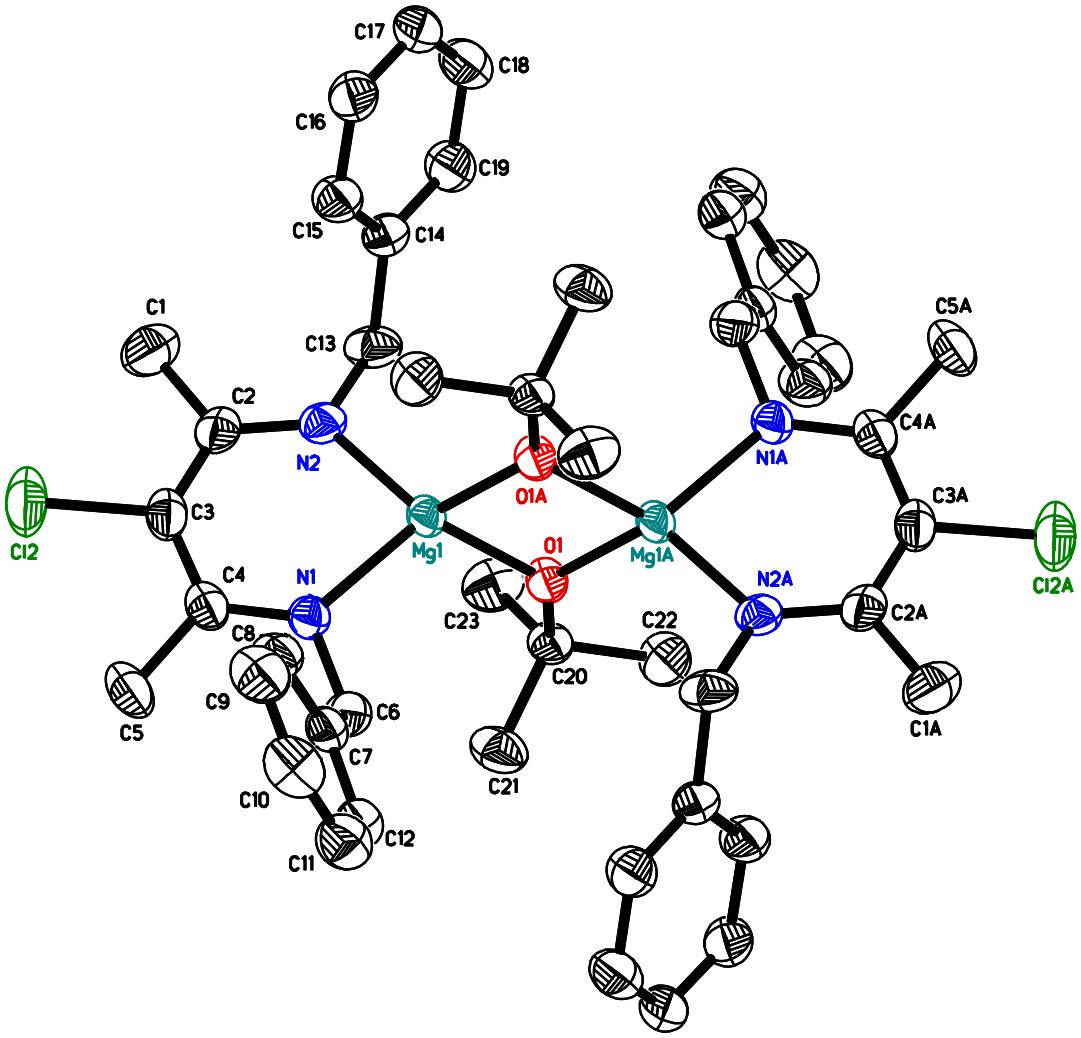

Figure 2.8 X-ray structure of **2.6e**. Hydrogen atoms omitted for clarity. Thermal ellipsoids are drawn at 50% probability. Bond distances/Å: Mg1-N1: 2.035(2), Mg1-N2: 2.038(2), Mg1-O1: 1.952(2), Mg1-O1A: 1.964(2), Mg1-Mg1A: 2.915(1). Bond angles/deg: N1-Mg1-N2: 91.92(8), O1-Mg1-O1A: 83.79(7), N1-Mg1-O1: 125.38(8), N1-Mg1-O1A: 116.45(8), N2-Mg1-O1: 122.26(8), N2-Mg1-O1A: 120.25(8).

Reactions of **2.8a** with magnesium amide mirror the reactivity observed for the non-chlorinated analog **2.5a** in that preparation of the amide complex **2.8d** was straightforward, but we were unable to obtain an isolable alkoxide complex (Scheme 2.6). The X-ray structure of **2.8d** (Fig 2.9) suffered from weak diffraction intensities and the presence of two independent molecules, one of which was severely disordered. We thus refrain from a detailed discussion of the structure, which is overall very similar to that of **2.5d**. A single crystal of the homoleptic bis(diketiminate) complex, (Cl-*nacnac*^{An})$_2$Mg, **2.8f**, was obtained as a minor byproduct with clearly different morphology in one recrystallization of **2.8d**. The

structure of **2.8f** (Fig 2.10) shows π-stacking interactions between the anthryl moiety and the chloro-diketiminate backbone for two anthrylmethyl substituents, while the remaining two are in a coplanar arrangement with each other. Mg-N bond distances in **2.8f** are slightly longer by 0.04° and N-Mg-N bite angles are slightly smaller by 2° than in the respective *N*-benzyl complex **2.6f** (Table 2.3), indicating some small increase in steric bulk. It should be noted, however, that replacing phenyl by anthryl seems to have only a minor steric impact, comparable to that of chlorination of the β-position.

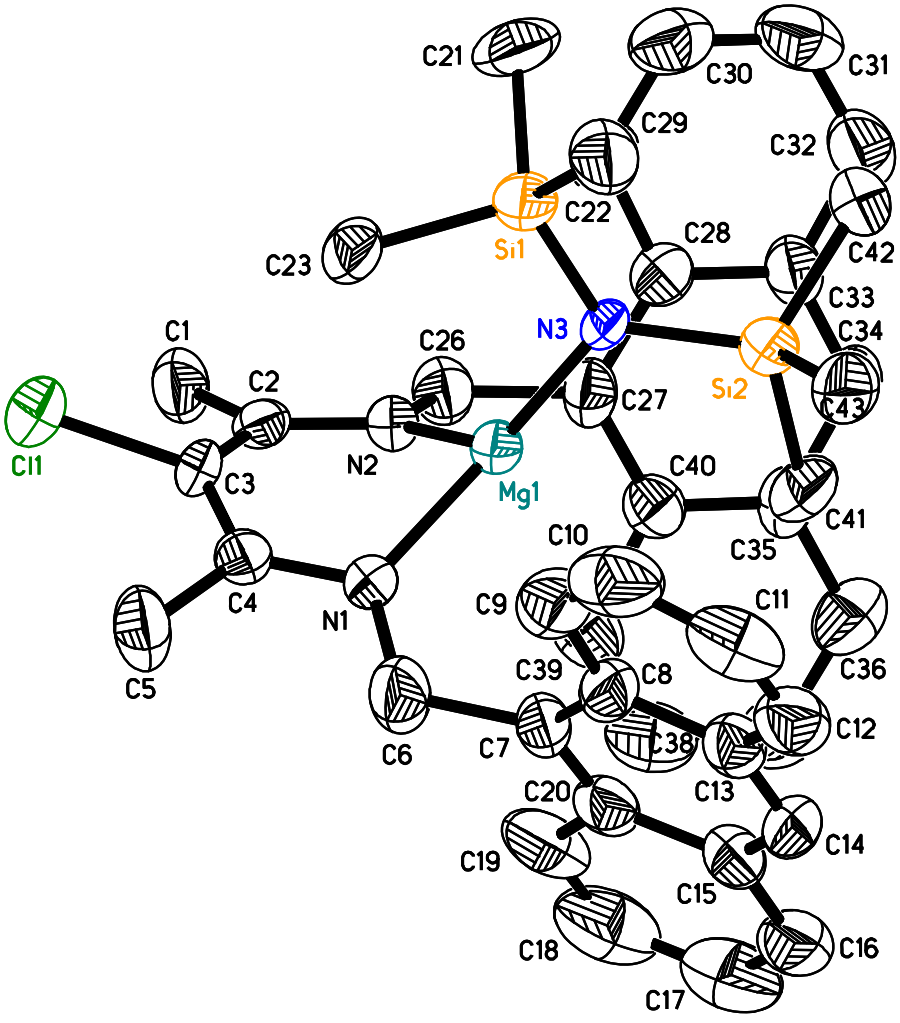

Figure 2.9 X-ray structure of **2.8d**. Hydrogen atoms and the second, strongly disordered molecule in the unit cell omitted for clarity. Thermal ellipsoids are drawn at 50% probability. Bond distances/Å: Mg-N1/N2/N4N5: 2.008(4) – 2.027(4), Mg-N3/6: 1.968(4)/ 1.960(4). Bond angles/deg: N1/4-Mg-N2/5: 91.90(17)/91.98(17), N1/2/4/5-Mg-N3/6: 128.28(17) – 131.49(16).

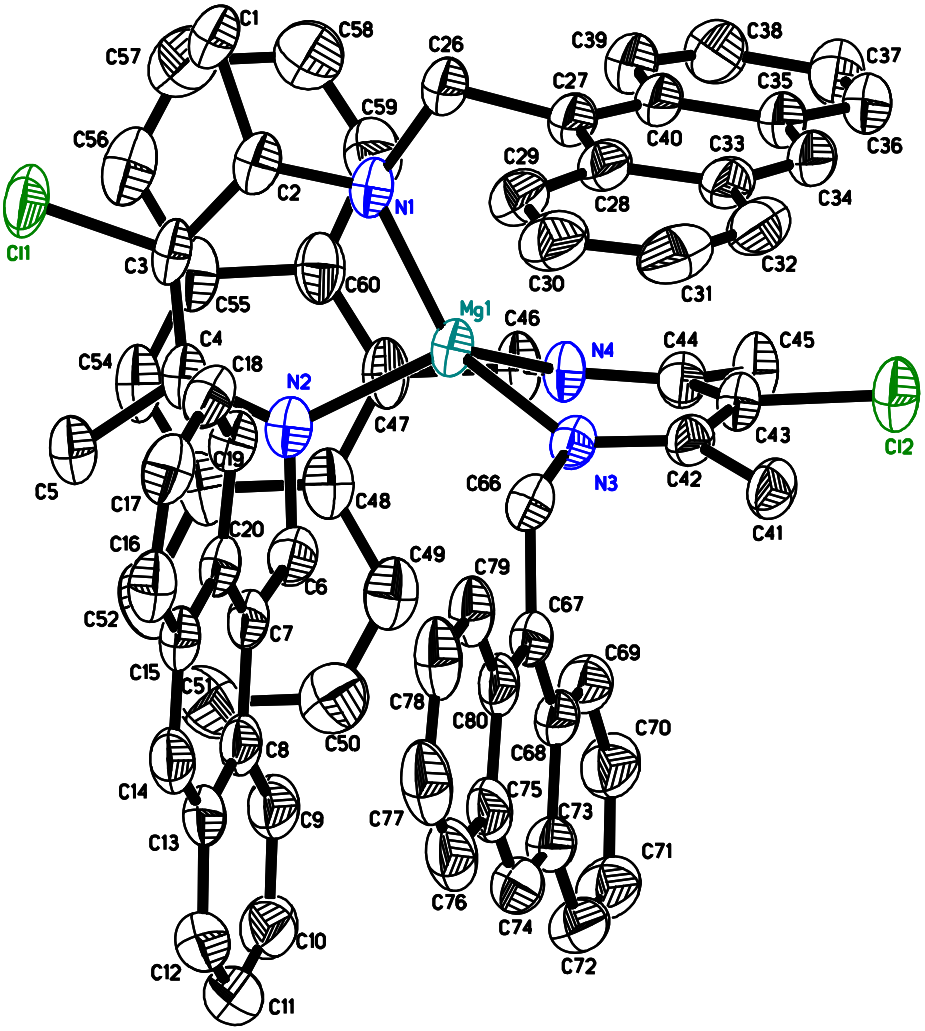

Figure 2.10 X-ray structure of **2.8f**. Hydrogen atoms omitted for clarity. Thermal ellipsoids are drawn at 50% probability. Bond distances/Å: Mg-N: 2.065(2) – 2.076(2). Bond angles/deg: N1-Mg1-N2: 88.04(7), N3-Mg1-N4: 87.20(7), N_{Lig1}-Mg1-N_{Lig2}: 108.30(8) – 128.65(7).

In the absence of an isolable alkoxide complex, lactide polymerization was again performed with the amide complex **2.8d** in the presence of benzyl alcohol. An activity lower than that of **2.5d**/BnOH, significant catalyst decomposition and an uninteresting P_r-value of 0.48 were observed (Table 2.2, #15; Fig S2.9). Polymerizations with **2.8d**/BnOH were thus not investigated further. Complex **2.6e**, on the

other hand, was very active in lactide polymerization, reaching conversions above 70 – 80% after 10 min (Table 2.2, #12-#14). As for **2.3**, a notable induction period was observed in conversion vs. time plots which, accompanied by increased polydispersities, indicated slow initiation through insertion into the Mg-O*t*Bu bond (Fig S2.10). Addition of benzyl alcohol removed the induction period and reduced polydispersities to 1.0 – 1.2 (Fig S2.10). However, observed activities, number of polymer chains obtained per Mg and final conversions varied widely, the latter being as low as 30%. This indicates that *tert*-butanol, liberated by reaction with BnOH, remained active as a chain transfer reagent and that catalyst decomposition occurs in the presence of free alcohol. Side reactions can be suppressed by lowering the polymerization temperature to –30 °C, yielding reproducible results, polydispersities of 1.1 and only one polymer chain per metal centre.

While **2.6e**, as **2.3**, has a slight heterotactic bias at room temperature (P_r = 0.54), addition of benzyl alcohol inexplicably reduced the P_r value to 0.46 – 0.49. Chain-transfer reactions due to the free alcohol present should not affect stereoselectivity in the case of a highly flexible ligand. However, catalyst decomposition (indicated by the lack of complete conversion) might yield species which are polymerization-active, but lack the slight heterotacticity of **2.6e**. Alternatively, decomposition products might be capable to catalyze transesterification to a higher degree than **2.6e**, which would lower the apparent P_r, since the statistical method used for its calculation does not allow the presence of rr-triads.[8b] Lowering the polymerization temperature to –30 °C reduced P_r to 0.43, which is a slightly higher isotactic preference than observed for **2.3** under the same conditions (P_r = 0.46). Since chain transfer and catalyst decomposition are absent at this temperature, this reflects a small, but reproducible isotactic preference of **2.6e**, the highest observed so far for a diketiminate complex.

Conclusions

Despite the minor changes undertaken in the steric and electronic environment of *N*-alkyl Zn and Mg diketiminate complexes, clear structure-reactivity relationships cannot be drawn. Replacing phenyl by anthryl increased heterotacticity in Zn complexes, but did not affect activity. In the respective Mg

complexes, on the other hand, ring-annulation or ortho-substitution of the *N*-benzyl substituent significantly increased reactivities, but had no or only minor effects on polymer tacticity. Chlorination of the C_β position slightly and reproducibly reduced the P_r value of Zn and Mg complexes with *N*-benzyl substituents by 3-4%, but did not affect complexes with *N*-anthrylmethyl substituents. Given the high preference of diketiminate zinc complexes for heterotactic monomer enchainment in general, which was also found for *N*-alkyl diketiminate ligands, it seems unlikely that even major changes in a diketiminate ligand would lead to an "isotactic" Zn-based catalyst. The isotactic preference observed for **2.3** increased slightly in the chlorinated analogue **2.6e** which supports an isoselective mechanism operating in *rac*-lactide polymerizations with *N*-alkyl diketiminate magnesium complexes. However, to increase this stereoselectivity to notable levels more drastic variations of the ligand framework will be required.

Experimental Section

General. All reactions were carried out using Schlenk and glove box techniques under a nitrogen atmosphere. *Nacnac*^{Bn}H was prepared according to literature,[12, 20] as was (9-anthryl)methylamine,[21] acetyl acetone ethylene glycol monoketal,[14b] and $Zn(N(SiMe_3)_2)_2$.[22] Solvents were dried by passage through activated aluminum oxide (MBraun SPS), de-oxygenated by repeated extraction with nitrogen, and stored over molecular sieves. C_6D_6 was dried over sodium and degassed by three freeze-pump-thaw cycles. $CDCl_3$ and CD_2Cl_2 were dried over 3 Å molecular sieves. *rac*-Lactide (98%) was purchased from Sigma–Aldrich, purified by 3x recrystallization from dry ethyl acetate and kept at –30 °C. All other chemicals were purchased from common commercial suppliers and used without further purification. ^{1}H and ^{13}C NMR spectra were acquired on a Bruker AVX 400 spectrometer. The chemical shifts were referenced to the residual signals of the deuterated solvents (C_6D_6: ^{1}H: d 7.16 ppm, ^{13}C: d 128.38 ppm, $CDCl_3$: ^{1}H: d 7.26 ppm, CD_2Cl_2: 1H: d 5.32 ppm). Elemental analyses were performed by the Laboratoire d'analyse élémentaire (Université de Montréal). Molecular weight analyses were performed on a Waters 1525 gel permeation chromatograph equipped with three Phenomenex columns and a refractive index detector at 35 °C. THF was used as the eluent at a flow rate of 1.0 mL·min^{-1} and polystyrene standards (Sigma–

Aldrich, 1.5 mg·mL^{-1}, prepared and filtered (0.2 mm) directly prior to injection) were used for calibration. Obtained molecular weights were corrected by a Mark-Houwink factor of 0.58.[23]

***N,N'*-di(9-anthrylmethyl)-2-amino-4-imino-2-pentene, *nacnac*^{An}H, 2.5a.** In a sealed vessel acetylacetone ethylene glycol monoketal (0.70 g, 4.39 mmol) and (9-anthryl)methylamine (1.82 g, 8.79 mmol) were added. The vessel was closed and stirred at 110 ºC for 4 hours or until the mixture had completely solidified. The solid was washed with cold diethyl ether, dried under reduced pressure and used for without further purification (1.30 g, 62%, 90% purity according to NMR).

^{1}H NMR (400 MHz, C_6D_6): δ 11.70 (s, 1H, NH), 7.88 (s, 2H, Ar), 7.68 (m, 8H, Ar), 7.09 (m, 4H, Ar), 6.81 (m, 4H, Ar), 4.73 (s, 5H, CH, NCH_2), 1.86 (s, 6H, CH_3). ^{13}C{^{1}H} NMR (100 MHz, C_6D_6): 194.3 (C=N), 131.5 (Ar), 131.2 (Ar), 130.1 (Ar), 128.0 (Ar), 127.3 (Ar), 125.2 (Ar), 124.5 (Ar), 124.4 (Ar), 94.9 (H*C*$(CN)_2$), 43.4 (NCH_2), 19.8 (Me). EI-HR-MS (*m*/*z*): calcd. for $C_{35}H_{30}N_2$ $[M+H]^+$: 479.2482; found: 479.2485.

The main contamination was the monocondensation product 4-(9-anthryl)methylamino-3-penten-2-one, *acnac*^{An}H, which was also the main product in unsuccessful condensation attempts described in the text. ^{1}H-NMR ($CDCl_3$, 400 MHz): δ 10.97 (s, 1H, NH), 8.48 (s, 1H, Ar), 8.20 (m, 2H, Ar), 8.01 (m, 2H, Ar), 7.57 (m, 2H, Ar), 7.48 (m, 2H, Ar), 5.37 (d, 2H, NCH_2), 5.05 (s, 1H, CH), 2.29 (s, 1H, CH_3), 1.90 (s, 1H, CH_3). ^{13}C{^{1}H} NMR (100 MHz, $CDCl_3$): 195.1 (C=O), 162.2 (C=N), 131.7 (Ar), 130.4 (Ar), 129.5 (Ar), 128.7 (Ar), 127.4 (Ar), 126.9 (Ar), 125.2 (Ar), 123.5 (Ar), 95.7 (H*C*CN), 39.8 (NCH_2), 28.9 (Me), 19.8 (Me). Anal. Calcd. for $C_{20}H_{19}NO$: C, 83.01; H, 6.62; N, 4.84. Found: C, 82.84; H, 6.54; N, 4.80.

***nacnac*^{An}ZnN(SiMe$_3$)$_2$, 2.5b. 2.5a** (0.34g, 0.71 mmol) was added to a solution of Zn(N(SiMe$_3$)$_2$)$_2$ (0.27 g, 0.71 mmol) in toluene or hexane in the glove box, forming a suspension. Stirring was continued for 4 days or until the mixture became homogeneous. Solvent and formed amine were removed under reduced pressure. The crude solid can be used in further reaction without purification. Recrystallization from toluene yielded analytically pure, colourless crystals (0.38 g, 76%).

^{1}H NMR (400 MHz, C_6D_6): 8.33 (s, 2H, Ar), 8.20(m, 8H, Ar), 7.91(m, 4H, Ar), 7.37(m, 4H, Ar), 5.54(s, 4H, NCH_2), 4.41(s, 1H, CH), 1.71 (s, 6H, Me), -0.59(s, 18H, $SiMe_3$). $^{13}C\{^1H\}$ NMR (100 MHz, C_6D_6): 169.5 (C=N), 131.9 (Ar), 131.7 (Ar), 130.4 (Ar), 129.4 (Ar), 127.9 (Ar), 126.0 (Ar), 124.9 (Ar), 124.8 (Ar), 96.2 (H*C*$(CN)_2$), 48.7 (NCH_2), 24.7 (Me), 4.6 ($SiMe_3$). Anal. Calcd. for $C_{41}H_{47}N_3Si_2Zn$: C, 70.01; H, 6.74; N, 5.97. Found: C, 69.72; H, 6.57; N, 5.73.

***nacnac*^{An}ZnO*i*Pr·CH_2Cl_2, 2.5c.** To a solution of **2.5b** (0.38 g, 0.54 mmol) in toluene (5 mL), isopropanol (41 μL, 0.54 mmol) was added and allowed to react for 3 hr during which time a white precipitate appeared. The solvent was removed under reduced pressure, yielding the crude product as a white solid. Purification was carried out by recrystallisation in dichloromethane (0.11 g, 34%).

^{1}H NMR (400 MHz, $CDCl_3$): 8.35 (m, 4H, Ar), 8.22(s, 2H, Ar), 7.82(m, 4H, Ar), 7.25 (m, 8H, Ar), 5.37 (s, 4H, NCH_2), 4.12 (s, 1H, CH), 3.89 (sept., 1H, C*H*Me_2), 1.39 (s, 6H, Me), 1.07 (d, 6H, CH*Me*$_2$). $^{13}C\{^1H\}$ NMR (100 MHz, $CDCl_3$): 169.4 (C=N), 133.4 (Ar), 131.6 (Ar), 130.3 (Ar), 129.1 (Ar), 127.1 (Ar), 125.6 (Ar), 125.4 (Ar), 124.7 (Ar), 94.3 (H*C*$(CN)_2$), 53.6 (*C*HMe_2), 49.5 (NCH_2), 28.1 (Me), 24.7 (Me). Anal. Calcd. for $C_{38}H_{36}N_2OZn·CH_2Cl_2$: Anal. Calcd. for $C_{38}H_{36}N_2OZn$ (CH_2Cl_2): C, 68.18; H, 5.57; N, 4.08. Combustion Analysis, found: C, 68.08; H, 5.29; N, 4.10. (One equivalent of dichloromethane per Zn was also observed in the crystal structure of **2.5c**.)

***nacnac*^{An}MgN$(SiMe_3)_2$, 2.5d. 2.5a** (1.07 g, 2.2 mmol) was added to a solution of $Mg(N(SiMe_3)_2)_2$ (0.86g, 2.5 mmol) in toluene or hexane, forming a suspension. The mixture was allowed to stir overnight, after which solvent and formed amine were removed under reduced pressure. The crude solid could be used either directly for further reactions or recrystallized from toluene (colourless crystals, 1.21 g, 82%).

^{1}H NMR (400 MHz, C_6D_6): δ 8.27 (d, 4H, Ar), 8.11 (s, 2H, Ar), 7.76 (d, 4H, Ar), 7.27 (8H, Ar), 5.25 (s, 4H, NCH_2), 4.69 (s, 1H, CH), 1.83(s, 6H, (NC)Me), -0.50 (s, 18H, $SiMe_3$). $^{13}C\{^1H\}$ NMR (100 MHz, C_6D_6): δ 170.2 (C=N), 132.3 (Ar), 131.5 (Ar), 131.2 (Ar), 129.8 (Ar), 128.6 (Ar), 126.8 (Ar), 125.3 (Ar), 124.7 (Ar), 95.8 (CH), 47.9 (NCH_2), 24.1 ((NC)Me), 4.4 ($SiMe_3$). Anal. Calcd. for $C_{41}H_{47}MgN_3Si_2$: C, 74.35; H, 7.15; N, 6.34. Found C, 74.45; H, 7.25; N, 6.20.

***nacnac*^{An}MgO*t*Bu, 2.5e.** A solution of **2.5d** in C_6D_6 was slowly titrated with a solution of *tert*-butanol in C_6D_6. After addition of 0.25 equiv the solution contained **2.5d** and **2.5e**. ^{1}H NMR (C_6D_6, 400 MHz): δ 8.82 (d, 4H Ar), 8.24 (d, 4H Ar), 8.20 (s, 2H Ar), 8.10 (s, 2H Ar), 7.82 (d, 4H Ar), 7.76 (d, 4H Ar), 5.80 (s, 4H, NCH_2), 4.43 (s, 1H, CH), 1.53 (s, 6H, (NC)Me), 1.10 (s, 9H, $OCMe_3$). Further addition of *tert*-butanol led to the formation of the ligand **2.5a** and unidentified side-products.

***N,N'*-dibenzyl-2-amino-3-chloro-4-imino-2-pentene, Cl*nacnac*^{Bn}H, 2.6a.** To a solution of *nacnac*^{Bn}H (5.48 g, 19.7 mmol) in dry THF (150 mL) was added *N*-chlorosuccinimide (3.00 g, 22.4 mmol). After stirring at room temperature for 45 minutes, a white precipitate formed which was removed by filtration. H_2O (500 mL) was then added. The product was extracted using hexanes (2 x 600 mL). After drying over Na_2SO_4 the solvent was evaporated. The obtained yellow oil was crystallized from dry ethanol at –80 °C, washed with cold dry ethanol and recrystallized from refluxing ethanol. The eluate yielded a second fraction at –80 °C (colourless crystals, 3.41 g, 55%).

^{1}H-NMR ($CDCl_3$, 400 MHz, 298 K): δ 12.22 (bs, 1H, NH), 7.25-7.19 (m, 10H, Ph), 4.49 (s, 4H, NCH_2), 2.18 (s, 6H, Me). ^{13}C{^{1}H} NMR ($CDCl_3$, 75 MHz, 298 K): δ 160.3 (*C*=N), 140.5 (*ipso* Ph), 128.6 (*ortho* or *meta* Ph), 127.3 (*ortho* or *meta* Ph), 126.8 (*para* Ph), 127.7 (ClC), 51.5 (NCH_2), 17.3 (Me). Anal. Calcd. for $C_{19}H_{21}ClN_2$: C, 72.95; H, 6.77; N, 8.95. Found C, 72.89; H, 6.66; N, 9.17.

Cl*nacnac*^{Bn}ZnO*i*Pr, 2.6c. $Zn(N(SiMe_3)_2)_2$ (0.86 g, 2.2 mmol) was added to a solution of **2.6a** (0.70 g, 2.2 mmol) in toluene (30 mL) over 5 min. The solvent was removed under reduced pressure, yielding Cl*nacnac*^{Bn}ZnN($SiMe_3$)$_2$, **2.6b**, as an orange oil (1.25g, 2.21 mmol, ^{1}H NMR (400 MHz, C_6D_6): 7.22-7.14 (m, 10H, Ph), 4.85 (s, 4H, NCH_2), 2.21 (s, 6H, Me(C=N)$_2$), 0.20 (s, 18H, $SiMe_3$).

Toluene (30 mL), followed by isopropanol (0.13 g, 2.20 mmol) were added. After 5 min of stirring, a white precipitate formed, which was isolated by filtration and washed with toluene (15 mL). 0.30 g, 26%.

^{1}H NMR (400 MHz, C_6D_6): δ 7.16-7.05 (m, 10H, Ph), 4.57 (s, 4H, NCH_2), 3.85 (sep., 1H, OC(*H*)Me$_2$), 2.11 (s, 6H, Me(C=N)$_2$), 0.96 (d, 6H, OC(H)*Me*$_2$). ^{13}C{^{1}H} NMR (75 MHz, C_6D_6): δ 169.5 (C=N), 140.6 (Ph), 128.3 (Ph), 126.5 (Ph), 126.4 (Ph), 101.2 (Cl*C*), 66.2 (O*C*HMe$_2$ or NCH_2), 55.0 (O*C*HMe$_2$ or

NCH_2), 27.9 (Me) 20.8 (Me). Anal. Calcd. for $C_{22}H_{27}ClN_2OZn$: C, 60.56; H, 6.24; N, 6.42. Found C, 60.10; H, 6.21; N, 6.35.

Cl*nacnac*^{Bn}MgO*t*Bu, 2.6e. To a solution of **2.6a** (0.100 g, 0.32 mmol) in dry THF (6 mL), $Mg(N(SiMe_3)_2)_2$ (0.110 g, 0.32 mmol) was added. The yellow-golden solution was stirred overnight followed by solvent evaporation under reduced pressure yielding a yellow solid; identified as a mixture of Cl*nacnac*^{Bn}MgO*t*Bu, **2.6d**, and (Cl*nacnac*^{Bn})$_2$Mg, **2.6f.** After re-dissolution in THF (6 mL), *tert*-butanol (0.024 g, 0.32 mmol) was added. The reaction mixture was stirred for 3 hours. Evaporating the solvent yielded a yellow solid, which was washed with hexane and dried under reduced pressure. Recrystallization from CH_2Cl_2/hexane at room temperature afforded colourless crystals after 24 h (0.04 g, 33%).

^{1}H-NMR (C_6D_6, 400 MHz): δ 7.35-6.95 (m, 10H, Ph), 4.68 (s, 4H, NCH_2), 2.19 (s, 6H, (NC)Me), 0.91 (s, 9H, $OCMe_3$). $^{13}C\{^1H\}$ NMR (100 MHz, C_6D_6): δ 170.6 (*C*=N), 141.0 (*ipso* Ph), 128.7 (*ortho* or *meta* Ph), 128.1 (*ortho* or *meta* Ph), 127.8 (*para* Ph), 126.7 (CCl), 67.5 (O*C*Me$_3$), 53.5 (NCH_2), 33.8 (OC*Me*$_3$), 20.9 ((NC)*Me*). Anal. Calcd. for $C_{23}H_{29}ClMgN_2O$: C, 67.50; H, 7.14; N, 6.85. Found C, 66.28; H, 7.28; N, 6.74.

(Cl*nacnac*^{Bn})$_2$Mg, 2.6f. To a solution of **2.6a** (0.100 g, 0.32 mmol) in dry toluene (5 mL), $Mg(N(SiMe_3)_2)_2$ (0.055 g, 0.16 mmol) was added. The yellow-golden solution was stirred overnight. After evaporation of the solvent, the product, a bright solid, was identified by NMR spectroscopy. The obtained solid was re-dissolved in a minimum of toluene and crystallized at -35 °C to yield yellow crystals (0.09 g, 91%).

^{1}H-NMR (C_6D_6, 400 MHz): δ 7.28-6.89 (m, 20H, Ph), 4.15 (s, 8H, NCH_2), 2.05 (s, 12H, Me). $^{13}C\{^1H\}$ NMR (100 MHz, C_6D_6): δ 169.3 (C=N), 140.9 (*ipso* Ph), 128.5 (*ortho*/*meta* Ph), 128.1 (*ortho*/*meta* Ph), 126.8 (*para* Ph), 126.6 (CCl), 53.3 (NCH_2), 20.1 (Me). Anal. Calcd. for $C_{38}H_{40}Cl_2MgN_4$: C, 70.44; H, 6.22; N, 8.65. Found C, 70.33; H, 6.37; N, 8.48.

***N,N'*-di(mesitylmethyl)-2-amino-4-imino-2-pentene, *nacnac*^{Mes}H, 2.7a.** In a sealed vessel with a stir bar, acetylacetone ethylene glycol monoketal (0.19 g, 1.68 mmol) and mesitylmethylamine (0.5 g, 3.35

mmol) were added along with activated 3Å molecular sieve. The vessel was closed and heated to 110 ºC for 4 hours or until the reaction had completely solidified. The solid product was dissolved in ethanol and crystallized (0.32 g, 52%).

^{1}H NMR (400 MHz, C_6D_6): 11.17 (s, 1H, NH), 6.72 (s, 4H, Ar), 4.63 (s, 1H, CH), 4.10 (s, 4H, NCH_2), 2.28 (s, 6H, ArCH_3), 2.00 (s, 12H, ArCH_3), 1.80 (s, 6H, CH_3). ^{13}C{^{1}H} NMR (100 MHz, C_6D_6): 159.9 (C=N), 136.8 (*ipso* Mes), 135.5 (*ortho/meta* Mes), 134.3 (*ortho/meta* Mes), 129.2 (*para* Mes), 94.7 (H$C(CN)_2$), 44.9 (NCH_2), 21.2 (Me), 19.5 (Me), 19.4 (Me). Anal. Calcd. for $C_{25}H_{42}N_2$: C, 82.82; H, 9.45; N, 7.73. Found C, 82.84; H, 9.46; N, 7.89.

***nacnac*^{Mes}MgN(SiMe$_3$)$_2$, 2.7d.** Following the procedure described for **2.5d**, **2.7a** (0.30 g, 0.83 mmol), $Mg(N(SiMe_3)_2)_2$ (0.29 g, 0.83 mmol) to yield colourless crystals (0.17 g, 37%).

^{1}H NMR (400 MHz, C_6D_6): δ 6.74 (s, 4H, Ar), 4.64 (s, 1H, CH), 4.28 (s, 4H, NCH_2), 2.28 (s, 6H, CN)Me), 2.09 (s, 12H, ArMe), 1.80 (s, 6H, ArMe) 0.00 (s, 18H, $SiMe_3$). ^{13}C{^{1}H} NMR (75 MHz, C_6D_6): δ 169.7 (C=N), 137.1 (Ar), 137.0 (Ar), 134.3 (Ar), 130.4 (Ar), 95.1 (CH), 48.8 (NCH_2), 23.4 (Me), 20.9 (Me), 20.7 (Me), 4.6 ($SiMe_3$). Anal. Calcd. for $C_{31}H_{51}MgN_3Si_2$: C, 68.16; H, 9.41; N, 7.69. Found .23 ; H, 9.50; N, 7.70.

***nacnac*^{Mes}MgO*t*Bu·½CH$_2$Cl$_2$, 2.7e.** As in **2.5c**, substituting **2.5b** for **2.7d** (0.13 g, 0.24 mmol), isopropanol for *tert*-butanol (23 μL, 0.24 mmol) colourless crystals (0.72 mg, 66%) after recrystallization from dichloromethane.

^{1}H-NMR (400 MHz, C_6D_6): δ 6.82 (s, 4H, Ar), 4.85 (s, 4H, NCH_2), 4.67 (s, 1H, CH), 2.48 (s, 12H, Ar*Me*), 2.16 (s, 6H, (CN)Me), 1.82 (s, 6H, Ar*Me*), 1.06 (s, 9H, $OCMe_3$). ^{13}C{^{1}H} NMR (100 MHz, C_6D_6): δ 169.9 (C=N), 136.5 (*ipso* Mes), 135.7 (*ortho/meta* Mes), 135.3 (*ortho/meta* Mes), 130.5 (*para* Mes), 80.9 (CH), 67.2 (O$C(CH_3)_3$), 44.9 (NCH_2), 33.1 (Me, *ortho*), 23.5 (Me, *para*), 21.6 (OC*Me*$_3$), 20.9 (NC*Me*). Anal. Calcd. for $C_{29}H_{42}MgN_2O·½CH_2Cl_2$: C, 70.66; H, 8.64; N, 5.59. Found 69.65; H, 8.68; N, 5.68. (Half an equivalent of CH_2Cl_2 per Mg was observed in the crystal structure.)

***N,N'*-di(9-anthrylmethyl)-2-amino-3-chloro-4-imino-2-pentene, Cl*nacnac*^{An}H, 2.8a.** To a solution of **2.5a** (1.00 g, 2.1 mmol) in dry THF (40 mL) was added *N*-chlorosuccinimide (0.30 g, 2.3 mmol). After

stirring at room temperature for 45 minutes, a white precipitate formed which was removed by filtration. Water was then added. The product was extracted using dichloromethane (2 x 10 mL) and dried over Na_2SO_4. Evaporation of the solvent yielded a yellow oil which was crystallized from dry dichloromethane (0.45 g, 42%).

^{1}H NMR (400 MHz, C_6D_6): 12.32 (s, 1H, NH), 7.76 (s, 2H, Ar), 7.56 (m, 8H, Ar), 7.06 (m, 4H, Ar), 6.87 (m, 4H, Ar), 4.57 (s, 5H, CH, NCH_2), 2.12 (s, 6H, Me). $^{13}C\{^1H\}$ NMR (100 MHz, C_6D_6): 159.6 (C=N), 131.1 (Ar), 129.8 (Ar), 129.1(Ar), 127.5 (Ar), 125.3 (Ar), 125.1 (Ar), 124.4 (Ar), 124.0 (Ar), 100.6 (CCl), 44.1 (NCH_2), 17.2 (Me). Anal. Calcd. for $C_{35}H_{29}ClN_2$: C, 81.93; H, 5.70; N, 5.46. Found C, 81.73; H, 5.70; N, 5.47.

Cl*nacnac*^{An}MgN(SiMe$_3$)$_2$, 2.8d. Following the procedure described for **2.5d**, **2.5a** (0.12g, 0.23 mmol), $Mg(N(SiMe_3)_2)_2$ (0.08 g, 0.23 mmol), (crude 0.14 g, 87%) colourless crystals (0.05 g, 28%).

^{1}H NMR (400 MHz, C_6D_6): δ 8.13 (s, 2H, Ar), 8.10 (d, 4H, Ar), 7.75 (d, 4H, Ar), 7.31-7.21 (m, 8H, Ar), 5.16 (s, 4H, NCH_2), 2.31 (s, 6H, (NC)Me), -0.57 (s, 18H, $SiMe_3$). $^{13}C\{^1H\}$ NMR (100 MHz, C_6D_6): δ 169.3 (C=N), 132.2 (Ar), 131.2 (Ar), 130.5 (Ar), 129.9 (Ar), 129.1 (Ar), 127.0 (Ar), 125.4 (Ar), 124.4 (Ar), 102.4 (Cl*C*$(CN)_2$), 48.9 (NCH_2), 21.4 (Me), 4.4 ($SiMe_3$). Anal. Calcd. for $C_{41}H_{46}ClMgN_3Si_2$: C, 70.68; H, 6.65; N, 6.03. Found C, 71.27; H, 6.47; N, 5.71.

X-ray diffraction studies. Single crystals were obtained as described in table S4. Diffraction data were collected with Cu Kα radiation on a Bruker Smart 6000 or a Bruker Microstar/Proteum, both equipped with Helios MX mirror optics and rotating anode sources, or on a Bruker Microsource/APEX2 using the APEX2 software package.[24] Data reduction was performed with SAINT,[25] absorption corrections with SADABS.[26] Structures were solved with direct methods (SHELXS97).[27] All non-hydrogen atoms were refined anisotropic using full-matrix least-squares on F^2 and hydrogen atoms refined with fixed isotropic U using a riding model (SHELXL97).[27] In **2.8f**, disordered solvent was found around the inversion centre (93 electrons/unit cell), but the best modeled solution remained 12% higher in wR_2 (with appr. twice as high errors in bond lengths) than the solution after application of SQUEEZE. No notable structural

difference was found between solutions and thus the latter was used. Further experimental details can be found in Table 2.4 and in the supporting information (CIF).

Table 2.4 Details of X-ray Diffraction Studies

	2.5b	**2.5c**	**2.5d**	**2.5f**	**2.6e**
Formula	$C_{41}H_{47}N_3Si_2Zn \cdot C_7H_8$	$C_{76}H_{72}N_4O_2Zn_2 \cdot 2\ CH_2Cl_2$	$C_{41}H_{47}MgN_3Si_2 \cdot 2\ CH_2Cl_2$	$C_{82}H_{68}Mg_2N_4O_2 \cdot 2.5\ CH_2Cl_2$	$C_{46}H_{58}Cl_2Mg_2N_4O_2$
M_w (g/mol); $d_{calcd.}$ (g/cm^3)	795.50; 1.246	1373.97; 1.387	747.23; 1.224	1402.33; 1.314	818.48; 1.236
Crystal size (mm)	0.15·0.15·0.18	0.27·0.27·0.36	0.16·0.09·0.09	0.18·0.14·0.11	0.14·0.14·0.14
T (K); F(000)	150; 1688	150; 716	200; 792	100; 1466	150; 872
Crystal System	Triclinic	Triclinic	Triclinic	Triclinic	Monoclinic
Space Group	P-1	P-1	P-1	P-1	$P2_1/c$
Unit Cell: a (Å)	13.0063(3)	11.8196(4)	11.4629(5)	14.4200(5)	9.1499(2)
b (Å)	15.7472(4)	12.4402(5)	12.8758(6)	16.6394(6)	22.1705(3)
c (Å)	20.9693(5)	12.4806(5)	14.0056(6)	17.0800(6)	10.8809(2)
α (°)	84.7981(11)	95.050(1)	92.665(3)	72.642(2)	
β (°)	86.8527(12)	115.269(2)	98.376(3)	73.431(2)	95.103(1)
γ (°)	83.0374(10)	92.814(1)	96.507(3)	67.467(2)	
V (Å^3); Z	4241.4(2); 4	1645.4(1); 1	2027.74(16); 2	3544.4(2); 2	2198.53(7); 2
θ range (°); completeness	2-73; 0.96	4-72; 0.95	3-73; 0.96	3-73; 0.96	4-73; 0.97
collected reflections; R_σ	56188; 0.026	21587; 0.021	26826; 0.070	47715; 0.039	28207; 0.038
unique reflections; R_{int}	16111; 0.034	6223; 0.035	7708; 0.089	13541; 0.035	4271; 0.072
μ (mm^{-1}); Abs. Corr.	1.246; multiscan	2.790; multiscan	2.402; multiscan	2.447; multiscan	1.926; multiscan
R1(F); wR(F^2) ($I > 2\sigma(I)$)	0.040; 0.114	0.054; 0.139	0.050; 0.144	0.049; 0.138	0.058; 0.155
R1(F); wR(F^2) (all data)	0.045; 0.118	0.055; 0.140	0.070; 0.153	0.062; 0.147	0.066; 0.183
GoF(F^2)	0.91	1.04	1.01	1.08	1.15
Residual electron density	1.08; -0.73	1.34; -1.44	0.71; -0.55	0.41; -0.42	0.47; -0.72

	2.6f	**2.7d**	**2.7e**	**2.8d**	**2.8f**
Formula	$C_{38}H_{40}Cl_2MgN_4$	$C_{31}H_{51}MgN_3Si_2$	$C_{29}H_{43}MgN_2O \cdot 0.5\ CH_2Cl_2$	$C_{41}H_{46}ClMgN_3Si_2$	$C_{70}H_{56}Cl_2MgN_4$
M_w (g/mol); $d_{calcd.}$ (g/cm^3)	647.9; 1.290	546.24; 1.111	501.42; 1.167	696.75; 1.228	1048.39; 1.224
Crystal size (mm)	0.18·0.16·0.16	0.14·0.11·0.07	0.15·0.15·0.15	0.06·0.06·0.06	0.13·0.08·0.08
T (K); F(000)	150; 1368	100; 1192	100; 2168	150; 1480	100; 1100
Crystal System	Monoclinic	Orthorhombic	Monoclinic	Triclinic	Triclinic
Space Group	$P2_1/c$	$Pnma$	$P2_1/n$	P-1	P-1
Unit Cell: a (Å)	14.5416(5)	17.4882(2)	15.0133(8)	10.256(1)	12.5041(8)
b (Å)	11.1177(4)	18.0767(2)	17.0252(9)	18.732(2)	14.3017(8)
c (Å)	20.7327(7)	10.3297(1)	22.8695(13)	20.538(2)	18.1609(10)
α (°)				74.418(4)	104.305(2)
β (°)	95.640(2)		102.436(2)	88.915(4)	109.464(2)
γ (°)				82.638(4)	100.227(2)
V (Å^3); Z	3335.6(2); 4	3265.52(6); 4	5708.4(5); 8	3768.6(6); 4	2844.6(3); 2
θ range (°); completeness	3-73; 0.97	5-72; 0.98	3-72; 0.99	3-57; 0.97	3-58; 0.98
collected reflections; R_σ	40209; 0.021	45504; 0.011	80320; 0.026	10043; 0.142	52174; 0.046
unique reflections; R_{int}	6473; 0.037	3233; 0.025	11142; 0.042	4485; 0.112	7765; 0.029
μ (mm^{-1}); Abs. Corr.	2.185; multiscan	1.334; multiscan	1.567; multiscan	1.913; multiscan	1.484; multiscan
R1(F); wR(F^2) ($I > 2\sigma(I)$)	0.039; 0.107	0.034; 0.095	0.056; 0.155	0.054; 0.118	0.048; 0.136
R1(F); wR(F^2) (all data)	0.043; 0.111	0.035; 0.096	0.061; 0.159	0.143; 0.141	0.051; 0.139
GoF(F^2)	1.05	1.06	1.04	0.86	1.04
Residual electron density	0.28; -0.43	0.40; -0.28	0.99; -0.77	0.31; -0.31	0.30; -0.52

Acknowledgements. Johannes T. Wendler's, Simon Cassegrain's and Marine Cros' contributions to these studies during their internships are gratefully acknowledged. We thank F. Bélanger for support with X-ray diffraction studies and Prof. R. E. Prud'homme and P. Ménard-Tremblay for access to GPC. Funding was provided by NSERC, Centre en chimie verte et catalyse (CCVC) and FQRNT (Ph. D. stipend for T. W.).

Supporting Information. Tables S1-S4. Lactide conversion/time plots (Fig S2.1-S2.10). Single-crystal diffraction data (CIF).

References

(1) (a) Patel, R. G.; Sen, D. J. *Int. Pharm. Sciencia* **2011**, *1*, 29. (b) Kishan, K.; Carmen, S. In *Degradable Polymers and Materials: Principles and Practice (2nd Edition)*, American Chemical Society: 2012; Vol. 1114, pp 3. (c) Luckachan, G. E.; Pillai, C. K. S. *J. Polym. Environ.* **2011**, *19*, 637.
(2) Thompson, R. C.; Moore, C. J.; Saal, F. S. v.; Swan, S. H. *Phil. Trans. R. Soc. B* **2009**, *364*, 2153.
(3) (a) Hammer, J.; Kraak, M. S.; Parsons, J. In *Reviews of Environmental Contamination and Toxicology*, Whitacre, D. M., Ed. Springer New York: 2012; Vol. 220, pp 1. (b) Barnes, D. K. A.; Galgani, F.; Thompson, R. C.; Barlaz, M. *Philos Trans R Soc Lond B Biol Sci.* **2009**, *364*, 1985. (c) Cole, M.; Lindeque, P.; Halsband, C.; Galloway, T. S. *Marine Pollution Bulletin* **2011**, *62*, 2588.
(4) (a) Williams, C. K.; Hillmyer, M. A. *Polym. Rev.* **2008**, *48*, 1. (b) Ahmed, J.; Varshney, S. K. *International Journal of Food Properties* **2011**, *14*, 37. (c) Inkinen, S.; Hakkarainen, M.; Albertsson, A.-C.; Södergård, A. *Biomacromolecules* **2011**, *12*, 523.
(5) (a) Dutta, S.; Hung, W.-C.; Huang, B.-H.; Lin, C.-C. In *Synthetic Biodegradable Polymers*, Rieger, B.; Künkel, A.; Coates, G. W.; Reichardt, R.; Dinjus, E.; Zevaco, T. A., Eds. Springer-Verlag: Berlin, 2011; Vol. pp 219. (b) Dijkstra, P. J.; Du, H.; Feijen, J. *Polym. Chem.* **2011**, *2*, 520. (c) Carpentier, J.-F. *Macromol. Rapid Comm.* **2010**, *31*, 1696. (d) Ajellal, N.; Carpentier, J.-F.; Guillaume, C.; Guillaume, S. M.; Helou, M.; Poirier, V.; Sarazin, Y.; Trifonov, A. *Dalton Trans.* **2010**, *39*, 8363. (e) Wheaton, C. A.; Hayes, P. G.; Ireland, B. J. *Dalton Trans.* **2009**, 4832 . (f) Platel, R. H.; Hodgson, L. M.; Williams, C. K. *Polym. Rev.* **2008**, *48*, 11 . (g) Chisholm, M. H.; Zhou, Z. *J. Mater. Chem.* **2004**, *14*, 3081.
(6) El-Zoghbi, I.; Whitehorne, T. J. J.; Schaper, F. *Dalton Trans.* **2013**, *42*, 9376
(7) Whitehorne, T. J. J.; Schaper, F. *Chem. Commun.* **2012**, *48*, 10334.
(8) (a) Drouin, F.; Whitehorne, T. J. J.; Schaper, F. *Dalton Trans.* **2011**, *40*, 1396. (b) Drouin, F.; Oguadinma, P. O.; Whitehorne, T. J. J.; Prud'homme, R. E.; Schaper, F. *Organometallics* **2010**, *29*, 2139.
(9) (a) Cheng, M.; Attygalle, A. B.; Lobkovsky, E. B.; Coates, G. W. *J. Am. Chem. Soc.* **1999**, *121*, 11583. (b) Chamberlain, B. M.; Cheng, M.; Moore, D. R.; Ovitt, T. M.; Lobkovsky, E. B.; Coates, G. W. *J. Am. Chem. Soc.* **2001**, *123*, 3229. (c) Chisholm, M. H.; Huffman, J. C.; Phomphrai, K. *J. Chem. Soc., Dalton Trans.* **2001**, 222. (d) Chisholm, M. H.; Gallucci, J.; Phomphrai, K. *Inorg. Chem.* **2002**, *41*, 2785. (e) Chisholm, M. H.; Phomphrai, K. *Inorg. Chim. Acta* **2003**, *350*, 121. (f) Dove, A. P.; Gibson, V. C.; Marshall, E. L.; White, A. J. P.; Williams, D. J. *Dalton Trans.* **2004**, 570. (g) Chisholm, M. H.; Gallucci, J. C.; Phomphrai, K. *Inorg. Chem.* **2005**, *44*, 8004. (h) Ayala, C. N.; Chisholm, M. H.; Gallucci, J. C.; Krempner, C. *Dalton Trans.* **2009**, 9237 . (i) Tong, R.; Cheng, J. *Angew. Chem., Int. Ed.* **2008**, *47*, 4830.

(j) Yu, K.; Jones, C. W. *J. Catal.* **2004**, *222*, 558. (k) Yu, K.; Jones, C. W. *Polym. Prepr. (Am. Chem. Soc., Div. Polym. Chem.)* **2004**, *45*, 1005. (l) Kroeger, M.; Folli, C.; Walter, O.; Doering, M. *Adv. Synth. Catal.* **2006**, *348*, 1908. (m) Helou, M.; Miserque, O.; Brusson, J.-M.; Carpentier, J.-F.; Guillaume, S. M. *Macromol. Rapid Comm.* **2009**, *30*, 2128. (n) Poirier, V.; Duc, M.; Carpentier, J.-F.; Sarazin, Y. *ChemSusChem* **2010**, *3*, 579. (o) Chen, H.-Y.; Huang, B.-H.; Lin, C.-C. *Macromolecules* **2005**, *38*, 5400. (p) Athar, T.; Hakeem, A.; Topnani, N. *J. Chil. Chem. Soc.* **2011**, *56*, 887. (q) Chen, H.-Y.; Peng, Y.-L.; Huang, T.-H.; Sutar, A. K.; Miller, S. A.; Lin, C.-C. *J. Mol. Catal. A: Chem.* **2011**, *339*, 61.

(10) (a) Sanchez-Barba, L. F.; Hughes, D. L.; Humphrey, S. M.; Bochmann, M. *Organometallics* **2006**, *25*, 1012. (b) Tong, R.; Cheng, J. *Bioconjugate Chem.* **2010**, *21*, 111. (c) Chisholm, M. H.; Choojun, K.; Gallucci, J. C.; Wambua, P. M. *Chem. Sci.* **2012**, *3*, 3445. (d) Collins, R. A.; Unruangsri, J.; Mountford, P. *Dalton Trans.* **2013**, *42*, 759.

(11) Independent of their solid state structure, *nacnac*Zn(OR) complexes might be dimeric or monomeric in solution. Since solution structures of the (pre-)catalysts influence only the very first monomer insertion, they were not investigated in detail and all complexes are presented as monomers in the text to facilitate readability.

(12) El-Zoghbi, I.; Ased, A.; Oguadinma, P. O.; Tchirioua, E.; Schaper, F. *Can. J. Chem.* **2010**, *88*, 1040.

(13) Feldman, J.; McLain, S. J.; Parthasarathy, A.; Marshall, W. J.; Calabrese, J. C.; Arthur, S. D. *Organometallics* **1997**, *16*, 1514.

(14) (a) Fisher, K. J. *Tetrahedron Lett.* **1970**, 2613. (b) Vela, J.; Zhu, L.; Flaschenriem, C. J.; Brennessel, W. W.; Lachicotte, R. J.; Holland, P. L. *Organometallics* **2007**, *26*, 3416.

(15) (a) Cheng, M.; Moore, D. R.; Reczek, J. J.; Chamberlain, B. M.; Lobkovsky, E. B.; Coates, G. W. *J. Am. Chem. Soc.* **2001**, *123*, 8738. (b) Piesik, D. F. J.; Range, S.; Harder, S. *Organometallics* **2008**, *27*, 6178.

(16) (a) Moore, D. R.; Cheng, M.; Lobkovsky, E. B.; Coates, G. W. *Angew. Chem., Int. Ed.* **2002**, *41*, 2599. (b) Boese, R.; Blaser, D.; Eisenmann, T.; Schulz, S. *Private communication to the Cambridge Structural Database* **2009**, CCDC 730654. (c) Schulz, S.; Eisenmann, T.; Bläser, D.; Boese, R. *Z. Anorg. Allg. Chem.* **2009**, *635*, 995. (d) Bendt, G.; Schulz, S.; Spielmann, J.; Schmidt, S.; Bläser, D.; Wölper, C. *Eur. J. Inorg. Chem.* **2012**, *2012*, 3725.

(17) Dove, A. P.; Gibson, V. C.; Hormnirun, P.; Marshall, E. L.; Segal, J. A.; White, A. J. P.; Williams, D. J. *Dalton Trans.* **2003**, 3088.

(18) Latreche, S.; Schaper, F. *Inorg. Chim. Acta* **2011**, *43*, 49.

(19) Bailey, P. J.; Coxall, R. A.; Dick, C. M.; Fabre, S.; Henderson, L. C.; Herber, C.; Liddle, S. T.; Loroño-González, D.; Parkin, A.; Parsons, S. *Chem.-Eur. J.* **2003**, *9*, 4820.

(20) Oguadinma, P. O.; Schaper, F. *Organometallics* **2009**, *28*, 6721.

(21) Stack, D. E.; Hill, A. L.; Diffendaffer, C. B.; Burns, N. M. *Org. Lett.* **2002**, *4*, 4487.

(22) Rivillo, D.; Gulyás, H.; Benet-Buchholz, J.; Escudero-Adán, Eduardo C.; Freixa, Z.; van Leeuwen, Piet W. N. M. *Angew. Chem., Int. Ed.* **2007**, *46*, 7247.

(23) Save, M.; Schappacher, M.; Soum, A. *Macromol. Chem. Phys.* **2002**, *203*, 889.

(24) *APEX2*, Release 2.1-0; Bruker AXS Inc.: Madison, USA, 2006.

(25) *SAINT*, Release 7.34A; Bruker AXS Inc.: Madison, USA, 2006.

(26) Sheldrick, G. M. *SADABS*, Bruker AXS Inc.: Madison, USA, 1996 & 2004.

(27) Sheldrick, G. M. *Acta Crystallogr.* **2008**, *A64*, 112.

2. Supporting Information

Lack of polymer weight control and transesterification

Presence of transesterification can lead to changes in the apparent P_r value, if determined as described in Table 1 or 2 from the intensities of homodecoupled ^{1}H NMR spectra. Unselective transesterification has a 50% chance of forming an *rr*-triad, from a polymer chain ending on an *r*-dyad. Since *rr*-triads overlap with *mmm*-tetrads and since the statistical model used for P_r calculation does not account for their presence, transesterification leads to an artificial decrease in P_r. In reality, given that the majority of dyads are *m*-dyads, unselective transesterification decreases overall isotacticity, which can be shown by careful inspection of the ^{13}C NMR data (c. f. Drouin et al. *Organometallics* **2010**, *29*, 2139 for an example).

In two cases lack of polymer weight control, i. e. discrepancies between expected and obtained polymer molecular weight correlated with indications for transesterification. This follows similar arguments made previously in the literature. Since transesterification itself does **not** affect M_n, changes in M_n require that parts of either the high or the low molecular weight fraction are lost during work-up. Given that none of the catalysts produced isotactic PLA, we did not investigate this in detail, nor did we conduct model polymerizations at low lactide:catalyst ratio for MALDI analysis.

Table S2.1 Comparison of geometric data for 2.5b and 2.5c with other nacnacZnX a complexes (see text for references).

	2.5b	**Typical values**	**2.5c**	**Typical values**
Zn-N	1.93 – 1.99	1.93 – 1.99	1.96 – 1.97	1.96 – 2.07
Zn-X [a]	1.90	1.89 – 1.95	1.97 – 1.98	1.93 – 2.02
N-Zn-N	100	97 – 100	100.66(8)	94 – 100
Si-N-Zn-N	68-80	60 - 82		
Angle OZnO/NZnN			45 – 46	36 -60

2.5b : X = N_{amide}; **2.5c** : X = O

Table S2.2 Comparison of geometric data for 2.5d and 2.7d with *nacnac*^{dipp}Mg(N(SiMe$_3$)$_2$).

	2.5d	**2.7d**	*nacnac*^{dipp}Mg(N(SiMe$_3$)$_2$)
Mg-N	2.026(2), 2.029(2)	2.036(1)	2.013(2), 2.044(2)
Mg-N$_{amide}$	1.972(2)	1.975(2)	1.961(2)
N-Mg-N	96.80(8)	95.28(6)	95.11(6)
N-Mg-N$_{amide}$	125.34(9), 126.55(8)	129.39(3)	131.28(7) – 133.57(7)
Angle C$_\beta$NNC$_\beta$/NMgN	29	31	16

Table S2.3 Comparison of geometric data with other {*nacnac*Mg(μ-OR)}$_2$ complexes (see text for references).

	2.5f	**2.6e**	**2.7e**	*Typical values*
Mg-N	2.02 – 2.06	2.03 – 2.04	2.05 – 2.07	2.04 – 2.12
Mg-O	1.97 – 1.99	1.95 – 1.96	1.96 – 1.98	1.94 – 2.03
N-Mg-N	95	92	91	91 – 94
N-Mg-O	105 – 136	116 - 125	110 – 139	110 – 126
O-Mg-O	81	84	82	81 – 84
Angle C$_\beta$NNC$_\beta$/NMgN	3 – 5	6	33 – 35	18 – 29
Angle O$_2$Mg$_2$/NMgN	79 – 82	87	74 – 76	80 – 89
N-CH$_2$-R orientation	anti	syn	syn	

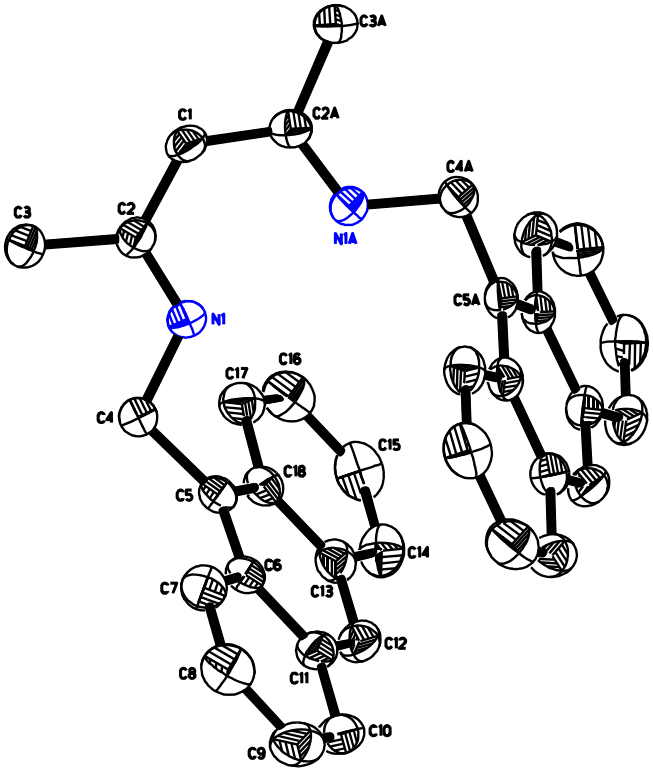

Figure S2.1 X-ray structure of **2.5a**. Hydrogen atoms omitted for clarity. Thermal ellipsoids are drawn at 50% probability.

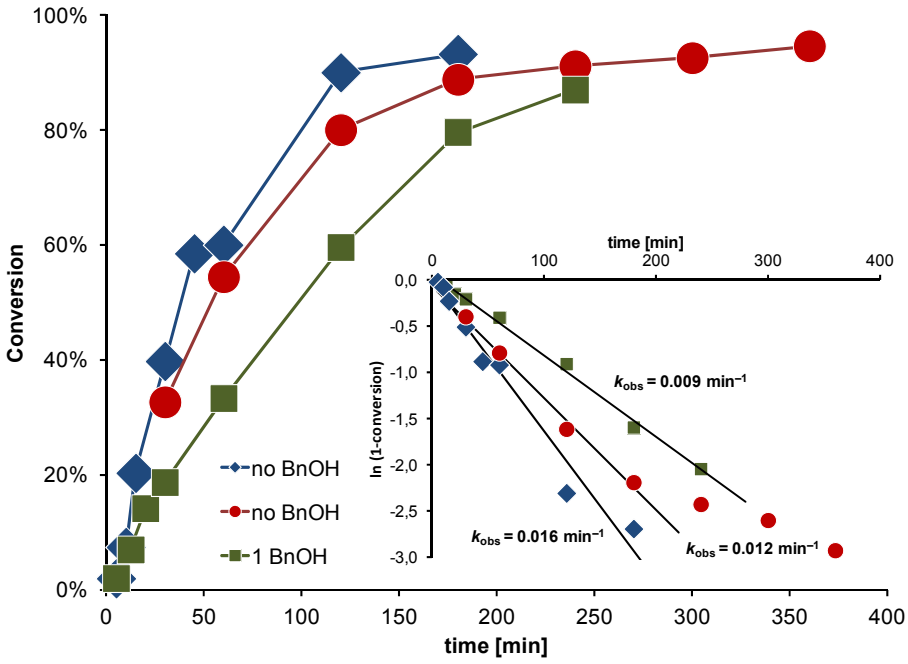

Figure S2.2 Conversion/time plot for polymerizations with **2.5c** in the absence (diamonds + circles) and in the presence (squares) of benzyl alcohol.

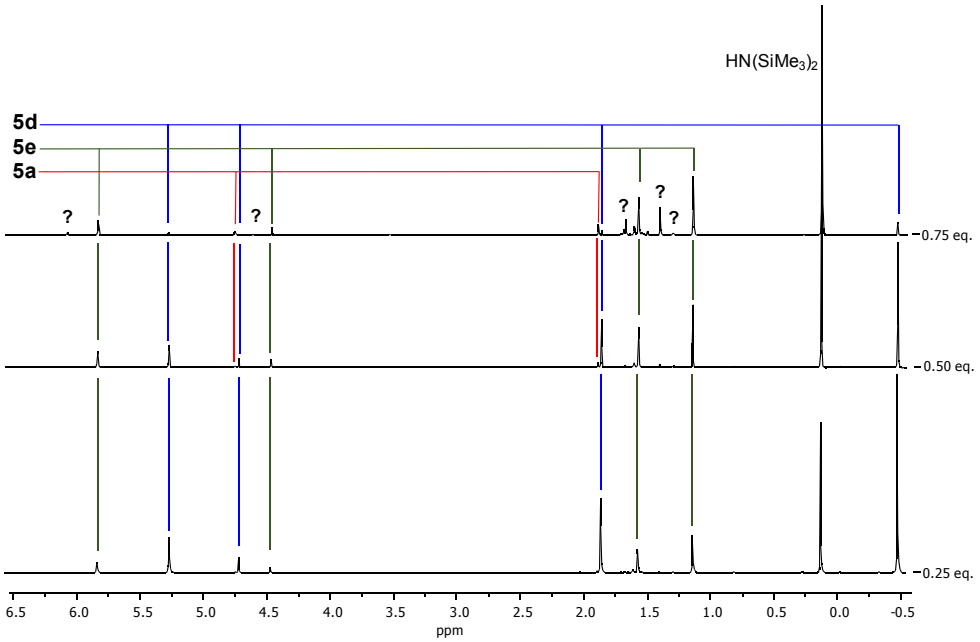

Figure S2.3 ^{1}H NMR spectra of the titration of **2.5d** with *tert*-butanol.

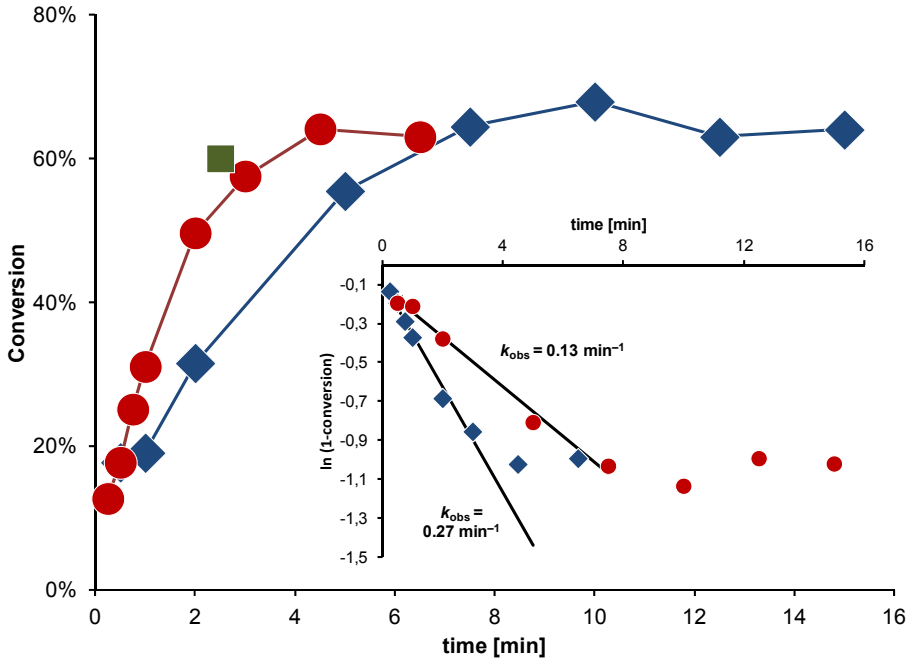

Figure S2.4 Conversion/time plot for polymerizations with **2.5d** in the absence of benzyl alcohol. All polymerizations failed to reach completion.

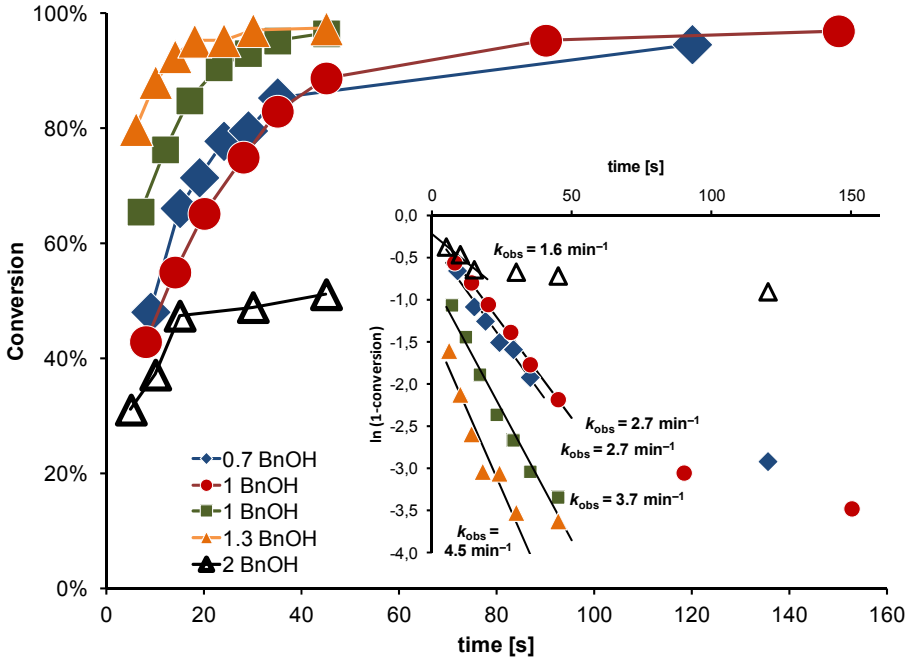

Figure S2.5 Conversion/time plot for polymerizations with **2.5d** in the presence of different amounts of benzyl alcohol. Lactide:Mg ratio was constant at 300:1.

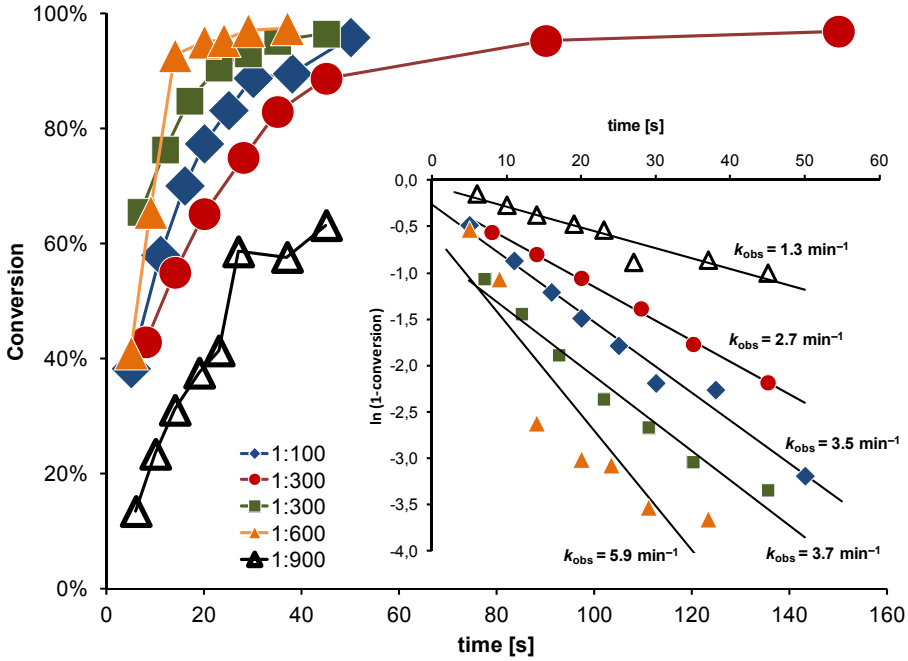

Figure S2.6 Conversion/time plot for polymerizations with **2.5d** + 1 equiv BnOH at different lactide:Mg ratios.

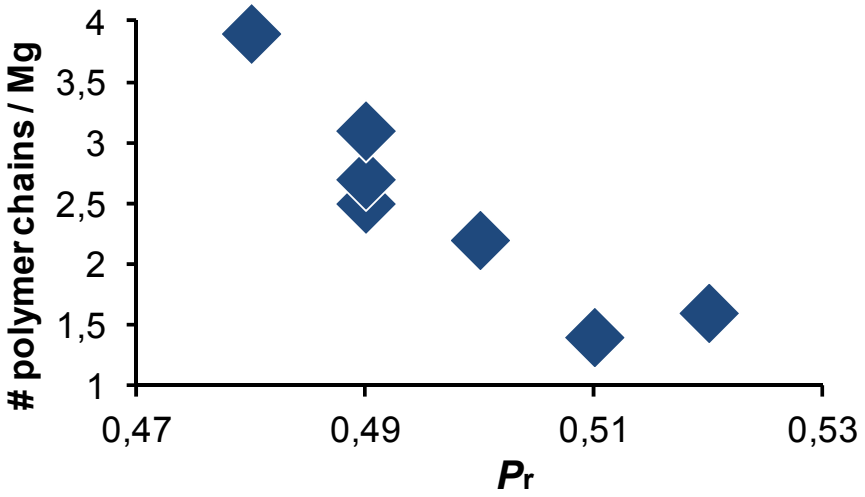

Figure S2.7 Correlation of the P_r value and the number of polymer chains per Mg obtained (= M_n(expected) /M_n(obtained)) for polymerizations with **2.5d**/BnOH.

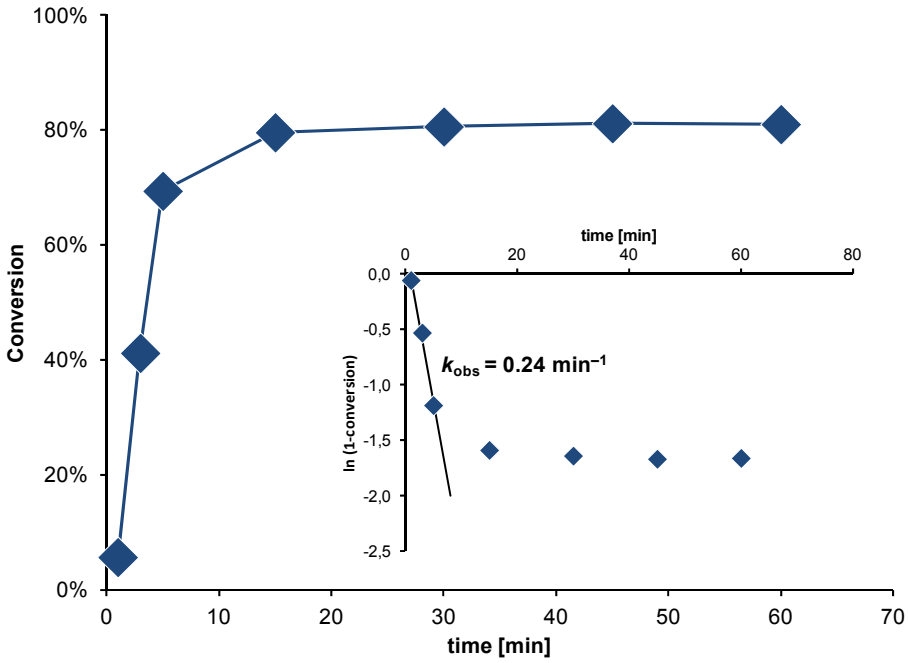

Figure S2.8 Conversion/time plot for polymerization with **2.7e**.

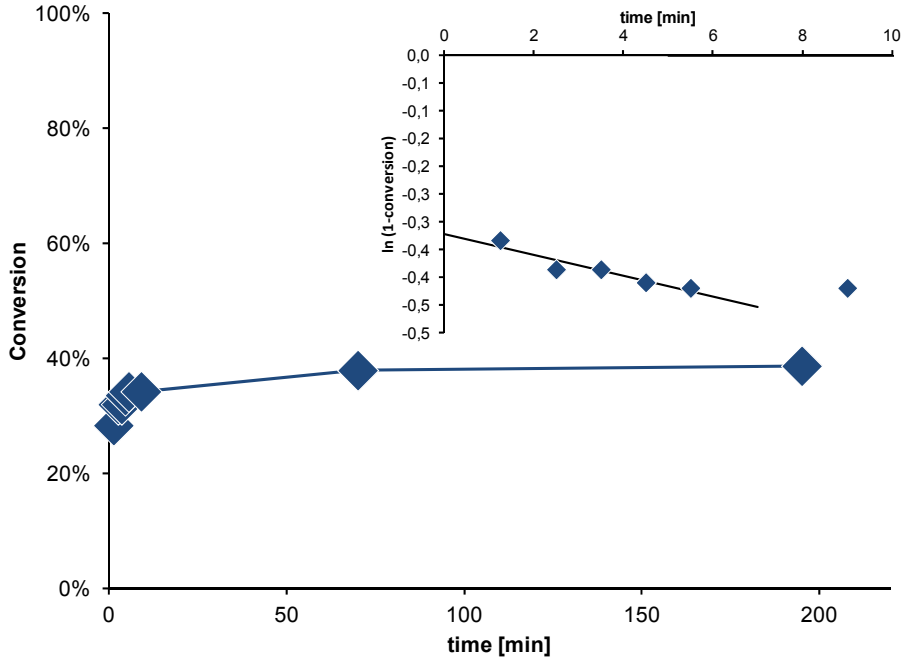

Figure S2.9 Conversion/time plot for polymerizations with **2.8d**/BnOH. Polymerization failed to reach completion with kinetic traces indicating catalyst decomposition.

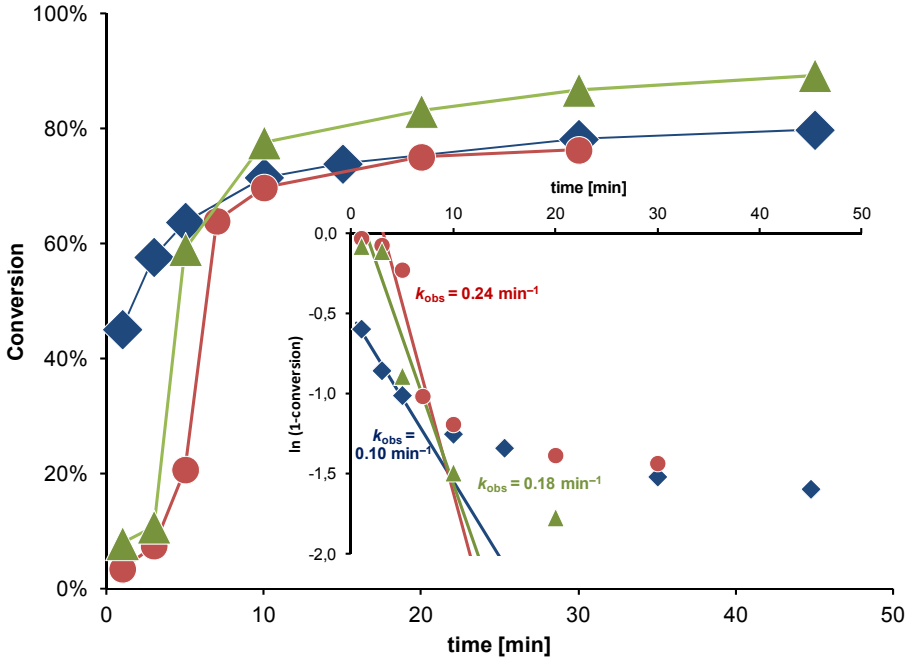

Figure S2.10 Conversion/time plot for (selected) polymerizations with **2.6e** in the absence of benzyl alcohol (red circles, green triangles) and in the presence of benzyl alcohol (blue diamonds). Polymerizations failed to reach completion.

Table S2.4 Crystallization conditions for X-ray diffractions studies

nacnac^{An}H, **2.5a**	dichloromethane, –15 °C
nacnac^{An}ZnN(SiMe$_3$)$_2$, **2.5b**	toluene, –30 °C
nacnac^{An}ZnO*i*Pr, **2.5c**	dichloromethane, –30 °C
nacnac^{An}MgN(SiMe$_3$)$_2$, **2.5d**	toluene, –30 °C
nacnac^{An}MgOPh, **2.5f**	dichloromethane, –30 °C
Cl*nacnac*^{Bn}MgO*t*Bu, **2.6e**	dichloromethane, –30 °C
(Cl*nacnac*^{Bn})$_2$Mg, **2.6f**	dichloromethane/hexane, –30 °C
nacnac^{Mes}MgN(SiMe$_3$)$_2$, **2.7d**	toluene, –30 °C
nacnac^{Mes}MgO*t*Bu, **2.7e**	dichloromethane, –30 °C
(Cl*nacnac*^{An})$_2$Mg, **2.8f**	toluene, –30 °C

3. *Nacnac*^{Bn}CuO*i*Pr: A strained geometry resulting in very high lactide polymerization activity

Chem. Commun., **2012***,48,* 10334-10336

*Todd J. J. Whitehorne, Frank Schaper**

Abstract

N,N'-Dibenzyl diketiminate copper isopropanolate, (*nacnac*^{Bn}CuO*i*Pr)$_2$, polymerizes *rac*- and *S,S*-lactide in the presence or absence of isopropanol as a chain-transfer reagent with very high activity (k_2 = 32 M^{-1} s^{-1}), narrow polydispersities and without evidence of side reactions such as transesterification, epimerization or catalyst decomposition.

Introduction

N,N'-dibenzyl diketiminate copper isopropanolate, (*nacnac*^{Bn}CuO*i*Pr)$_2$, polymerizes *rac*- and *S,S*-lactide in the presence or absence of isopropanol as a chain-transfer reagent with very high activity (k_2 = 32 $M^{-1}\cdot s^{-1}$), narrow polydispersities and without evidence of side reactions such as transesterification, epimerization or catalyst decomposition.

Since the introduction of polymeric materials and the resulting presence of plastic debris in the environment, the persistence of plastics is reason for ecological concern. In addition to the macroscopic level, i. e. choking and entanglement hazards for wildlife as well as purely aesthetic effects, recent findings suggest that physical and photochemical degradation of debris into microplastics renders them bio-available, particularly in marine environments.[1] Polylactic acid (PLA) is one possible candidate to replace traditional polymers which has found commercial application. PLA is obtained by ring-opening polymerization of lactide, the dimeric anhydride of lactic acid, in the presence of a catalyst. While a large number of catalysts have been investigated in academia, often in an attempt to control the stereochemistry of polymerization,[2] commercial production relies on tin(II) octoate as a catalyst due to its "*solubility in molten lactide, high catalytic activity, and low rate of racemisation of the polymer*".[3] We recently started to investigate the performance

of *N*-alkyl diketiminate metal complexes with fixed or flexible ligand frameworks in lactide polymerization.[4] Here we present a catalyst with square-planar geometry, of which only a limited number of examples have been reported for lactide polymerization based on copper(II)[5] and nickel(II)[5b,6], and none for Cr(II), Pd(II), Pt(II), Rh(I) or Ir(I).

Complex Synthesis

Addition of the free ligand **3.1** to Cu(O*i*Pr)$_2$ in hexanes or toluene yielded (*nacnac*^{Bn}CuO*i*Pr)$_2$, **3.2**, by protonation of one equivalent of isopropanolate in 63% recrystallized yield (Scheme 3.1).

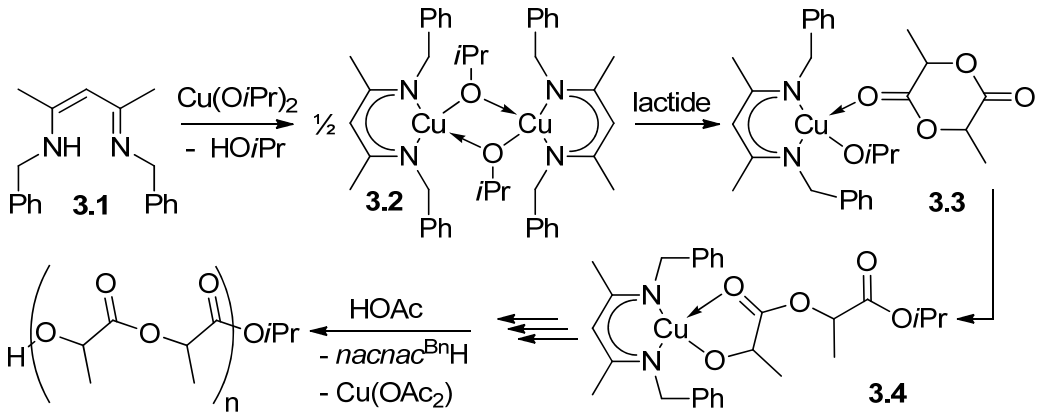

Scheme 3.1 Synthesis of 3.2 and *rac*-lactide polymerization

The only other example of a diketiminate Cu(II) alkoxide, *nacnac*^{Ar}CuO*t*Bu, was obtained by oxidation of *nacnac*^{Ar}Cu(I) with *tert*-butyl peroxide.[7] Diketiminate Cu(II) phenolate complexes, *nacnac*^{Ar}CuOAr, have been previously obtained from salt metathesis between *nacnac*^{Ar}CuCl and thallium phenolates.[8]

Complex **3.2** crystallizes as alkoxide-bridged dimer on a crystallographic inversion centre (Figure 3.1, Table S3.1). Cu-N bond lengths in **3.2** (1.921(3) – 1.953(3) Å) are in the range typically observed for four-coordinated *nacnac*$_2$Cu (1.95±0.04 Å)[9] and {*nacnac*Cu(μ-X)}$_2$ (1.93±0.01 Å),[7,10] but longer than those in three-coordinate *nacnac*^{Ar}CuOR (1.88±0.02 Å).[7-8]

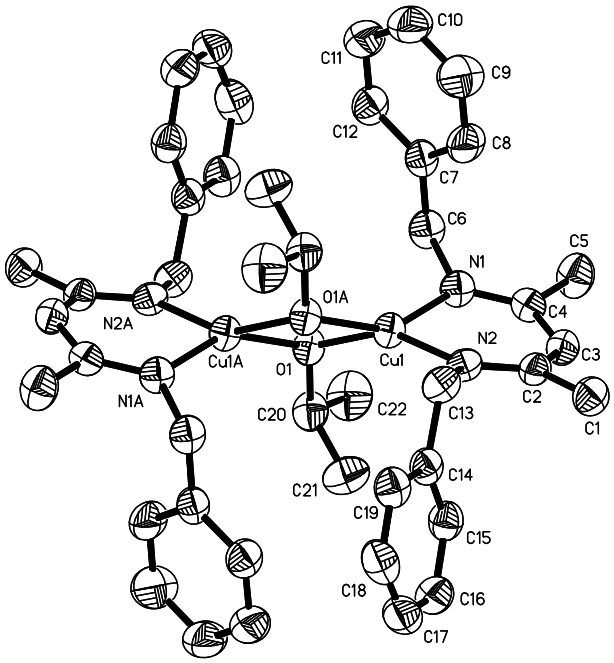

Figure 3.1 X-ray structure of **3.2**. Hydrogen atoms were omitted for clarity. Thermal ellipsoids were drawn at the 50% probability level. Only one of two independent molecules in the asymmetric unit is shown.

The most notable structural feature is the formation of a sterically strained, alkoxide-bridged dimer with a strongly distorted square-planar coordination environment around Cu. Previous examples of diketiminate copper alkoxide or aryloxide complexes contained *N*-aryl substituents and displayed monomeric structures with a trigonal coordination geometry around copper.[7-8] In **3.2**, on the other hand, the higher conformational flexibility of the *N*-alkyl substituent allows for the formation of a distorted bridged dimer (tilt angles of 41-43°, Table S3.1). Cu-O bond lengths in **3.2** (1.951(2) – 1.982(2) Å) are, as expected, longer than those in *nacnac*CuOR with terminal OR/OAr ligands (Cu-O: 1.80±0.02 Å),[7-8] but they are also appr. 0.04 Å longer than the average for bridged Cu(II) alkoxide complexes (1.92±0.06 Å),[11] indicative again of steric strain in the dimer.

Lactide Polymerization. Complex **3.2** polymerizes *rac*-lactide at room temperature in dichloromethane with very high activity, yielding, in less than 1 min, a primarily atactic

polymer (P_r = 56%). Polymerization of *rac*-lactide with **3.2** was well behaved, yielding polydispersities in the range of 1.04 to 1.08 under typical conditions (Table S3.2). This is indicative of polymerization initiation without a significant induction period. In fact, no induction period was observed when the polymerization was followed by ^{1}H NMR. Formation of the active, most likely monomeric species thus occurs fast upon addition of lactide.

The kinetics of polymerization was studied by quenching of samples from bulk reactions, followed by ^{1}H NMR analysis. In all cases, the polymerization kinetics was found to be first order with respect to monomer concentration. Over a concentration range of 0.125 < [Cu] < 2.5 mM, the obtained pseudo-1st-order rate constants depend linearly on the concentration of **3.2** (Figure 3.2, Table S3.2). The polymerization reaction is thus 1st order with respect to **3.2** and the active species does not participate in any dimerization equilibria under polymerization conditions.

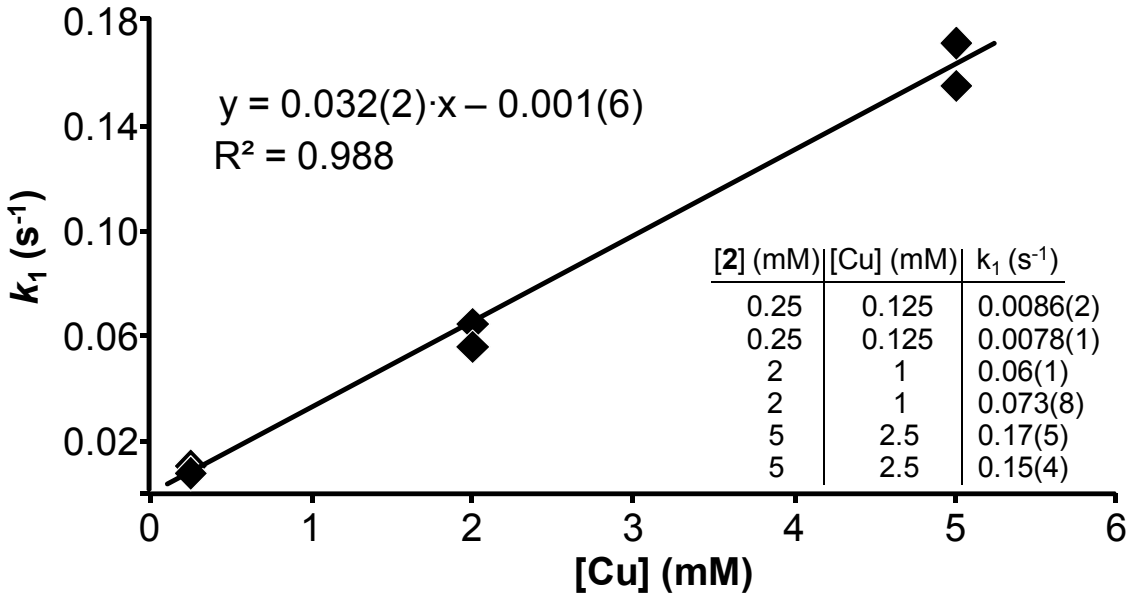

[**2**] (mM)	[Cu] (mM)	k_1 (s^{-1})
0.25	0.125	0.0086(2)
0.25	0.125	0.0078(1)
2	1	0.06(1)
2	1	0.073(8)
5	2.5	0.17(5)
5	2.5	0.15(4)

Figure 3.2 Dependence of pseudo-first order rate constants k_1 on the concentration of $(\mathbf{3.2})_{0.5}$.

A second order rate constant of k_2 = 32(2) $s^{-1} \cdot M^{-1}$ (based on $(\mathbf{3.2})_{0.5}$) indicates that complex **3.2** is far more active than previous Cu(II) lactide polymerization catalysts, which required temperatures of 70 °C or higher to achieve even moderate activity.[5] Magnesium and zinc alkoxide complexes, *nacnac*^{Bn}MOR, bearing the same diketiminate ligand, were less active by at least an order of magnitude.[4a,4b] In fact, **3.2** is among the most active lactide polymerization catalysts reported to date (Table 3.1).

Table 3.1 Highest activities in lactide polymerization at ambient temperature for different metal catalysts

	k_2 ($M^{-1}s^{-1}$)	PDI	P_r	ref.
$(\mathbf{3.2})_{0.5}$	32(2)	1.0-1.1	0.56	
Cu(II)	7.7×10^{-4}	1.5	-	5c
Ca(II)	2[a]	1.2-1.4	0.50	12
Mg(II)	60[b]	1.6	0.43	13
Zn(II)	2.2	1.4	-	14
Y(III)	80[a]	1.1-1.2	0.90	15
$SnOct_2$	no polymer obtained under conditions used for **3.2** [c]			

Conditions: room temperature (except for Cu(II): 70°C), solution polymerization. [a] Estimated from k_1, assuming a 2nd order rate law. [b] Estimated from time and conversion, assuming a 2nd order rate law. [c] 2 mM $SnOct_2$, 2 mM BnOH, CH_2Cl_2, ambient temperature, 1 h polymerization time

Polymerizations with **3.2** fail, in most cases, to reach 100% conversion. Given the sensitivity of **3.2** towards hydrolysis, it seemed reasonable to assume that catalyst decomposition is responsible for the failure to polymerize the final 4-5% of *rac*-lactide.

This, however, is not supported by the narrow molecular weight distributions generally observed (Table S3.2). In fact, upon addition of three consecutive portions of *rac*-lactide every 3 minutes, identical activities were observed for each addition, disproving death of the catalyst (Figure 3.3). Obtained M_n values were within 10% of predictions (Table S3.2); a tendency noted in all experiments and, most likely, due to weighing errors. The linear relationship between monomer addition and polymer molecular weight (Figure 3.3, inset) proves that neither irreversible termination nor catalyst decomposition occurs to a notable extent and that impurities in *rac*-lactide are not a significant source of catalyst decomposition. In the presence of active catalyst, incomplete conversion must thus be attributed to reversible polymerization, a well documented phenomenon in lactide polymerization.[16]

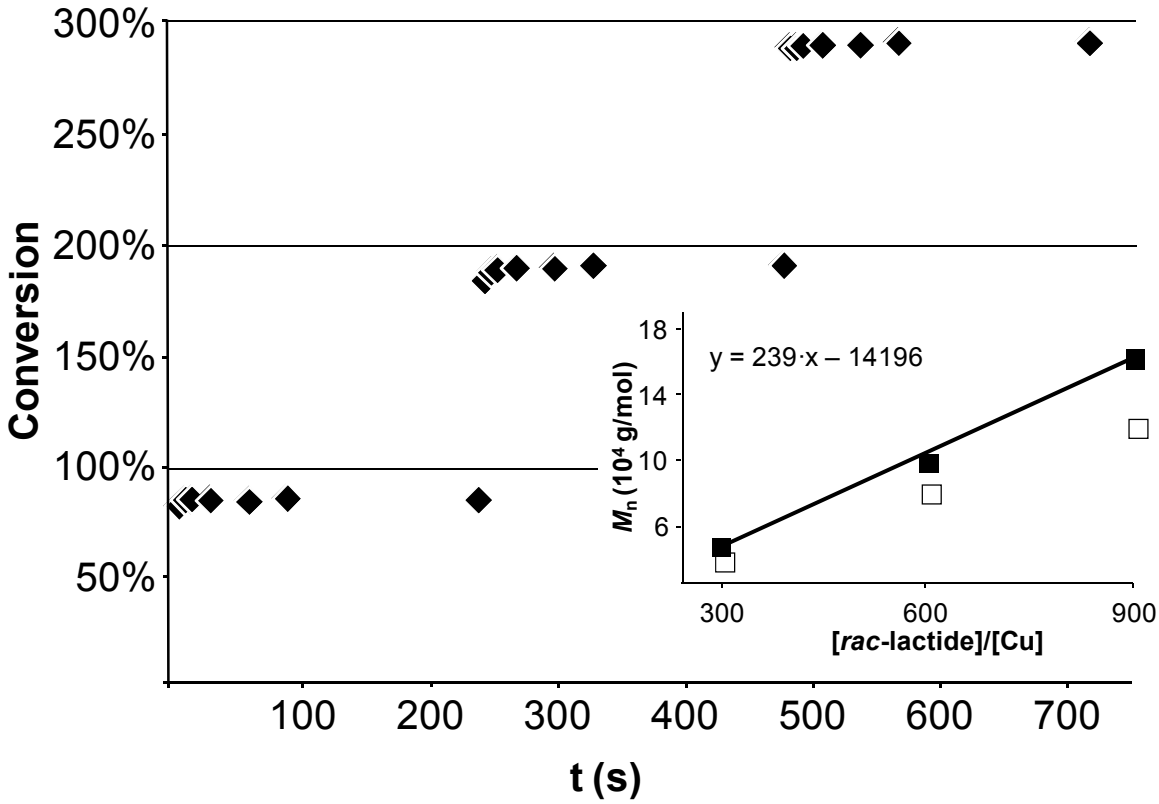

Figure 3.3 Repeated monomer addition (3 x 300 equiv) experiment. Conversion calculated as (total equiv of lactide polymerized)/300 equiv. The inset shows the obtained polymer molecular weight after each addition, expected M_n values in hollow squares.

Two often observed problems in lactide polymerization are transesterification of the polymer chain and epimerization of the chiral centres, leading to increased polydispersities and to reduced isotacticity in polymerizations with enantiopure lactide. A standard polymerization reaction of *rac*-lactide with **3.2** was studied via NMR for 12 h after polymerization was complete, during which the P_r value was found to decrease slightly from 60% to 50%. For *rac*-lactide polymerizations, decreases in the P_r values determined by homodecoupled NMR can be attributed to the formation of *rr*-triads, caused either by transesterification or epimerization.[4a] The same experiment was performed using *S*-lactide,

but no change in P_r was observed over the same period. Thus **3.2** does not lead to notable epimerization within the polymer. Transesterification does occur to a slight degree over 12 h, but is negligible during the short period of polymerization (<3 min), in agreement with the narrow molecular weight distributions obtained.

High molecular weight polymers were attainable (M_n up to 480 000 g/mol) using **3.2** as a catalyst (Table S3.2), and were found to be limited only by polymer solubility. Polymer precipitation occurred after 80% conversion, giving rise to increased polydispersity; the only time a PDI above 1.1 was obtained.

In polymerizations under "immortal" conditions[17] with isopropanol as a transfer reagent, the obtained M_n values agreed well with those predicted (Table S3.2, Figure 3.4). Overall, M_n values are slightly higher than expected, in agreement with partial catalyst decomposition due to solvent impurities. Polydispersities remained narrow (<1.08) in all cases, indicating that the polymerization remained well controlled in the presence of a chain-transfer agent.

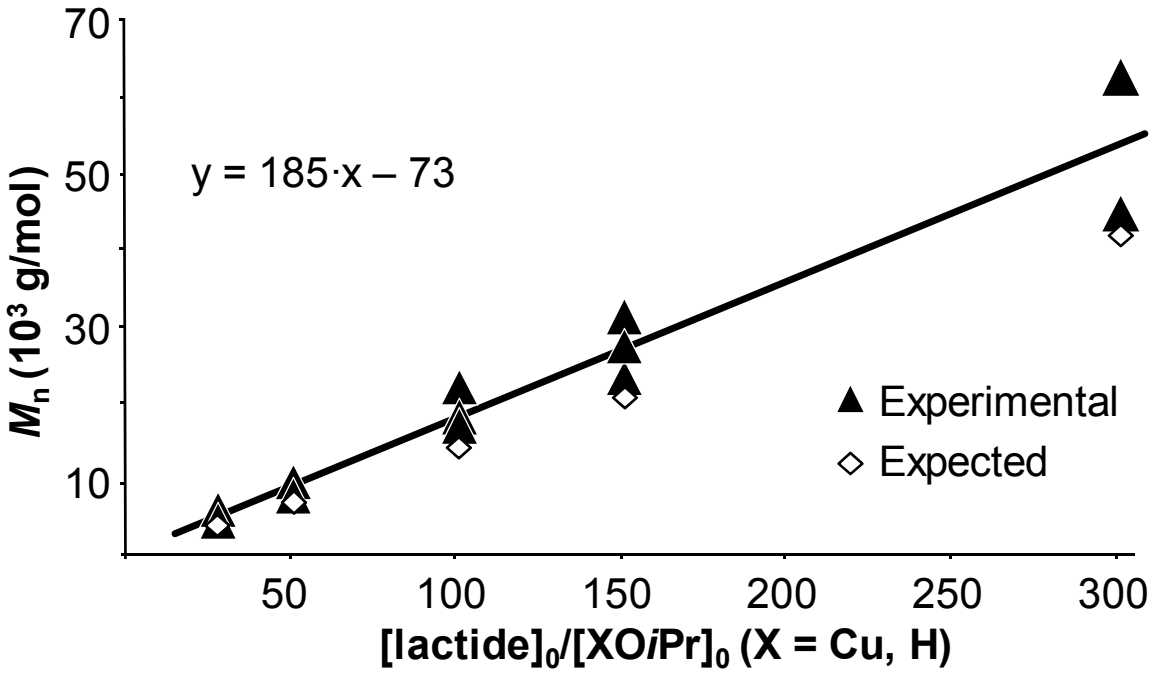

Figure 3.4 Obtained polymer molecular weight *vs*. monomer to initiator ratio in immortal polymerizations; expected M_n values shown as hollow diamonds.

Conclusions

(*Nacnac*^{Bn}CuO*i*Pr)$_2$, **3.2**, proved to be one of the most active (pre)catalysts reported for lactide polymerization so far. Its high activity is most likely related to the *N*-alkyl diketiminate ligand, which is flexible enough to allow monomer coordination, but presents sufficient steric bulk to destabilize a lactide-coordinated square-planar intermediate (**3.3**, Scheme 3.1), thus favouring insertion. Despite its high polymerization activity, the complex is stable and the polymerization is well controlled, yielding narrow polydispersities without evidence for transesterification, epimerization or catalyst decomposition even in presence of a chain-transfer agent. Although the current ligand system did not allow for control of the stereochemistry of polymerization, the activity and

polymerization control exhibited by **3.2** indicate that copper(II) catalysts are worthy candidates for further exploration.

This work was supported by the Natural Sciences and Engineering Research Council of Canada (NSERC) and the Centre in Green Chemistry and Catalysis (CGCC). We thank Pierre Ménard-Tremblay and Dr. R. E. Prud'homme for help with polymer molecular weight measurements.

Notes and references

1. (a) M. Cole, P. Lindeque, C. Halsband and T. S. Galloway, *Marine Pollution Bulletin*, 2011, **62**, 2588; (b) D. K. A. Barnes, F. Galgani, R. C. Thompson and M. Barlaz, *Philos Trans R Soc Lond B Biol Sci.*, 2009, **364**, 1985.

2. (a) P. J. Dijkstra, H. Du and J. Feijen, *Polym. Chem.*, 2011, **2**, 520; (b) N. Ajellal, J.-F. Carpentier, C. Guillaume, S. M. Guillaume, M. Helou, V. Poirier, Y. Sarazin and A. Trifonov, *Dalton Trans.*, 2010, **39**, 8363; (c) C. A. Wheaton, P. G. Hayes and B. J. Ireland, *Dalton Trans.*, 2009, 4832 ; (d) O. Dechy-Cabaret, B. Martin-Vaca and D. Bourissou, *Chem. Rev.*, 2004, **104**, 6147; (e) M. H. Chisholm and Z. Zhou, *J. Mater. Chem.*, 2004, **14**, 3081.

3. R. E. Drumright, P. R. Gruber and D. E. Henton, *Adv. Mater. (Weinheim, Ger.)*, 2000, **12**, 1841.

4. (a) F. Drouin, P. O. Oguadinma, T. J. J. Whitehorne, R. E. Prud'homme and F. Schaper, *Organometallics*, 2010, **29**, 2139; (b) F. Drouin, T. J. J. Whitehorne and F. Schaper, *Dalton Trans.*, 2011, **40**, 1396; (c) I. El-Zoghbi, S. Latreche and F. Schaper, *Organometallics*, 2010, **29**, 1551.

5. (a) J. Sun, W. Shi, D. Chen and C. Liang, *J. Appl. Polym. Sci.*, 2002, **86**, 3312; (b) A. John, V. Katiyar, K. Pang, M. M. Shaikh, H. Nanavati and P. Ghosh, *Polyhedron*, 2007, **26**, 4033; (c) S. Bhunora, J. Mugo, A. Bhaw-Luximon, S. Mapolie, J. Van Wyk, J. Darkwa and E. Nordlander, *Appl. Organomet. Chem.*, 2011, **25**, 133; (d) L.-L. Chen, L.-Q. Ding, C. Zeng, Y. Long, X.-Q. Lü, J.-R. Song, D.-D. Fan and W.-J. Jin, *Appl. Organomet. Chem.*, 2011, **25**, 310; (e) R. R. Gowda and D. Chakraborty, *J. Molec. Catal. A: Chem.*, 2011, **349**, 86.

6. (a) L. Ding, W. Jin, Z. Chu, L. Chen, X. Lü, G. Yuan, J. Song, D. Fan and F. Bao, *Inorg. Chem. Commun.*, 2011, **14**, 1274; (b) W.-J. Jin, L.-Q. Ding, Z. Chu, L.-L. Chen, X.-Q. Lü, X.-Y. Zheng, J.-R. Song and D.-D. Fan, *J. Molec. Catal. A: Chem.*, 2011, **337**, 25; (c) G. Xiao, B. Yan, R. Ma, W. J. Jin, X. Q. Lu, L. Q. Ding, C. Zeng, L. L. Chen and F. Bao, *Polym. Chem.*, 2011, **2**.

7. S. Wiese, Y. M. Badiei, R. T. Gephart, S. Mossin, M. S. Varonka, M. M. Melzer, K. Meyer, T. R. Cundari and T. H. Warren, *Angew. Chem., Int. Ed.*, 2010, **49**, 8850.

8. B. A. Jazdzewski, P. L. Holland, M. Pink, V. G. Young, D. J. E. Spencer and W. B. Tolman, *Inorg. Chem.*, 2001, **40**, 6097.

9. (a) G. Dessy and V. Fares, *Acta Crystallogr., Sect. C: Cryst. Struct. Commun.*, 1979, **8**, 101; (b) K.-H. Park and W. J. Marshall, *J. Am. Chem. Soc.*, 2005, **127**, 9330; (c) N. B. Morozova, P. A. Stabnikov, I. A. Baidina, P. P. Semyannikov, S. V. Trubin and I. K. Igumenov, *J. Struct. Chem.*, 2007, **48**, 889; (d) R. E. Marsh, *Acta Crystallogr., Sect.B : Struct. Sci.*, 2009, **65**, 782; (e) P. O. Oguadinma and F. Schaper, *Private communication to the Cambridge Structural Database*, 2010, CCDC 773447.

10. (a) X. Dai and T. H. Warren, *Chem. Commun.*, 2001, 1998; (b) D. J. E. Spencer, A. M. Reynolds, P. L. Holland, B. A. Jazdzewski, C. Duboc-Toia, L. Le Pape, S. Yokota, Y. Tachi, S. Itoh and W. B. Tolman, *Inorg. Chem.*, 2002, **41**, 6307; (c) S. Hong, L. M. R. Hill, A. K. Gupta, B. D. Naab, J. B. Gilroy, R. G. Hicks, C. J. Cramer and W. B. Tolman, *Inorg. Chem.*, 2009, **48**, 4514; (d) M. M. Melzer, S. Mossin, X. Dai, A. M. Bartell, P. Kapoor, K. Meyer and T. H. Warren, *Angew. Chem., Int. Ed.*, 2010, **49**, 904; (e) P. O. Oguadinma and F. Schaper, *Private communication to the Cambridge Structural Database*, 2010, CCDC 773445.

11. F. H. Allen, *Acta Crystallogr., Sect. B: Struct. Sci.*, 2002, **B58**, 380.

12. M. G. Cushion and P. Mountford, *Chem. Commun. (Cambridge, U. K.)*, 2011, **47**, 2276.

13. L. Wang and H. Ma, *Macromolecules*, 2010, **43**, 6535.

14. C. K. Williams, L. E. Breyfogle, S. K. Choi, W. Nam, V. G. Young, M. A. Hillmyer and W. B. Tolman, *J. Am. Chem. Soc.*, 2003, **125**, 11350.

15. T.-P.-A. Cao, A. Buchard, X. F. Le Goff, A. Auffrant and C. K. Williams, *Inorg. Chem.*, 2012, **51**, 2157.

16. (a) A. Duda and S. Penczek, *Macromolecules*, 1990, **23**, 1636; (b) J. Mosnáček, A. Duda, J. Libiszowski and S. Penczek, *Macromolecules*, 2005, **38**, 2027.

17. S. Inoue, *J. Polym. Sci., Part A: Polym. Chem.*, 2000, **38**, 2861.

3. Supporting information

Table S3.1 Selected bond lengths [Å] and angles [°] for **3.2**

Cu-N1/31	1.921(3), 1.923(3)	N-Cu-N	95.2(1), 94.9(1)
Cu-N2/32	1.951(3), 1.946(3)	Cu-Cu-N1/31	129, 128
Cu-O	1.951(2), 1.979(2), 1.954(2), 1.982(2)	Cu-Cu-N2/32	136, 137
		(N,Cu)-(O,Cu)[a]	41, 43

[a] tilt angle between (N,N,Cu) and (Cu,O,O,Cu) least-square planes.

Table S3.2 Selected data for the polymerization of *rac*-lactide in CH_2Cl_2.

#	Catalyst/lactide	Equiv. *i*PrOH	[Cu]/(mmol·L^{-1})	*t*/s	Conversion[a] (%)	$M_{n,calc}$[c]/(g·mol^{-1})	M_n[d]/(g·mol^{-1})	M_w/M_n[d]
1	1/300	-	2.0	25	97	42005	44604	1.07
2	1/300	-	0.50	90	93	40275	37472	1.06
3	1/300	-	0.25	180	80	34654	34255	1.03
4	1/3000	-	0.25	150	95[b]	410859[b]	487976	1.48[b]
5	1/300	1	2.0	45	96	20816	27302[e]	1.04[e]
6	1/300	2	2.0	45	95	13849	19103[e]	1.04[e]
7	1/300	5	2.0	45	97	7003	8491[e]	1.07[e]
8	1/300	10	2.0	45	96	3834	5329[e]	1.11[e]
9	1/300	-	2.0	90	85	36816	45260	1.03
	1/600	-	2.0	90	91	78328	96290	1.05
	1/900	-	2.0	90	91	118111	159959	1.08

[a] Calculated from ^{1}H NMR spectra. [b] PLA precipitates at 80% conversion, final conversion estimated. [c] Calculated from ([lactide]$_0$/[*i*PrOH]$_0$+[Cu])·conversion·144 + 60. [d] Determined by size exclusion chromatography *vs.* polystyrene standards, corrected by a Mark-Houwink factor of 0.58.[1] [e]Average of multiple experiments.

Experimental

All reactions were carried out using Schlenk and glove box techniques under a nitrogen atmosphere. *Nacnac*BnH, **3.1**,[2] and Cu(O*i*Pr)$_2$ starting material[3] was synthesized according to literature methods. Solvents were dried by passage through activated aluminum oxide (MBraun SPS), de-oxygenated by repeated extraction with nitrogen, and stored over molecular sieves. C_6D_6 was dried over sodium and degassed by three freeze-pump-thaw cycles. $CDCl_3$ and CD_2Cl_2 were dried over 3 Å molecular sieves. *rac*-Lactide (98%) was purchased from Sigma–Aldrich, purified by 3 times recrystallization from dry ethyl acetate and kept at -30 °C. All other chemicals were purchased from common commercial suppliers and used without further purification. ^{1}H and ^{13}C NMR spectra were acquired on a Bruker AVX 400 spectrometer. The chemical shifts were referenced to the residual signals of the deuterated solvents (C_6D_6: ^{1}H: δ 7.16 ppm, ^{13}C: δ 128.38 ppm, $CDCl_3$: ^{1}H: δ 7.26 ppm, CD_2Cl_2: ^{1}H: δ 5.32 ppm). Elemental analyses were performed by the Laboratoire d'analyse élémentaire (Université de Montréal). Molecular weight analyses were performed on a Waters 1525 gel permeation chromatograph equipped with three Phenomenex columns and a refractive index detector at 35 °C. THF was used as the eluent at a flow rate of 1.0 mL·min^{-1} and polystyrene standards (Sigma–Aldrich, 1.5 mg·mL^{-1}, prepared and filtered (0.2 mm) directly prior to injection) were used for calibration. Obtained molecular weights were corrected by a Mark-Houwink factor of 0.58.[1]

***Nacnac*^{Bn}CuO*i*Pr, 3.2.** Cu(O*i*Pr)$_2$ (500 mg, 2.75 mmol) was suspended in hexanes or toluene (20 mL). **1** (610 mg, 2.20 mmol) was added slowly to the mixture and allowed to react at room temperature for 18 h. The reaction mixture changed colour from deep green to deep blue. Solvent and *i*PrOH was removed under reduced pressure. The blue solid was then taken up in toluene (15 mL) and filtered through a fine frit. The filtrate was placed at -35 °C, yielding X-ray quality crystals (550 mg, 63%). Anal. calcd for $C_{22}H_{28}CuN_2O_1$: C 66.1, H 7.1, N 7.0. Found: C 66.3, H 7.2, N 6.8. UV/vis (toluene): λ/nm (ε·M·cm) 357 (10000), 431 (570), 523 (560), 720 (sh, 100). UV/vis (THF): λ/nm (ε·M·cm) 421 (sh 470), 533 (400).

Lactide Polymerizations. Typical example: In a dry box, a vial was charged with a stir bar, *rac*-lactide (170 mg, 1.2 mmol) and CH_2Cl_2 (2 mL). After dissolution of lactide, a solution of **2** in CH_2Cl_2 (53 µL, 75 mM, 4 µmol) was added and a stopwatch initiated. Every 5 sec, a sample of the reaction mixture (100 µL) from the polymerization mixture was transferred to a test tube, charged with a solution of acetic acid in CH_2Cl_2 (100 µL, 4 mM, 0.4 µmol). After one minute, the remaining reaction mixture was quenched by addition of a solution of acetic acid in CH_2Cl_2 (0.8 mL, 4 mM, 3.2 µmol). Samples and polymerization mixture were then removed from the dry box and the solvent evaporated immediately under reduced pressure. If not analyzed directly, polymers were stored at –80 °C.

Microstructure analysis. P_r-values were determined from the integration of the methine region in homonuclear decoupled ^{1}H NMR spectra of PLA in $CDCl_3$ and calculated according to $P_r = 2 \cdot I_1/(I_1+I_2)$, with I_1 = 5.20 – 5.25 ppm (*rmr, mmr/rmm*), I_2 = 5.13 – 5.20 ppm (*mmr/rmm, mmm, mrm*).[4] Resonances in ^{1}H spectra were assigned according to literature.[5]

X-ray crystallography. Diffraction data were collected on a Bruker Smart 6000 with a Helios monochromator, equipped with a rotating anode source for Cu Kα radiation. Cell refinement and data reduction were done using APEX2.[6] The crystal was found to be twinned. Two twin domains were identified by CELLNOW and included with scale factors refined to 0.45, 0.45, 0.06, and 0.04. Alternative integration with 2, 3 or 5 twin domains yielded higher R_{int} values. Reported R_{int} were obtained from TWINABS[6] based on agreement between observed single and composite intensities and those calculated from refined unique intensities and twin fractions. Absorption corrections were applied using TWINABS.[6] Structures were solved by direct methods using SHELXS97 and refined on F^2 by full-matrix least squares using SHELXL97.[7] All non-hydrogen atoms were refined anisotropically. Hydrogen atoms were refined isotropically on calculated positions using a riding model.

Table S3.3 Details of the X-ray crystal structure of **3.2**.

Formula	$C_{22}H_{28}N_2OCu$
Formula Mass/g·mol^{-1}	400.00
Crystal system	triclinic
a/Å	11.3590(4)
b/Å	12.1536(4)
c/Å	15.8854(5)
α/°	76.981(2)
β/°	80.639(2)
γ/°	71.993(2)
Unit cell volume/Å^3	2021.7(1)
T/K	150
Space group	P-1
No. of formula units per unit cell, Z	4
Absorption coefficient, μ/mm^{-1}	1.606
No. of reflections measured	82878
No. of independent reflections	7954
R_{int}	8.59
Final *R1* values (I > 2σ(I))	0.059
Final *wR*(F^2) values (I > 2σ(I))	0.159
Final *R1* values (all data)	0.083
Final *wR*(F^2) values (all data)	0.169
Goodness of fit on F^2	1.025
Residual elec. density	0.72

Polymerization kinetics

Polymerization kinetics were studied at room temperature in CH_2Cl_2 solution. For polymerizations with [**3.2**] = 0.125 mM or 1 mM, samples were taken in the desired intervals, quenched with AcOH and analyzed by NMR. For polymerizations with [**3.2**] = 2.5 mM, acquiring samples was not possible and each data point corresponds to an independent experiment, resulting in increased errors for this concentration. At least two experimental rate constants were determined for each concentration, which differed by less than 20%.

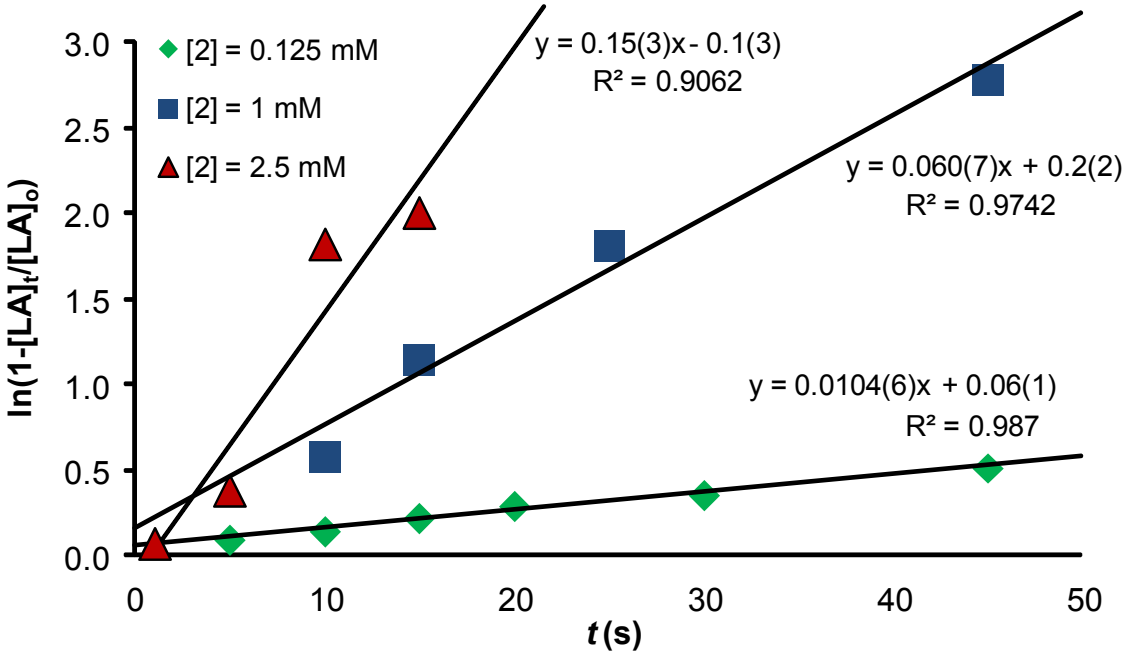

Figure S3.1: Selected examples of 1st order rate law determinations for varied concentrations of **3.2**, with [Cu]/[lactide] = 1/300.

1. M. Save, M. Schappacher and A. Soum, *Macromol. Chem. Phys.*, 2002, **203**, 889.
2. F. Drouin, P. O. Oguadinma, T. J. J. Whitehorne, R. E. Prud'homme and F. Schaper, *Organometallics*, 2010, **29**, 2139.
3. J. V. Singh, B. P. Baranwal and R. C. Mehrotra, *Z. Anorg. Allg. Chem.*, 1981, **477**, 235.
4. B. M. Chamberlain, M. Cheng, D. R. Moore, T. M. Ovitt, E. B. Lobkovsky and G. W. Coates, *J. Am. Chem. Soc.*, 2001, **123**, 3229.
5. (a) J. E. Kasperczyk, *Macromolecules*, 1995, **28**, 3937; (b) J. E. Kasperczyk, *Polymer*, 1999, **40**, 5455; (c) M. T. Zell, B. E. Padden, A. J. Paterick, K. A. M. Thakur, R. T. Kean, M. A. Hillmyer and E. J. Munson, *Macromolecules*, 2002, **35**, 7700.
6. *APEX2*, (2006) Bruker AXS Inc., Madison, USA.
7. G. M. Sheldrick, *Acta Crystallogr.*, 2008, **A64**, 112.

4. Square-planar Cu(II) diketiminate complexes in lactide polymerization

Inorg. Chem., **2013**,*52,* 13612

*Todd J. J. Whitehorne, Frank Schaper**

Département de chimie, Université de Montréal, 2900 Boul. E.-Montpetit, Montréal, QC, H3T 1J4, Canada

Abstract

Cu(O*i*Pr)$_2$ was reacted with several β-diketimine ligands, *nacnac*^{R}H. Sterically undemanding ligands with *N*-benzyl substituents afforded the dimeric heteroleptic complexes [*nacnac*^{Bn}Cu(μ-O*i*Pr)]$_2$ and [3-Cl-*nacnac*^{Bn}Cu(μ-O*i*Pr)]$_2$ (Bn = benzyl). With sterically more demanding amines, dimerization was not possible, and the putative *nacnac*CuO*i*Pr intermediate underwent ligand exchange to the homoleptic bisdiketiminate complexes Cu(*nacnac*^{ipp})$_2$ and Cu(*nacnac*^{Naph})$_2$ (ipp = 2-isopropylphenyl, Naph = 1-naphthyl). Homoleptic complexes were also prepared with *N*-benzyl ligands, i. e. Cu(*nacnac*^{Bn})$_2$ and Cu(3-succinimido-*nacnac*^{Bn})$_2$. All complexes were characterized by single-crystal X-ray diffraction. Even bulkier ligands with *N*-anthrylmethyl, *N*-mesitylmethyl or *N*-methylbenzyl substituents failed to react with Cu(O*i*Pr)$_2$. In the case of *nacnac*$^{di^{pp}}$CuO*i*Pr, putative *nacnac*^{dipp}CuO*i*Pr decomposed by β-hydride elimination. Heteroleptic complexes [*nacnac*^{Bn}Cu(μ-O*i*Pr)]$_2$ and [3-Cl-*nacnac*^{Bn}Cu(μ-O*i*Pr)]$_2$ are very highly active *rac*-lactide polymerization catalysts, with complete monomer conversion at ambient temperature in solution in 0.5 – 5 min. In the presence of free alcohol, the homoleptic complexes seem to be in equilibrium with small amounts of the respective heteroleptic complex, which are sufficient to complete polymerization in less than 60 min at room temperature. All catalysts show high control of the polymerization with polydispersities of 1.1 and below. The obtained polymers were essentially atactic, with a slight heterotactic bias at ambient temperature and at –17 °C.

Introduction

With the increasing use of plastics, concerns about the accumulation of plastic debris in the environment favour the use of polymers that are 100% biodegradable. One such polymer is polylactic acid (PLA), the condensation polymer of lactic acid.[1] PLA is currently marketed, albeit on a small scale for commodity polymers. It is biodegradable given the right conditions, since hydrolysis yields easily metabolized lactic acid. An additional advantage stems from the fact that lactic acid can be obtained by fermentation of natural products and does not depend – directly – on fossil fuels.[2]

Industrial production of PLA currently relies on the polymerization of lactide, the dimeric anhydride of lactic acid, using a non-selective tin catalyst, in particular $Sn(Oct)_2$, at elevated temperatures. Although only isotactic PLA is currently of commercial interest, the use of an unselective catalyst is possible since lactic acid is obtained from fermentation of natural products in enantiopure form. The polymerization of lactide has attracted in the last two decades considerable attention in the scientific community. This interest is fuelled partly by the potential of commercial applications, and partly by the lack of stereoselective catalysts with acceptable properties such as stability, activity, polymer molecular weight control, etc.

Establishing clear structure-reactivity relationships for lactide polymerization catalysts, which would enable rational catalyst design, is handicapped by the overall reversibility of the reaction, the presence of two important transition states for insertion and ring-opening of comparable energy,[3] the multitude of possible reaction pathways given the chirality of the catalyst, the polymer chain and the monomer, and interfering site reactions, such as chain transfer between catalyst centres or transesterification. While the existing literature is already too vast to be easily summarized,[4] some very general trends with regard to the central metal and typical coordination geometries can be seen: Following Spassky's initial work, five- or six-coordinated aluminum complexes can provide high stereocontrol towards isotactic monomer enchainment, but suffer from reduced activities.[5] Indium (or gallium) analogs show in general higher activity and retain (some) of the isospecifity, but no highly specific and active catalyst has yet been reported.[6] Group 3 and rare earth catalysts with a variety of coordination geometries are among the most

active catalysts known and can yield highly heterotactic to moderately isotactic polymer.[7] Alkaline and earth alkaline compounds, again with a variety of coordination geometries, show low to high activities and in rare cases a moderate preference for isotactic monomer enchainment.[8] Group 4 metal catalysts, mostly of octahedral geometries, can show moderate amounts of isospecificity, but have in general low to moderate activity.[9] Tetrahedral Mg and Zn complexes have been investigated widely, following the seminal work of Coates *et al.*,[10] and show moderate to high activities.[11] However, they tend to produce heterotactic PLA by a chain-end control mechanism and only in rare cases were low isospecificities observed.[12]

Despite the number of investigations into metal-catalyzed lactide polymerization, the use of catalysts with square-planar geometry was somewhat neglected. We are aware only of a limited number of examples reported for lactide polymerization based on copper(II)[13] and nickel(II) (Fig. 4.1),[13b, 14] and none for Cr(II), Pd(II), Pt(II), Rh(I) or Ir(I). The initial literature survey on copper(II) catalyzed lactide polymerization seems less than promising. While several catalysts were able to provide decent molecular weight control, they all required high temperatures, typically in molten monomer and showed only low activities even under those conditions.

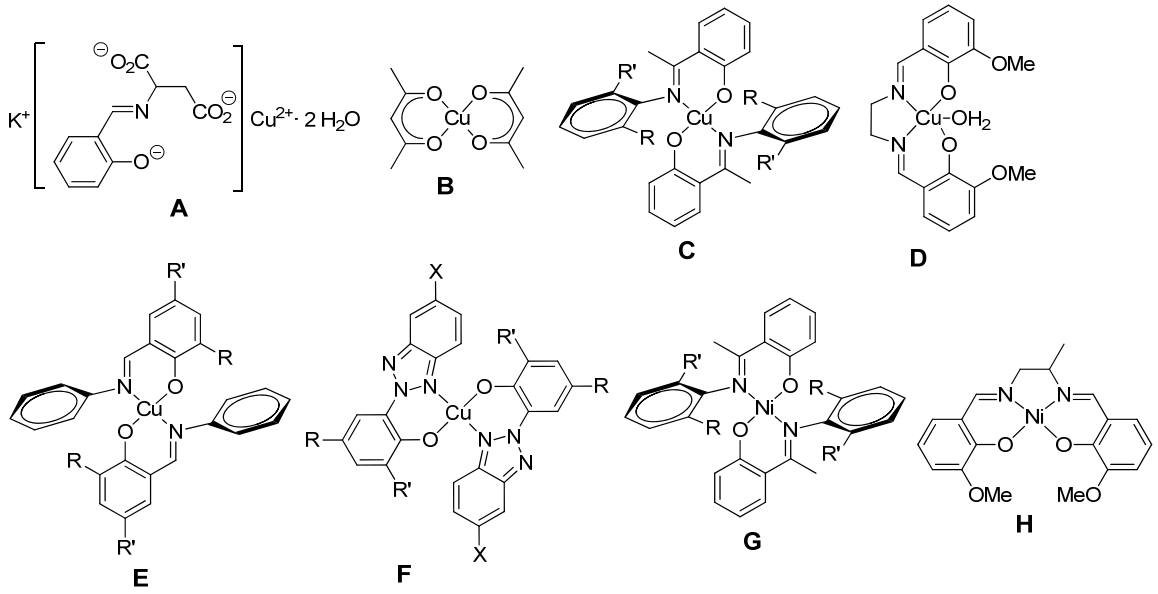

Figure 4.1. A : 97%, 24 h, 130 °C, molten monomer.[13a] **B** : 97%, 8 h, 145 °C, molten monomer.[13e] **C** : 76%, 4 h, 160 °C, molten monomer.[13b] **D** : 50%, 24 h, 130 °C, molten monomer.[13d] **E** : 80%, 35 h, 70 °C, toluene.[13c] **F** : >95%, 6 h, 110 °C, toluene.[13f] **G** : no polymerization, 160 °C, molten monomer.[13b] **H** : 78%, 24 h, 130 °C, molten monomer.[14]

A serendipitous choice of the right spectator ligand, however, showed that square-planar copper complexes can indeed be interesting candidates for lactide polymerization and we recently reported preliminary results that [(*nacnac*^{Bn}Cu(μ-O*i*Pr)]$_2$ is highly active in lactide polymerization, reaching complete conversion of monomer in less than 1 min at room temperature (*nacnac*^{Bn} = *N,N*-dibenzyl-pentane-2,4-diiminato).[15] In the present manuscript, we extend these investigations to other *N*-alkyl and *N*-aryl copper(II) diketiminate complexes.

Results and discussion

Complex syntheses. Only two examples of Cu(II) diketiminate alkoxide or aryloxide complexes have been reported in the literature. Tolman and coworkers prepared *nacnac*^{dipp}CuOAr, **4.1**, (dipp = 2,6-diisopropylphenyl, Scheme 4.1) from the reaction of *nacnac*^{dipp}CuCl with thallium aryl oxides.[16] Warren and coworkers obtained *nacnac*^{Ar}CuO*t*Bu, **4.2**, by oxidation of the respective Cu(I) complex with *tert*-butyl peroxide.[17] Since aryl oxides, as well as *tert*-butoxide groups tend to give slow polymerization initiation, our interest was focused on more reactive alkoxides, such as isopropoxide. We thus reacted

nacnac^{dipp}H, **4.3a**, with Cu(O*i*Pr)$_2$ in an attempt to prepare *nacnac*^{dipp}CuO*i*Pr, **4.4a**, by a protonation route. Upon addition of the ligand, green Cu(O*i*Pr)$_2$ solubilised and the colour changed to brown, indicating that the ligand did indeed react with Cu(O*i*Pr)$_2$. However, no isolable product could be obtained. Analysis of the volatiles of the reaction showed the presence of acetone. We speculate that **4.4a** was indeed formed as an intermediate. Contrary to the reported **4.1** and **4.2**, however, **4.4a** contains a β-hydrogen atom on the alkoxide ligand, which is available for β-H elimination. The latter yields acetone and a putative Cu(II) hydride which, unsurprisingly, is unstable (Scheme 4.1). Probably due to steric hindrance, *nacnac*^{dipp}H failed to react with Cu(O*t*Bu)$_2$ even at 100 °C (toluene) and only starting materials were observed. Surprisingly, Cu(OMe)$_2$ was unreactive as well. Other bulky diketimine ligands, such as *nacnac*^{An}H (An = 9-antrhylmethyl), *nacnac*^{Mes}H (Mes = mesitylmethyl), or *nacnac*$^{CMe(H)Ph}$H, failed to react even with Cu(O*i*Pr)$_2$.

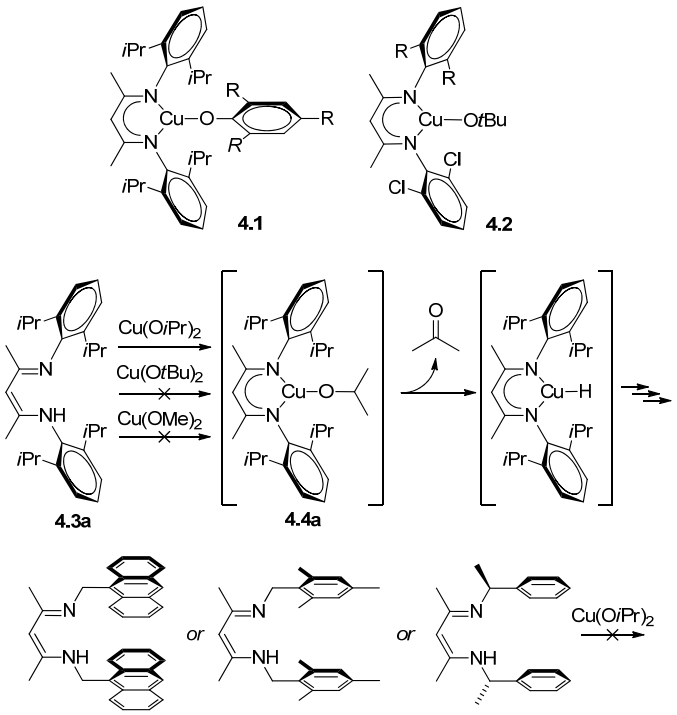

Scheme 4.1

Given the lack of reactivity with sterically encumbered diketimines, monosubstituted *nacnac*^{ipp}H, **4.3b**, (ipp = 2-isopropylphenyl, Scheme 4.2) was reacted with Cu(O*i*Pr)$_2$. However, instead of heteroleptic *nacnac*^{ipp}CuO*i*Pr, **4.4b**, the homoleptic bisdiketiminate complex (*nacnac*^{ipp})$_2$Cu, **4.5b**, was obtained, at a variety of reaction conditions. For comparison purposes, **4.5b** was prepared independently by reaction of

two equiv. **4.3b** with Cu(O*i*Pr)$_2$. Attempts to obtain *nacnac*^{ipp}CuO*t*Bu by a route similar to the one used by Warren and co. for **4.2** failed due to the instability of the respective Cu(I) complex **4.6**, which disproportionated into Cu(0) and **4.5b**. An increased tendency for decomposition by disproportionation has been observed previously for Cu(I) diketiminate complexes with *N*-alkyl ligands, which required stabilization with an ancillary ligand.[18] Mono-substituted *N*-aryl diketimines seem to suffer from similar stability problems. Reaction of the lithiated ligand *nacnac*^{ipp}Li with $CuCl_2$[16] yielded the respective copper(II) chloride complex, **4.7**, but subsequent reaction with KOtBu did not yield the heteroleptic complex. Instead homoleptic **4.5b** was obtained again. The latter reaction provided some indications with regard to the inaccessibility of **4.4b**. In protonations of Cu(O*i*Pr)$_2$ with **4.3b**, the putative intermediate **4.4b** might either be kinetically labile, given that it might be more reactive towards a second protonation than insoluble Cu(O*i*Pr)$_2$ (Scheme 4.2, path A) or it is thermodynamically labile and undergoes ligand exchange to **4.5b** and Cu(O*i*Pr)$_2$ without further participation of **4.3b** (Scheme 4.2, path B). The fact that changing reaction conditions, i. e. order of addition, reagent concentrations, or temperature, did not affect the reaction outcome already indicated that **4.4b** might rather be thermodynamically labile. This was confirmed in the salt metathesis reaction of **4.7** with KOtBu, since there is no possible pathway in which **4.5b** can be obtained as the kinetic product. Heteroleptic Cu(II) alkoxides with mono-substituted *N*-aryl substituents thus seem to be inherently labile towards ligand redistribution to form homoleptic, four-coordinate complexes. With the disubstituted *N*-aryl ligand **4.3a**, formation of a homoleptic bis(diketiminate) complex (*nacnac*^{dipp})$_2$Cu was most likely not possible due to the increased steric bulk of the disubstituted *N*-aryl and the presumed intermediate **4.4a** decomposed via β-H elimination. A reactivity similar to that of **4.3b** was observed with *nacnac*^{Naph}H, **4.3c** (Naph = 1-naphtyl, Scheme 4.2), which also yielded the homoleptic complex (*nacnac*^{Naph})$_2$Cu, **4.5c**, upon reaction with Cu(O*i*Pr)$_2$.

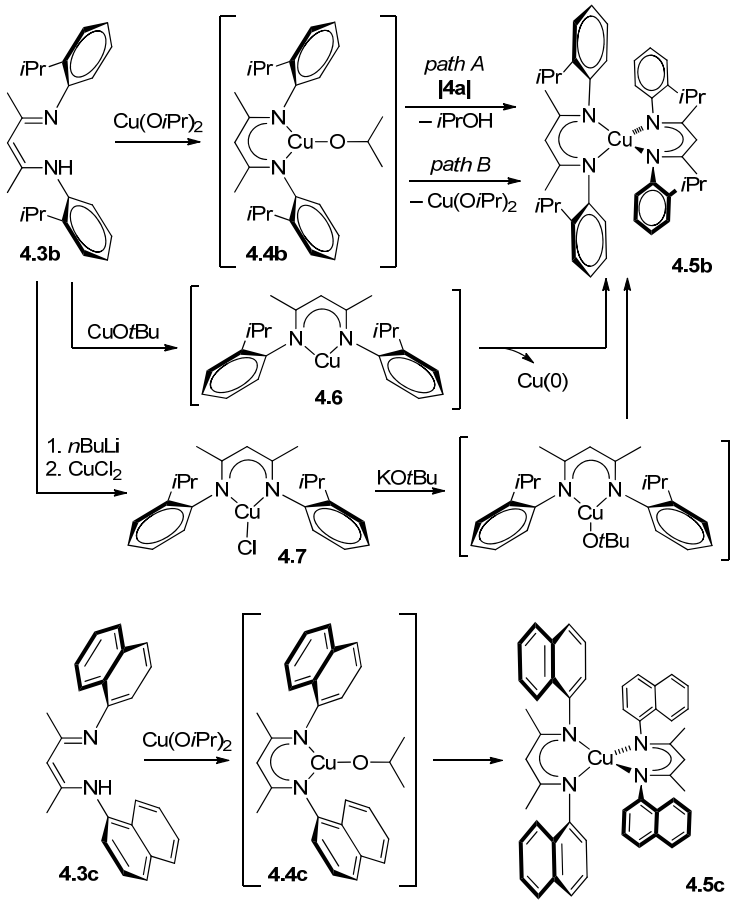

Scheme 4.2

Reaction of Cu(O*i*Pr)$_2$ with *nacnac*^{Bn}H, **4.3d**, finally afforded the heteroleptic complex (*nacnac*^{Bn}CuO*i*Pr)$_2$, **4.4d** (Scheme 4.3).[15] In Cu(I) chemistry, diketiminate ligands with primary *N*-alkyl ligands have been shown to be sterically significantly less bulky than those with *N*-aryl substituents.[18b, 18c] Given the propensity of *nacnac*CuOR to undergo ligand exchange to the homoleptic complexes, isolation of **4.4d** with a sterically undemanding spectator ligand was counter-intuitive. It seems unlikely that formation of the homoleptic complex Cu(*nacnac*^{Bn})$_2$, **4.5d**, should not be possible with an *N*-benzyl substituent. Indeed, **4.5d** could not only be prepared from the reaction of two equivalents of **4.3d** with Cu(O*i*Pr)$_2$, but was also formed in the reaction of **4.4d** with a second equivalent of **4.3d** (Scheme 4.3).[19] Given the easy access to **4.5d**, an additional mechanism has thus to be responsible for the stabilization of **4.4d**. The solid-state structure of **4.4d** yielded further insights. Contrary to **4.1** and **4.2**, complex **4.4d** crystallized as an alkoxide-bridged dimer in the solid state (*vide infra*). A UV/vis study of **4.4d** confirmed that the dimeric structure is most likely retained in solution: UV/vis-spectra of **4.4d** in toluene did not

change notably and obeyed the Beer-Lambert law over a concentration range of 0.050 – 6.5 mM (Fig. S4.1), indicating the absence of any monomer-dimer equilibria in this concentration range. Likewise, addition of 0.25 – 10 equiv pyridine did not affect the UV/vis spectra of **4.4d** in toluene (Fig. S4.2). Subtle, but more notable changes were observed between UV/vis spectra of **4.4d** in non-coordinating solvents, such as dichloromethane or toluene, and coordinating solvents, such as THF or pyridine (Fig. 4.2). Spectra similar to those obtained in coordinating solvents were obtained in toluene after addition of 1 equiv methyl lactate or 10 equiv of lactide. Based on these UV/vis studies, it appears that **4.4d** is dimeric in solution in the absence of strong donors without any noticeable dissociation. In the presence of intermolecular or intramolecular Lewis bases, the dimer can break apart to yield a tetracoordinated monomeric species (Fig. 4.2).

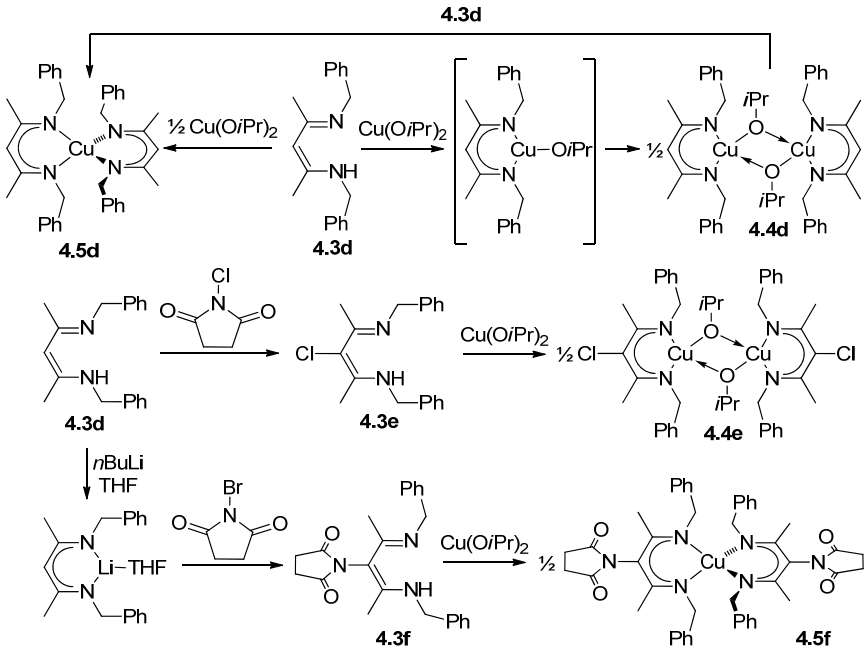

Scheme 4.3

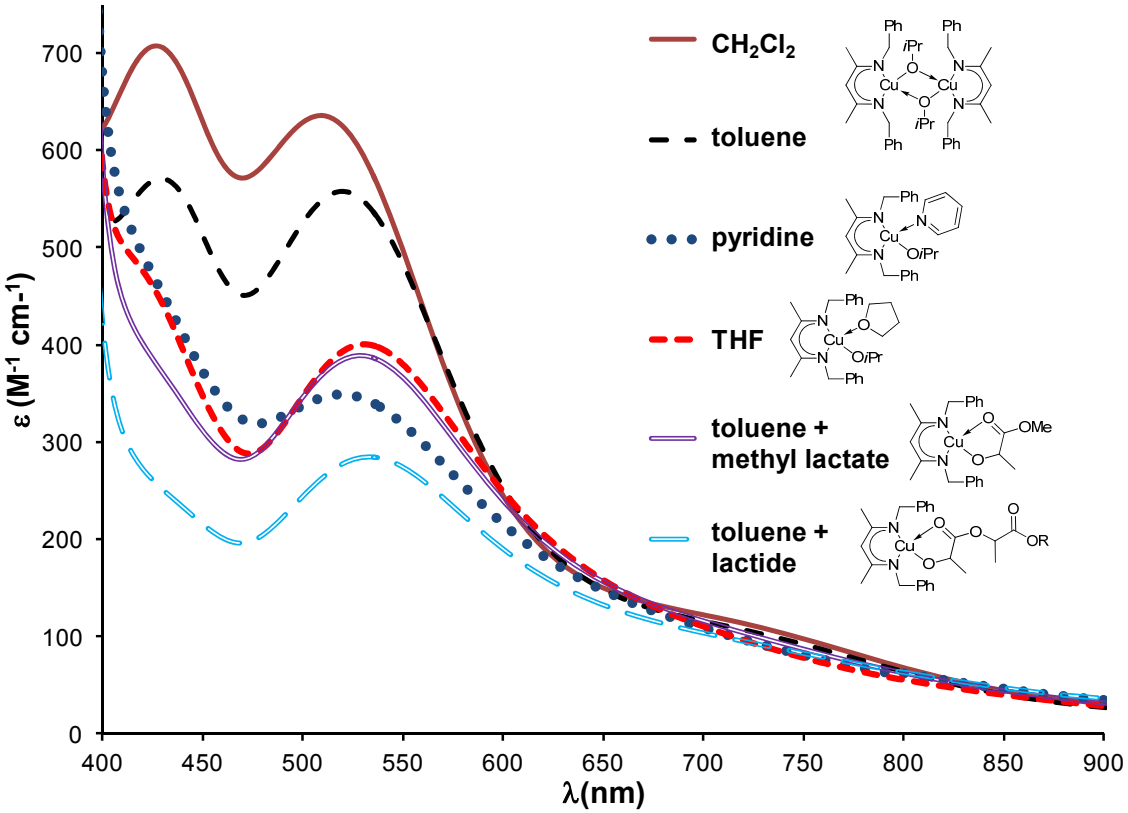

Figure 4.2. UV/vis spectra of **4.4d** in different solvents or after addition of methyl lactate or lactide, respectively.

Since *N*-benzyl diketimines were the only ligands which yielded a heteroleptic copper(II) complex, we attempted to slightly vary the electronic and steric nature of the ligand by substitution in 3-position. Reaction of **4.3d** with *N*-chlorosuccinimide afforded the expected 3-chlorosubstituted ligand **4.3e** (Scheme 4.3). Reaction of the lithiated ligand *nacnac*^{Bn}Li(THF) with *N*-bromosuccinimide, on the other hand, afforded the 3-succinimido substituted ligand **4.3f**, probably by reaction of the initially formed 3-bromosubstituted ligand with lithium succinimide.[18a] Despite their minor differences, both ligands reacted differently. Reaction of **4.3e** with Cu(O*i*Pr)$_2$ yielded the heteroleptic complex **4.4e**, while reaction of **4.3f** with Cu(O*i*Pr)$_2$ afforded homoleptic **4.5f**, at least under the conditions applied here.

Solid state structures. Crystal structures were obtained for the homoleptic complexes **4.5b**, **4.5c**, **4.5d** and **4.5f** (Fig. 4.3, Table 4.1). The coordination geometry in (L^L)$_2$M complexes can be described using the θ angles introduced by White and coworkers,[20] where $\theta_x = \theta_y = \theta_z = 90°$ represent ideal tetrahedral coordination and $\theta_x = \theta_y = 90°$, $\theta_z = 0°$ ideal square-planar geometry (Scheme 4.4). All bisdiketiminate

copper complexes, Cu(*nacnac*)$_2$, described here or elsewhere[21] show distorted geometries with $\theta_z \approx 60°$ (Table 4.1). Distortion from ideal geometry might occur for electronic reasons in tetrahedral copper complexes due to their d^9 electron configuration and for steric reasons in square-planar complexes due to the in-plane interactions of the *N*-substituents. (Pseudo-)tetrahedral Cu(II) complexes are not uncommon and the fact that the value of θ_z does not correlate with the steric demand of the *N*-substituent would argue to assign the coordination geometries as distorted tetrahedral. However, complexes electronically very similar to Cu(*nacnac*)$_2$, i. e. Cu(acac)$_2$ and Cu(*acnac*)$_2$ (acnac = 4-imino-penta-2-nonate), show square-planar geometries. Closer inspection of the structure of the sterically least encumbered bisdiketiminate complex, Cu(*nacnac*^{Me})$_2$,[22c, 22d] shows that $\theta_z \approx 60°$ actually represents the closest sterically possible approach to square-planar symmetry, even for *N*-substituents as small as methyl. Coordination geometries in **4.5b-d** and **4.5f** (Fig. 4.3) are thus best described as distorted square-planar, even though the θ_z-values are closer to a tetrahedral geometry. In **4.5b**, steric demands of the *N*-isopropylphenyl substituent lead to further distortion from ideal geometry. Although some of the steric strain is released (as often encountered in sterically demanding diketiminate complexes) by a strong bending of the Cu metal out of the mean plane of the diketiminate ligand ($\theta_M \approx 30°$, Scheme 4.4, Table 4.1), coordination around Cu in **4.5b** is highly unsymmetrical with differences in Cu-N bond lengths of 0.07 Å, $\Delta\theta_x = 15°$ and $\Delta\theta_y = 9°$ (Table 4.1). The *N*-naphtyl substituent in **4.5c** likewise introduces strong additional distortions, with one the disordered diketiminate ligands close to perpendicular to the other. Interligand π-stacking between naphtyl substituents and between naphtyl and diketiminate is observed in **4.5c**, which was absent in **4.5b** probably due to the isopropyl substituent. While θ_z values remain ≈60°, reduction of the steric impact of the *N*-substituent reduces additional distortions caused by steric interactions. Complexes **4.5d** and **4.5f** thus display only small differences in Cu-N bond lengths ($\Delta = 0.01 – 0.02$ Å), a much smaller bending of the Cu atom out of the ligand mean plane ($\theta_M = 5 – 9°$), and a symmetry much closer to the (crystallographic) C_2 symmetry observed for Cu(*nacnac*^{Me})$_2$ ($\Delta\theta_x < 3°$, $\Delta\theta_y < 5°$).

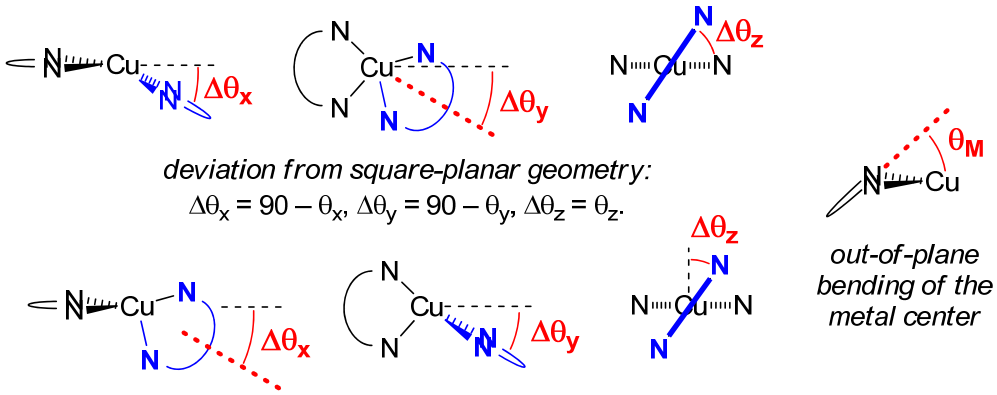
N
Cu
N
Δθx
N
Cu
N
N
Δθy
N
Δθz
N
Cu
N
N
θM
N
Cu
out-of-plane
bending of the
metal center
deviation from square-planar geometry:
Δθx = 90 – θx, Δθy = 90 – θy, Δθz = θz.
N
Cu
N
N
Δθx
N
Cu
N
N
Δθy
Δθz
N
N
Cu
N
N
deviation from tetrahedral geometry:
Δθx = 90 – θx, Δθy = 90 – θy, Δθz = 90 – θz.

Scheme 4.4

Table 4.1 Selected geometric data for homoleptic complexes **4.5b-d**, and **4.5f**.

	4.5b	**4.5c**	**4.5d**	**4.5f**	***nacnac*$^{Me}_{2}$Cu**[21c, 2] 1d	***nacnac*$_2$Cu** 21
Cu-N_A (Å)	1.943(1), 2.016(1)	1.952(3), 1.967(3)	1.946(1), 1.951(1)	1.945(1), 1.958(1) .	1.95	1.93 – 1.99
Cu-N_B (Å)	1.947(1), 2.019(1)	1.909(5) – 1.975(3)	1.974(1), 1.976(1)	1.945(1); 1.958(1)	1.95	
Δ(Cu-N)	0.07	0.02– 0.06	0.02	0.01	< 0.01	0 – 0.02
N_A-Cu-N_A, (°) N_B-Cu-N_B, (°)	90.99(6), 91.69(6)	92.21(12), 91.9(3), 94.74(16)	95.21(6), 95.58(6)	94.04(6), 93.31(6)	95	95 – 98
N_A-Cu-N_B (°)	104.29(6) – 147.23(6)	98.78(13)– 128.5(3)	101.74(6) – 135.41(6)	100.82(6) – 134.23(6)	135	98 – 137
$(N_A)_2$Cu/$(N_B)_2$Cu [a]	68	73, 81	67	62	62	60 – 67
θ_M [b]	29, 32	13, 25, 31	7, 9	5, 9	3	1 – 7
$\Delta\theta_x$ / $\Delta\theta_y$ / $\Delta\theta_z$	15 / 9 / 67	4 / 3 / 82, 8 / 9 / 72	3 / 5 / 64	3 / 0 / 59	0 / 1 / 60	
Orientation N-R [c]	syn, syn	syn, anti	syn, anti	anti, anti		

$\Delta\theta_z$ given for deviations from square-planar geometry (Scheme 4.4). N_A and N_B denote the nitrogen atoms in the first and in the second diketiminate ligand, respectively. [a] Angle between the planes formed by the N atoms of each diketiminate and Cu, roughly comparable to θ_z. [b] Bending of Cu out of the ligand mean plane, described as the angle between the N_2Cu plane and the plane formed by the two nitrogen and the two α-carbon atoms of the diketiminate ligand. [c] Relative orientation of either the N-CH_2-R or the N-Ar-R substituents.

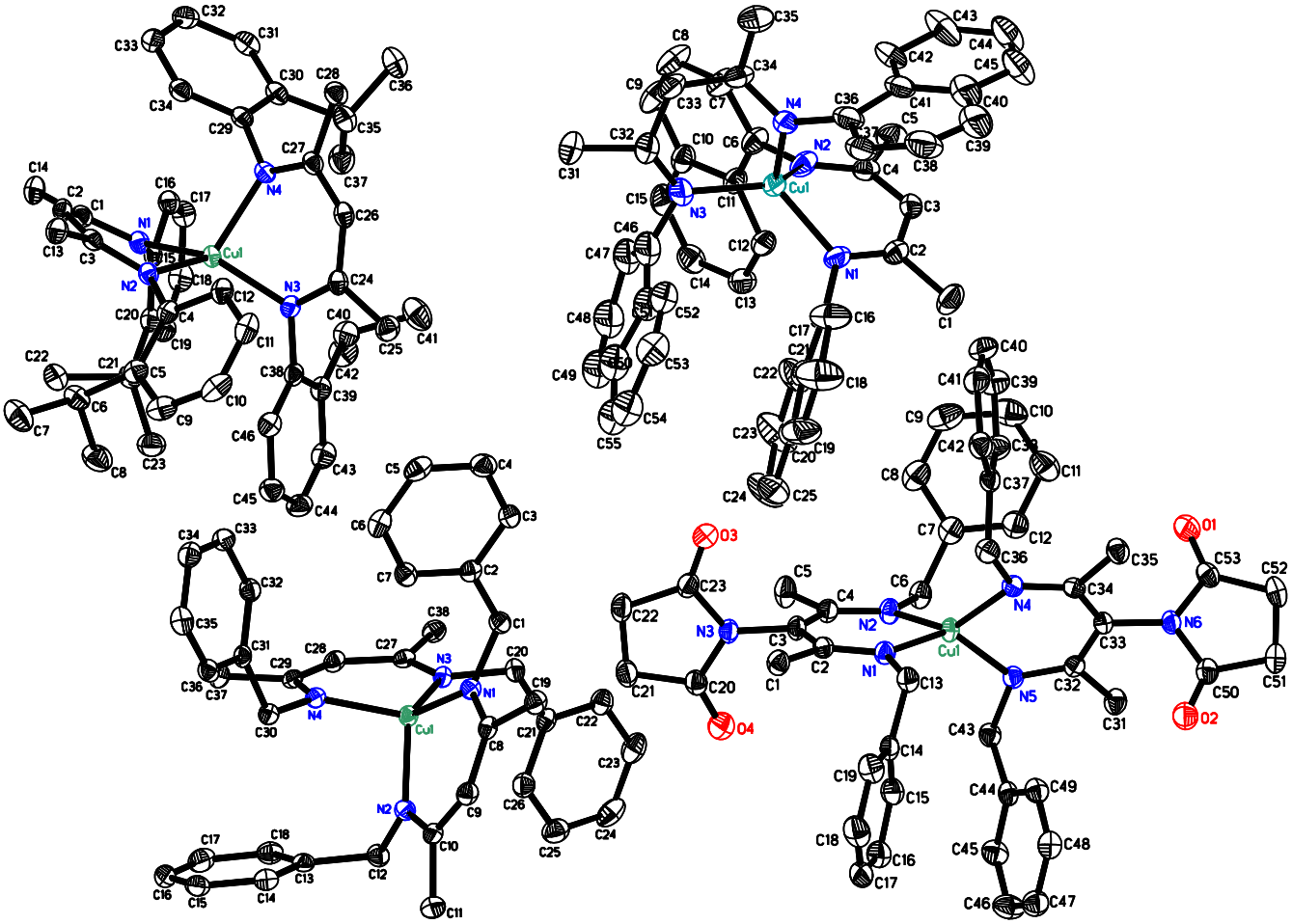

Figure 4.3. X-Ray structure of compounds **4.5b-d** and **4.5f**. Hydrogen atoms and disordered atoms in **4.5c** are omitted for clarity. Thermal ellipsoids are draw at 50% probability.

The alkoxide complexes **4.4d** and **4.4e** crystallize as oxygen-bridged dimers (Fig. 4.4). Their coordination geometry is best described as distorted square-planar, with a distortion from planarity ($\Delta\theta_z$ = 50 – 55) due to unfavourable steric interactions of the alkoxide ligands with the *N*-substituents. Cu-N distances are slightly longer than those in monomeric *nacnac*^{diip}CuOAr[16] or *nacnac*^{Ar}CuO*t*Bu[17a] (Table 4.2) and the bending of Cu out of the ligand mean plane (θ_M, Table 4.2) slightly more pronounced. Introduction of a chloride substituent in the 3-position of the ligand has barely noticeable steric consequences. Interaction between the chloride substituent and the ligand methyl groups, leads to a slight (1°) widening of the C_β-C_α-C_{Me} angles in the ligand (when compared to **4.4d**), which in turn very slightly increases the steric pressure in the front of the complex. Even this minor effect seems to be absent in the case of a succinimido substituent since structures **4.5d** and **4.5f** are practically identical.

Table 4.2. Selected geometric data for heteroleptic alkoxide complexes **4.4d**,[15] and **4.4e**.

	4.4d [15]	**4.4e**	*nacnac*^{diip}CuOAr[16]	*nacnac*^{Ar}CuO*t*Bu[17a]
Cu-N (Å)	1.921(3), 1.951(3); 1.923(3), 1.946(3)	1.917(3), 1.932(2)	1.86 – 1.90	1.88 – 1.89
Cu-O (Å)	1.951(2), 1.979(2); 1.954(2), 1.982(2)	1.948(2), 1.977(2)	1.75 – 1.82	1.78 – 1.79
N-Cu-N (°)	95.19(12); 94.92(11)	94.63(10)	96 – 97	96
N-Cu-O (°)	96.14(11) – 152.75(11)	98.46(9) – 149.23(9)	129 – 135	118 – 146
N_2Cu / Cu_2O_2 [a]	41, 43	45		
θ_M [b]	13, 14	15	0 – 6	1 – 10
$\Delta\theta_x$ / $\Delta\theta_y$ / $\Delta\theta_z$	2 / 4 / 35	0 / 2 / 40		
Orientation N-R	anti	anti		

[a] Angle between the planes formed by the N atoms of the diketiminate and Cu and by the $Cu_2(\mu\text{-}O)_2$ core. [b] Bending of the Cu out of the ligand mean plane, described as the angle between the N_2Cu plane and the plane formed by the two nitrogen and two α-carbon atoms of the diketiminate ligand. [c] Relative orientation of the N-CH_2-R substituents.

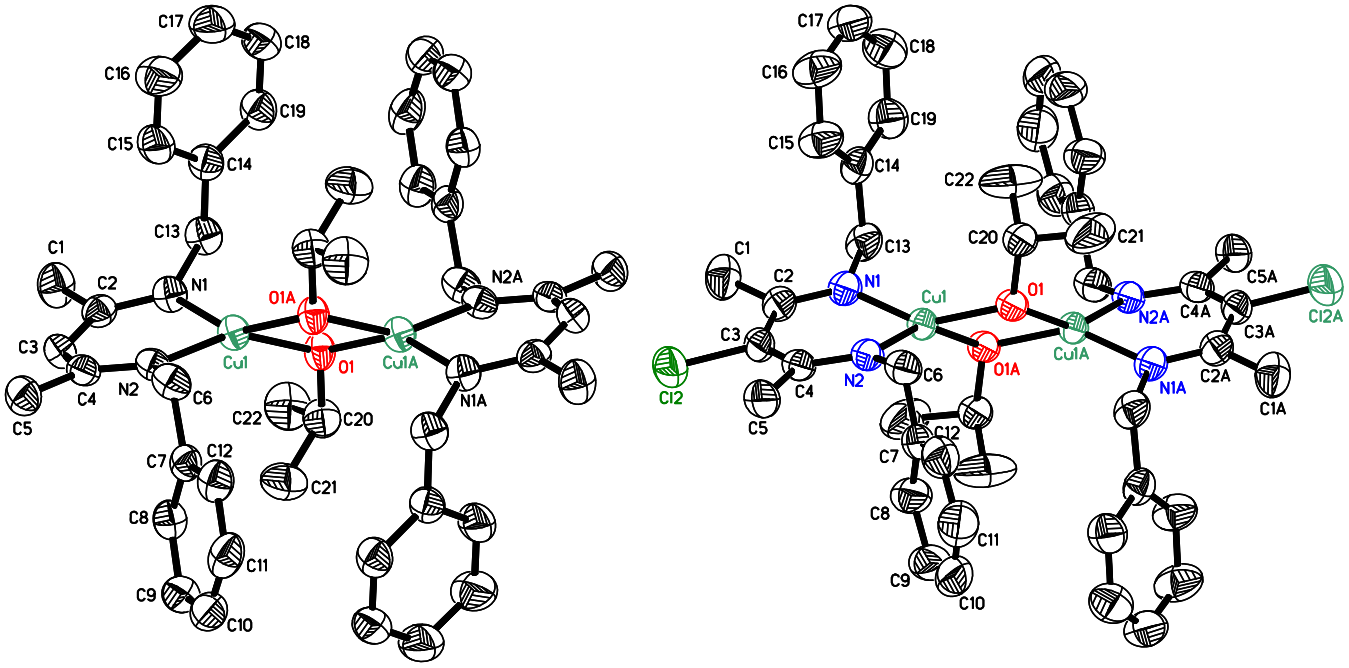

Figure 4.4. X-Ray structure of **4.4d**[15] (left) and **4.4e** (right). Hydrogen atoms are omitted for clarity. Thermal ellipsoids are drawn at 50% probability.

Lactide polymerization. Performance in *rac*-lactide polymerization was first investigated using heteroleptic **4.4d** and **4.4e** (Table 4.3). Preliminary results on the surprisingly high activity of **4.4d** (Table 4.3), given the generally low activity reported for copper(II) complexes in lactide polymerization,[13a-e] have been reported recently.[15] Structurally very similar **4.4e** was also highly active in lactide polymerization. With 1 mM **4.4d** or **4.4e** in dichloromethane at room temperature, polymerizations reached completion in <1 min or 3 min, respectively. Polymerizations with both catalysts were highly controlled and narrow polydispersities below 1.1 were obtained, indicating fast activation and the absence of side reactions. The obtained polymers were atactic, with a slight heterotactic bias *(P_r* = 0.56 for **4.4d**, 0.53 for **4.4e**. P_r = probability of alternating monomer insertion). Tetrahedral magnesium alkoxide complexes, carrying the same ligands as **4.4d** and **4.4e**, showed a slight isotactic preference for lactide polymerization at low temperatures.[12c, 22] In the case of square-planar **4.4d** and **4.4e**, polymerizations at –17 °C led only to a slight increase of the heterotactic bias. Despite very narrow polydispersities, the observed polymer molecular weight sometimes differed from expectations (e. g. Table 4.3, #1). Although experimental errors, such as weighing errors and catalyst decomposition, are more likely to be responsible

for the observed discrepancies than transesterification reactions, changes in P_r over time were investigated. (Due to the overlap of *rr*-triads, formed during transesterification, with *mm*-triads, transesterification results in an artificially low P_r value if the latter is determined from homonuclear decoupled NMR.) Thus, *rac*-lactide was polymerized with **4.4d** (> 95% conversion after 1 min) and kept for 12 h under polymerization conditions to allow transesterification of the formed polymer. Analysis of a polymer sample showed that the P_r value of the polymer decreased slightly by less than 10%, indicating a very low amount of transesterification over a time period 1000x longer than the polymerization time. In a similar experiment, polymer produced with **4.4d** from *S*,*S*-lactide was kept for 12 h without quenching. No change in the P_r value was observed. **4.4d** thus does not catalyze polymer epimerization. In both cases, addition of additional monomer confirmed that **4.4d** remained active.

Table 4.3. Polymerization of *rac*-lactide with heteroleptic and homoleptic copper complexes

#	Catalyst	Cu : lactide (: BnOH) [a]	[Cu] / mM [a]	Conversion	Time	P_r	M_n · g/mol	M_n (exp.) / M_n [b]	M_w / M_n	k_{obs} · min
1	**4.4d**	1:300	2	90 – 98%	1 – 3 min	0.56 – 0.57	27 400 – 62 300	0.7 – 1.5	1.04 – 1.07	3.6(4) – 4.4(5)
2	**4.4d**, –17 °C	1:300	2	80 – 98%	30 min	0.60 – 0.61	37 400	1.1	1.06	
3	**4.4d**	1:300:1 (**4.3d**)	2	36%	90 min	0.64	53 300	0.5	1.06	$5.1(1)\cdot10^{-3}$
4	**4.4e**	1:300	2	95 – 98%	3 – 11 min	0.53 – 0.54	29 400	1.4	1.04	0.8(1) – 1.3(2)
5	**4.4e**, –17 °C	1:300	2	95 – 98%	60 – 175 min	0.53 – 0.54	30 300	1.4	1.04	
6	**4.5d**	1:300	2	10%	10 min					$\approx10^{-2}$
7	**4.5d**	1:300:1 [c]	2	95%	45 min	0.60	26 400	1.6	1.04	$11.2(1)\cdot10^{-2}$
8	**4.5d**	1:300:1	2	95%	40 min	0.59	29 900	1.4	1.03	$9.6(2)\cdot10^{-2}$
9	**4.5d**	1:300:1 (*i*PrOH)	2	75%	40 min	0.60	41 600	0.8	1.04	$3.8(1)\cdot10^{-2}$
10	**4.5d**	1:300:1 (*i*PrOH)	2	97%	125 min	0.58	46 400	0.9	1.03	$4.4(1)\cdot10^{-2}$
11	**4.5b**	1:300	2	80%	85 min	0.63	487 700	0.07	1.12	
12	**4.5b**	1:300:1 [c]	2	98%	60 min	0.59	30 500	1.4	1.48	$12.0(4)\cdot10^{-2}$
13	**4.5b**	1:300:1	2	95%	60 min	0.60	35 300	1.2	1.07	$6.7(3)\cdot10^{-2}$
14	**4.5b**	1:300:25	2	98%	60 min	0.57	1400	1.3	1.12	$17.2(9)\cdot10^{-2}$

15	**4.5c**	1:300	2	7%	60 min		56 000	0.06	1.06	
16	**4.5c**	1:300:1	2	95%	60 min	0.52	4300	4.8	1.08	$6.4(3)\cdot10^{-2}$
17	**4.5f**	1:300	2	10%	60 min		79 300	0.06	1.14	
18	**4.5f**	1:300:1	2	95%	60 min	0.57	4300	4.8	1.53	$12.7(5)\cdot10^{-2}$

If a range is provided: minimum and maximum values of three experiments. GPC analysis performed only on selected examples. Conditions: CH_2Cl_2, ambient temperature. P_r determined from decoupled ^{1}H NMR by $P_r = 2\cdot I_1/(I_1+I_2)$, with I_1 = 5.20 – 5.25 ppm (*rmr, mmr/rmm*), I_2 = 5.13 – 5.20 ppm (*mmr/rmm, mmm, mrm*). M_n and M_w determined by size exclusion chromatography vs. polystyrene standards, with a Mark-Houwink correction factor of 0.58. [a] Concentrations and ratios provided per Cu atom, i. e. for (putative) monomeric complexes. [b] M_n(expected) = [lactide]/([Cu] + [ROH]) · conversion · $M_{lactide}$ + M_{ROH}. [c] Alcohol added after 10 min polymerization time.

Given that only homoleptic diketiminate complexes were obtained with ligands **4.3b**, **4.3c** and **4.3f**, their activity in rac-lactide polymerization was verified. Polymerization with **4.5d** under conditions identical to **4.4d** yielded, unsurprisingly, a very low activity due to the absence of a suitable initiator group and only 10% conversion was observed after 10 min (Table 4.4, Fig. S4.3). Addition of benzyl alcohol increased the activity by an order of magnitude. The polymerization was completely controlled with polydispersities below 1.05 and showed the molecular weight expected from the amount of added alcohol. The pseudo-first order rate constant $k_{obs} = 9 \cdot 10^{-2}$ min^{-1} was, however, 50× lower than the rate observed for the heteroleptic complex **4.4d**, although the same active species should have been obtained after the first monomer insertion. We thus assume that protonation of a diketiminate ligand by benzyl alcohol is unfavourable and that polymerization occurs under immortal polymerization conditions catalyzed by approx. 2% of heteroleptic complex present in the equilibrium under these conditions (Scheme 4.5). The latter mechanism is supported by the fact that **4.4d** is stable under immortal polymerization conditions,[15] that UV/vis absorbance titrations of **4.4d** with ligand **4.3d** yield the homoleptic complex **4.5d** and that addition of one equiv **4.3d** to *rac*-lactide polymerizations with **4.4d** reduced activities drastically by three orders of magnitude (Table 4.3, #3). If isopropanol instead of benzyl alcohol is employed as co-catalyst, a notably longer induction period and an overall lower activity was observed (Table 4.3, Fig. S4.3). While the induction period can be explained by the lower acidity of isopropanol compared to benzyl alcohol, activity is governed by the acidity of the polymeryl alcohol and should be independent of the starting alcohol, once all catalyst initiated. We have at the moment no explanation for this behaviour.

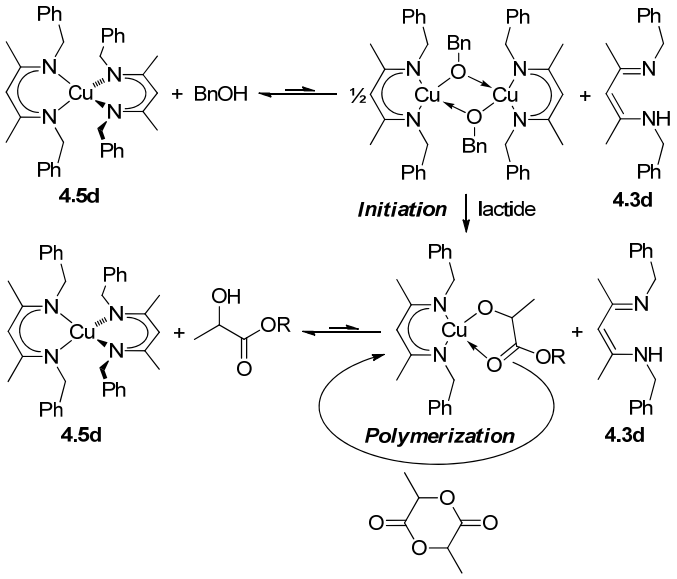

Scheme 4.5

Polymerizations with homoleptic **4.5b** in the absence of any co-catalyst again proceeded sluggishly. A positive curvature of the conversion/time plot up to 60 min (Fig. S4.4) and a polymer weight of 500 000 g/mol indicate slow activation of small amounts of **4.5b**, most likely by impurities in the monomer. It should be noted that although only 5% of **4.5b** were active in polymerization with an extremely slow initiation, and although polymerization had to be quenched at 80% when the solution became too viscous to stir, the obtained polymer still showed a very narrow polydispersity of 1.12. Addition of benzyl alcohol as a co-catalyst reduced the induction period to appr. 10 min and yielded an activity approximately half as high as that of **4.5d**. In the presence of 25 equiv of benzyl alcohol, the induction period disappeared and activity increased by a factor of 2 – 3, in agreement with the mechanism proposed in Scheme 4.5.

Homoleptic **4.5c** and **4.5f** likewise showed very low polymerization activity from a small number of catalyst centres in the absence of benzyl alcohol (Table 4.4), but became moderately active in its presence (Table 4.4, Fig. 4.5). Both catalysts show unexpectedly low polymer molecular weight in the presence of benzyl alcohol, and **4.5f** was the first Cu catalyst presented here which gave polydispersities above 1.1. Comparison of the conversion/time data in Fig. 4.5 reveals that the structurally similar *N*-benzyl complexes **4.5d** and **4.5f** also have very similar activities. Apart from the loss of polymer molecular weight control, there seems thus to be no noticeable impact of the succinimido substituent on

polymerization. Complexes **4.5b** and **4.5c** with mono-ortho-substituted *N*-aryl substituents also show very similar activity, about half as high as the *N*-alkyl derivatives. Contrary to **4.5d** and **4.5f**, they show the presence of an induction period. Both, delayed initiation as well as lower activity, would be expected in **4.5b** and **4.5c** due to the higher acidity of *N*-aryl diketimines compared to *N*-alkyl diketimines. All polymers obtained with **4.5b-d**, and **4.5f** were essentially atactic with a slight heterotactic bias (P_r = 0.52 – 0.60). The P_r-value obtained for **4.5d**/BnOH (P_r = 0.59 – 0.60) is 3% higher than for **4.4d**, although the active species should be identical in both polymerizations. Although the mechanistic reason for this slight change in stereospecifity is unclear, we noted a similar behaviour in diketiminate magnesium complexes, which showed a slightly decreased P_r value (change < 5%) in the presence of excess alcohol.[22]

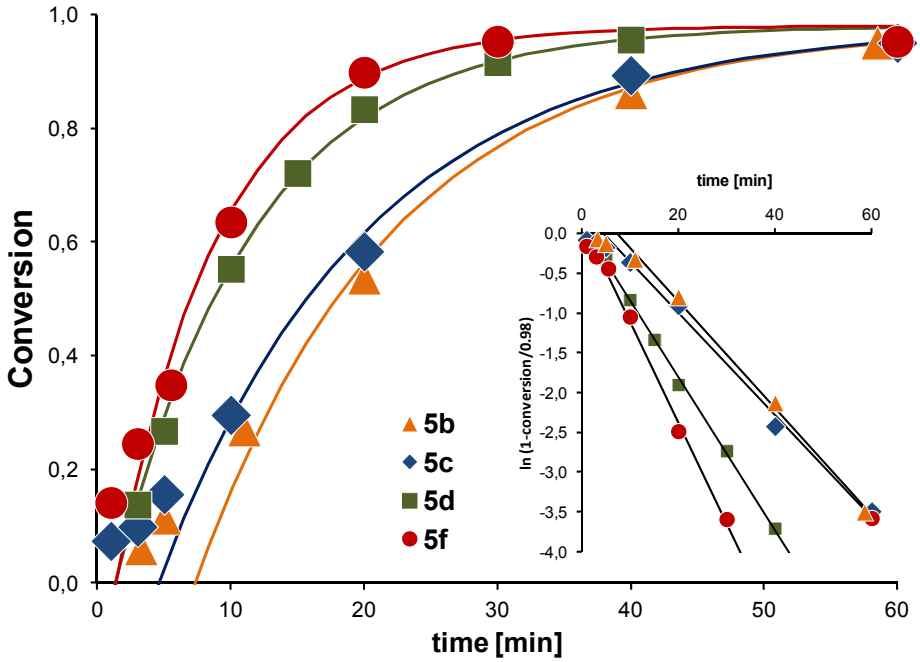

Figure 4.5. Conversion-time plots for *rac*-lactide polymerization with homoleptic **4.5b-d** and **4.5f**.

Conclusions

The chemistry of Cu(II) diketiminate alkoxide complexes is governed by their strong tendency to achieve four-coordination in square-planar geometry on one hand and the steric constraints of the diketiminate ligand on the other. In the case of sterically undemanding *N*-alkyl diketimines, the monomeric intermediate *nacnac*CuO*i*Pr, obtained upon reaction of Cu(O*i*Pr)$_2$ with diketimine, stabilizes

via simple dimerization. Sterically more demanding *mono-ortho*-substituted *N*-aryl substituents, such as 9-naphtyl nor 2-isopropylphenyl, do not yield a dimeric heteroleptic complex. Instead, homoleptic Cu(*nacnac*)$_2$ is obtained, which seems to be the thermodynamic rather than the kinetic product. Further increase in steric bulk, i. e. the use of 2,6-disubstituted *N*-aryl substituents such as the ubiquitous 2,6-diisopropylphenyl, prevents the formation of the homoleptic complex for steric reasons. In the absence of β-hydrogen atoms on the alkoxide ligand, the three-coordinated intermediate can then be isolated as the reaction product. If β-hydrogen atoms are present, β-H-elimination will produce the respective ketone or aldehyde, and Cu(II) hydride which will decompose.

Heteroleptic (X*nacnac*^{Bn}CuO*i*Pr)$_2$ showed activities in lactide polymerization comparable to the best catalysts reported. The catalysts show high molecular weight control with polydispersities typically below 1.1 even under immortal polymerization conditions and do not suffer from side reactions such as transesterification, epimerization or (undesired) chain transfer. Combined with their high activity, they are promising candidates for the production of block-copolymers and we are currently investigating the scope of these catalysts with regards to different monomers.

Homoleptic Cu(*nacnac*)$_2$ can be activated by alcohol as a co-catalyst to yield moderately active polymerization catalysts (1 h to completion at room temperature) which retain the high polymer molecular weight control of the heteroleptic complexes. Given that 1 h is a reasonable time-scale for polymerization experiments, the easy accessibility of Cu bisdiketiminate complexes drastically simplifies synthetic requirements. Since only a small part of the homoleptic complex is activated for polymerization, polymer molecular weight is determined from the monomer:alcohol ratio and small amounts of catalyst decomposition by impurities should be tolerated without impact on the obtained polymer molecular weight. These catalysts do not contain an initiating group and are thus suitable catalysts for the polymerization of macroinitiators.

Experimental Section

General considerations. All reactions were carried out using Schlenk or glove box techniques under nitrogen atmosphere. Cu(O*i*Pr)$_2$,[23] *nacnac*$^{d\text{ipp}}$H (**4.3a**),[24] *nacnac*$^{\text{ipp}}$H (**4.3b**),[25] *nacnac*$^{\text{Naph}}$H (**4.3c**),[26] and *nacnac*$^{\text{Bn}}$H (**4.3d**)[27] were prepared according to literature. Solvents were dried by passage through activated aluminum oxide (MBraun SPS), de-oxygenated by repeated extraction with nitrogen, and stored over molecular sieves. C_6D_6 was dried over sodium and degassed by three freeze-pump-thaw cycles. $CDCl_3$ and CD_2Cl_2 were dried over 3 Å molecular sieves. *rac*-Lactide (98%) was purchased from Sigma–Aldrich, purified by 3× recrystallization from dry ethyl acetate and kept at –30 °C. All other chemicals were purchased from common commercial suppliers and used without further purification. ^{1}H and ^{13}C NMR spectra were acquired on a Bruker AVX 400 spectrometer. The chemical shifts were referenced to the residual signals of the deuterated solvents (C_6D_6: ^{1}H: δ 7.16 ppm, ^{13}C: δ 128.38 ppm, $CDCl_3$: ^{1}H: δ 7.26 ppm, CD_2Cl_2: 1H: δ 5.32 ppm, CD_3CN: 1H: δ 1.94 ppm, ^{13}C: δ 1.32 ppm). Elemental analyses were performed by the Laboratoire d'analyse élémentaire (Université de Montréal). Molecular weight analyses were performed on a Waters 1525 gel permeation chromatograph equipped with three Phenomenex columns and a refractive index detector at 35 °C. THF was used as the eluent at a flow rate of 1.0 mL·min^{-1} and polystyrene standards (Sigma–Aldrich, 1.5 mg·mL^{-1}, prepared and filtered (0.2 mm) directly prior to injection) were used for calibration. Obtained molecular weights were corrected by a Mark-Houwink factor of 0.58.[28]

***N,N'*-dibenzyl-2-amino-3-chloro-4-imino-2-pentene, Cl*nacnac*$^{\text{Bn}}$H, 4.3e.** To a solution of **4.3d** (5.48 g, 19.7 mmol) in dry THF (150 mL) was added *N*-chlorosuccinimide (3.00 g, 22.4 mmol). After stirring at room temperature for 45 minutes, a white precipitate formed which was removed by filtration. H_2O (500 mL) was then added. The product was extracted using hexanes (2 x 600 mL). After drying over Na_2SO_4 the solvent was evaporated. The obtained yellow oil was crystallized from dry ethanol at –90 °C, washed with cold dry ethanol and recrystallized from refluxing ethanol. The eluate yielded a second fraction at –80 °C (colourless crystals, 3.41 g, 55%).

^{1}H-NMR ($CDCl_3$, 400 MHz, 298 K): δ 12.22 (bs, 1H, NH), 7.25-7.19 (m, 10H, Ph), 4.49 (s, 4H, NCH_2), 2.18 (s, 6H, Me). ^{13}C{^{1}H} NMR ($CDCl_3$, 75 MHz, 298 K): δ 160.3 (*C*=N), 140.5 (*ipso* Ph), 128.6 (*ortho*

or *meta* Ph), 127.3 (*ortho* or *meta* Ph), 126.8 (*para* Ph), 127.7 (ClC), 51.5 (NCH_2), 17.3 (Me). Anal. Calcd. for $C_{19}H_{21}ClN_2$: C, 72.95; H, 6.77; N, 8.95. Found: C, 72.89; H, 6.66; N, 9.17.

***N,N'*-dibenzyl-2-amino-3-succinimido-4-imino-2-pentene, 3-succinimido-*nacnac*^{Bn}H, 4.3f.** N-Bromosuccinimide (224 mg, 1.26 mmol) and *nacnac*^{Bn}Li(THF) (440 mg, 1.24 mmol) were suspended in THF (30 mL) and heated at 60 °C for 24 h to afford a brown solution. 1,4-dioxane (1 mL) was added to precipitate LiCl. After additional stirring for 15 min at room temperature, the mixture was filtered and the filtrate evaporated. The resulting brown residue was dissolved in dichloromethane (3 mL). Hexane (12 mL) was added, the mixture filtered and the filtrate allowed to slowly evaporate, yielding dark-yellow crystals (250 mg, 54%). ^{1}H-NMR (CD_3CN), 400 MHz, 298 K): δ 12.57 (bs, 1H, NH), 7.28–7.19 (m, 10H, Ph), 4.47 (s, 4H, CH_2), 2.76 (s, 4H, NCH_2), 1.76 (s, 6H, CH_3). ^{13}C{^{1}H} NMR (CD_3CN, 101 MHz, 298 K): δ 179.3 (*C*=O), 161.6 (*C*=N), 141.5 (*ipso* Ph), 129.5 (*ortho* or *meta* Ph), 128.4 (*ortho* or *meta* Ph), 127.7 (*para* Ph), 98.9 (NC), 51.5 (NCH_2), 28.8 (CH_2), 14.8 (Me). Anal. Calcd. for $C_{23}H_{25}N_3O_2$: C, 73.57; H, 6.71; N, 11.19. Found: C, 73.28; H, 6.69; N 10.84.

[*nacnac*^{Bn}Cu(μ-O)*i*Pr]$_2$, 4.4d.[15] Cu(O*i*Pr)$_2$ (500 mg, 2.75 mmol) was suspended in toluene (20 mL). **4.3d** (610 mg, 2.20 mmol) was added slowly to the mixture and allowed to react at room temperature for 18 h. The reaction mixture changed colour from deep green to deep blue. Solvent and isopropanol were removed under reduced pressure. The blue solid was taken up in toluene (15 mL) and filtered through a fine frit. The filtrate was placed at –25 °C yielding purple-red crystals (550 mg, 63%). Anal. Calcd. for $C_{22}H_{28}CuN_2O$: C, 66.06; H, 7.05; N, 7.00. Found: C, 66.33; H, 7.22; N 6.82. UV/vis (toluene): λ/nm (ε·M·cm) 357 (10000), 431 (570), 523 (560), 720 (sh, 100). UV/vis (THF): λ/nm (ε·M·cm) 421 (sh 470), 533 (400).

[*nacnac*^{Bn}Cu(μ-O)*i*Pr]$_2$, 4.4e. Using the same procedure as for **4.4d**. Cu(O*i*Pr)$_2$ (500 mg, 2.75 mmol), hexanes or toluene (20 mL), **4.3e** (690 mg, 220 mmol) yielded 350 mg (0.80 mmol, 36%) purple-red crystals.

Anal. Calcd. for $C_{22}H_{27}ClCuN_2O$: C, 60.82; H, 6.26; N, 6.45. Found: C 60.76, H 6.17, N 6.34.

Cu(*nacnac*^{ipp})$_2$, 4.5b. Diketimine **4.3b** (2.00 g, 5.98 mmol) was added to a heterogeneous solution of Cu(O*i*Pr)$_2$ (0.54g, 2.98 mmol) in toluene (20 mL) and allowed to stir overnight. The solvent was then removed in vacuo from the dark green solution, giving a dark green (unreacted Cu(O*i*Pr)$_2$) waxy solid. The mixture was dissolved in a minimum of hexanes and filtered over celite. Pure product was isolated by crystallization at –35 °C to yield purple crystals (0.68 g, 0.93 mmol, 63%). Mp: 154 °C. Anal. Calcd. for $C_{46}H_{58}CuN_4$: C, 75.63; H, 8.00; N, 7.67. Found: C, 75.47; H, 8.02; N, 7.47. UV/vis (toluene): λ/nm (ε·M·cm): 440 (sh, 1400), 460 (1300).

Cu(*nacnac*^{Naph})$_2$, 4.5c. Following the same procedure as for **4.5b**, **4.3c** (0.82 g, 1.1 mmol), Cu(O*i*Pr)$_2$ (0.10 g, 0.54 mmol), toluene (10 mL) gave a dark green waxy solid. The mixture was dissolved in a minimum of dichloromethane and filtered over celite. Crystallization by slow evaporation yielded green crystals (0.21 g, 0.28 mmol, 51%). Mp: 149 °C. Anal. Calcd. for $C_{50}H_{42}CuN_4$: C, 78.76; H, 5.55; N, 7.35. Found: C, 78.79; H, 5.63; N, 7.33. UV/vis (toluene): λ/nm (ε·M·cm) 537 (1000), 670 (1200).

Cu(*nacnac*^{Bn})$_2$, 4.5d. Following the same procedure as for **4.5b**, **4.3d** (0.70 g, 2.5 mmol), Cu(O*i*Pr)$_2$ (0.25 g, 1.2 mmol), toluene (20 mL) gave a purple wax-like solid. The mixture was dissolved in a minimum of hexanes and filtered over celite. **4.5d** was isolated by crystallization at –35 °C as purple crystals (0.98 g, 0.158 mmol, 64%). Mp: 62 °C. Anal. Calcd. for $C_{38}H_{42}CuN_4$: C, 73.81; H, 6.85; N, 9.06. Found: C, 73.74; H, 6.81; N, 9.02. UV/vis (toluene): λ/nm (ε·M·cm) 446 (550), 546 (1500).

Cu(3-succinimido-*nacnac*^{Bn})$_2$, 4.5f. Following the same procedure as for **4.5b**, **4.3f** (0.32 g, 0.74 mmol) , Cu(O*i*Pr)$_2$ (65 mg, 0.36 mmol), toluene (10 mL) gave a dark-purple waxy solid. The solid was dissolved in a minimum of dichloromethane and filtered over celite. Crystallization by slow evaporation yielded 0.30 g (0.74 mmol, 87%) of purple crystals. Mp: 174 °C. Anal. Calcd. for $C_{46}H_{48}CuN_6O_4 \cdot CH_2Cl_2$: C, 62.90; H, 5.62; N, 9.36. Found: C, 62.06; H, 5.71; N, 8.96. (One equivalent of dichloromethane was found in the X-ray structure.) UV/vis (toluene): λ/nm (ε·M·cm) 432 (620), 531 (1300), 726 (sh, 400).

***rac*-Lactide polymerization.** In the glove box a stock solution of the catalyst (100 μL, $5.0 \cdot 10^{-2}$ M in CH_2Cl_2, 5.0 μmol) was added to lactide (220 mg, 1.5 mmol) in dichloromethane (2.5 mL). If desired,

benzyl alcohol ($5.0 \cdot 10^{-2}$ M in CH_2Cl_2) was added to the reaction mixture. Samples for kinetic investigations were taken at the desired intervals and added to vials already containing a dichloromethane solution of acetic acid (5 mM). Reaction mixtures were quenched at the desired polymerization time by addition of a dichloromethane solution of acetic acid (5 mM). For samples as well as the bulk reaction, volatiles were immediately evaporated. Solid polymer samples were stored at –80 °C. Conversion was determined from ^{1}H NMR in $CDCl_3$ by comparison to remaining lactide. P_r values were determined from homodecoupled ^{1}H NMR spectra.

X-ray diffraction. Single crystals were obtained directly from isolation of the products as described above. Diffraction data were collected with Cu Kα radiation on Bruker Microstar/Proteum, equipped with Helios mirror optics and rotating anode source or on a Bruker APEXII with a Cu microsource/Quazar MX optics using the APEX2 software package.[29] Data reduction was performed with SAINT,[30] absorption corrections with SADABS.[31] Structures were solved with direct methods (SHELXS97).[32] All non-hydrogen atoms were refined anisotropic using full-matrix least-squares on F^2 and hydrogen atoms refined with fixed isotropic U using a riding model (SHELXL97).[32] In **4.5f**, cocrystallized dichloromethane was found to be disordered and refined with appropriate restraints (0.7:0.3 occupancy). In 5c, one diketiminate ligand was found disordered with N-naphtyl orientations inverted by 180 °C. The disorder was resolved using appropriate restraints (SIMU/SADI) and refined to 0.7:0.3 occupation. Additional fluxionality exists and electron density indicates even further *N*-naphthyl rotamers, which were not resolved. Further experimental details can be found in Table 4.4 and in the supporting information (CIF).

Table 4.4. Details of X-ray Diffraction Studies

	4.4e	**4.5b**	**4.5c**	**4.5d**	**4.5f**
Formula	$C_{44}H_{54}Cl_2Cu_2N_4O_2$	$C_{46}H_{58}CuN_4$	$C_{50}H_{42}CuN_4$	$C_{38}H_{42}CuN_4$	$C_{46}H_{48}CuN_6O_4 \cdot CH_2Cl_2$
M_w (g/mol); $d_{calcd.}$ (g/cm^3)	868.89; 1.400	730.50; 1.194	762.41; 1.291	618.29; 1.302	897.37;
T (K); F(000)	150; 908	100; 1564	100; 798	100; 654	150; 1876
Crystal System	monoclinic	monoclinic	triclinic	triclinic	monoclinic
Space Group	$P2_1/n$	$P2_1/c$	P-1	P-1	$P2_1/c$
Unit Cell: a (Å)	13.6092(14)	16.6129(5)	12.0601(13)	9.5454(6)	11.2594(4)
b (Å)	10.2310(10)	10.4872(3)	12.1002(13)	11.3169(7)	17.7065(7)
c (Å)	14.8126(16)	23.5375(7)	16.0178(18)	15.0776(10)	21.5097(8)
α (°)			78.080(4)	93.248(3)	
β (°)	91.846(5)	97.799(2)	75.677(4)	103.821(3)	91.886(2)
γ (°)			60.513(5)	92.335(3)	
V (Å^3); Z	2061.4(4); 2	4062.8(2); 4	1961.5(4); Z	1576.57(18); 2	4285.9(3); 4
μ (mm^{-1}); Abs. Corr.	2.786; multiscan	1.018; multiscan	1.089; multiscan	1.219; multiscan	2.283; multiscan
θ range (°); completeness	4 – 70; 0.99	3 – 71; 0.99	3 – 72; 0.97	3 – 70; 0.98	3 – 70; 1.00
collected reflections; R_σ	39607; 0.023	58938; 0.026	54014; 0.026	35571; 0.028	100806; 0.063
unique reflections; R_{int}	3895; 0.059	7830; 0.046	7430; 0.048	5844; 0.043	8180;
R1(F) ($I > 2\sigma(I)$)	0.047	0.037	0.076	0.037	0.036
wR(F^2) (all data)	0.145	0.103	0.1948	0.102	0.101
GoF(F^2)	1.04	1.03	1.04	1.06	1.04
Residual electron density	0.35; –0.82	0.44; –0.40	1.25; –1.18	0.71; –0.36	0.45; –0.39

Acknowledgments. We thank Lylia Dif-Yaiche for her contributions to the synthesis of **4.5d** during her internship. This work was supported by the Natural Sciences and Engineering Research Council of Canada (NSERC) and the Centre in Green Chemistry and Catalysis (CGCC). We thank Pierre Ménard-Tremblay and Dr. R. E. Prud'homme for access to GPC and Elena Nadezhina for elemental analyses.

Supporting information. Figures S3.1 – S3.4. Details of the crystal structure determinations (CIF).

Reference Section

(1) (a) Luckachan, G. E.; Pillai, C. K. S. *J. Polym. Environ.* **2011**, *19*, 637. (b) Ahmed, J.; Varshney, S. K. *Int.J. Food Prop.* **2011**, *14*, 37. (c) Inkinen, S.; Hakkarainen, M.; Albertsson, A.-C.; Södergård, A. *Biomacromolecules* **2011**, *12*, 523.

(2) Hottle, T. A.; Bilec, M. M.; Landis, A. E. *Polymer Degradation and Stability* **2013**, *98*, 1898.

(3) Marshall, E. L.; Gibson, V. C.; Rzepa, H. S. *J. Am. Chem. Soc.* **2005**, *127*, 6048.

(4) (a) Dutta, S.; Hung, W.-C.; Huang, B.-H.; Lin, C.-C. In *Synthetic Biodegradable Polymers*, Rieger, B.; Künkel, A.; Coates, G. W.; Reichardt, R.; Dinjus, E.; Zevaco, T. A., Eds. Springer-Verlag: Berlin, 2011; Vol. pp 219. (b) Dijkstra, P. J.; Du, H.; Feijen, J. *Polym. Chem.* **2011**, *2*, 520. (c) Ajellal, N.; Carpentier, J.-F.; Guillaume, C.; Guillaume, S. M.; Helou, M.; Poirier, V.; Sarazin, Y.; Trifonov, A. *Dalton Trans.* **2010**, *39*, 8363. (d) Stanford, M. J.; Dove, A. P. *Chem. Soc. Rev.* **2010**, *39*, 486. (e) Williams, C. K.; Hillmyer, M. A. *Polym. Rev.* **2008**, *48*, 1. (f) O'Keefe, B. J.; Hillmyer, M. A.; Tolman, W. B. *J. Chem. Soc., Dalton Trans.* **2001**, 2215.

(5) (a) Spassky, N.; Wisniewski, M.; Pluta, C.; Le Borgne, A. *Macromol. Chem. Phys.* **1996**, *197*, 2627. (b) Zhong, Z.; Dijkstra, P. J.; Feijen, J. *Angew. Chem., Int. Ed.* **2002**, *41*, 4510. (c) Chisholm, M. H.; Patmore, N. J.; Zhou, Z. *Chem. Commun. (Cambridge, U. K.)* **2005**, 127. (d) Chisholm, M. H.; Gallucci, J. C.; Quisenberry, K. T.; Zhou, Z. *Inorg. Chem.* **2008**, *47*, 2613.

(6) Dagorne, S.; Normand, M.; Kirillov, E.; Carpentier, J.-F. *Coord. Chem. Rev.* **2013**, *257*, 1869.

(7) (a) Cao, T.-P.-A.; Buchard, A.; Le Goff, X. F.; Auffrant, A.; Williams, C. K. *Inorg. Chem.* **2012**, *51*, 2157. (b) Thomas, C. M. *Chem. Soc. Rev.* **2010**, *39*, 165.

(8) (a) Cushion, M. G.; Mountford, P. *Chem. Commun. (Cambridge, U. K.)* **2011**, *47*, 2276. (b) Calvo, B.; Davidson, M. G.; Garcia-Vivo, D. *Inorg. Chem.* **2011**, *50*, 3589.

(9) Sauer, A.; Kapelski, A.; Fliedel, C.; Dagorne, S.; Kol, M.; Okuda, J. *Dalton Trans.* **2013**, *42*, 9007.

(10) Cheng, M.; Attygalle, A. B.; Lobkovsky, E. B.; Coates, G. W. *J. Am. Chem. Soc.* **1999**, *121*, 11583.

(11) (a) Wheaton, C. A.; Hayes, P. G. *Comments on Inorganic Chemistry* **2011**, *32*, 127. (b) Wheaton, C. A.; Hayes, P. G.; Ireland, B. J. *Dalton Trans.* **2009**, 4832

(12) (a) Wang, L.; Ma, H. *Macromolecules* **2010**, *43*, 6535. (b) Buffet, J.-C.; Davin, J. P.; Spaniol, T. P.; Okuda, J. *New J. Chem.* **2011**, *35*, 2253. (c) Drouin, F.; Whitehorne, T. J. J.; Schaper, F. *Dalton Trans.* **2011**, *40*, 1396. (d) Sung, C.-Y.; Li, C.-Y.; Su, J.-K.; Chen, T.-Y.; Lin, C.-H.; Ko, B.-T. *Dalton Trans.* **2012**, *41*, 953.

(13) (a) Sun, J.; Shi, W.; Chen, D.; Liang, C. *J. Appl. Polym. Sci.* **2002**, *86*, 3312. (b) John, A.; Katiyar, V.; Pang, K.; Shaikh, M. M.; Nanavati, H.; Ghosh, P. *Polyhedron* **2007**, *26*, 4033. (c) Bhunora, S.; Mugo, J.; Bhaw-Luximon, A.; Mapolie, S.; Van Wyk, J.; Darkwa, J.; Nordlander, E. *Appl. Organomet. Chem.* **2011**, *25*, 133. (d) Chen, L.-L.; Ding, L.-Q.; Zeng, C.; Long, Y.; Lü, X.-Q.; Song, J.-R.; Fan, D.-D.; Jin, W.-J. *Appl. Organomet. Chem.* **2011**, *25*, 310. (e) Gowda, R. R.; Chakraborty, D. *J. Molec. Catal. A: Chem.* **2011**, *349*, 86. (f) Li, C.-Y.; Hsu, S.-J.; Lin, C.-l.; Tsai, C.-Y.; Wang, J.-H.; Ko, B.-T.; Lin, C.-H.; Huang, H.-Y. *J. Polym. Sci., Part A: Polym. Chem.* **2013**, *51*, 3840.

(14) Ding, L.; Jin, W.; Chu, Z.; Chen, L.; Lü, X.; Yuan, G.; Song, J.; Fan, D.; Bao, F. *Inorg. Chem. Commun.* **2011**, *14*, 1274.

(15) Whitehorne, T. J. J.; Schaper, F. *Chem. Commun.* **2012**, *48*, 10334.

(16) Jazdzewski, B. A.; Holland, P. L.; Pink, M.; Young, V. G.; Spencer, D. J. E.; Tolman, W. B. *Inorg. Chem.* **2001**, *40*, 6097.

(17) (a) Wiese, S.; Badiei, Y. M.; Gephart, R. T.; Mossin, S.; Varonka, M. S.; Melzer, M. M.; Meyer, K.; Cundari, T. R.; Warren, T. H. *Angew. Chem., Int. Ed.* **2010**, *49*, 8850. (b) Melzer, M. M.; Mossin, S.; Cardenas, A. J. P.; Williams, K. D.; Zhang, S.; Meyer, K.; Warren, T. H. *Inorg. Chem.* **2012**, *51*, 8658.

(18) (a) Oguadinma, P. O.; Schaper, F. *Organometallics* **2009**, *28*, 4089. (b) Oguadinma, P. O.; Schaper, F. *Organometallics* **2009**, *28*, 6721. (c) Oguadinma, P. O.; Schaper, F. *Can. J. Chem.* **2010**, *88*, 472.

(19) In several instances, **5d** was obtained even when only 1 equiv of diketimine was used, complicating the preparation of **4d**. The reason for the differences in reaction outcome remains unclear and they do not correlate with the source of starting material, the operator, reaction times or changes in reaction temperature.

(20) Dobson, J.; Green, B.; Healy, P.; Kennard, C.; Pakawatchai, C.; White, A. *Aust. J. Chem.* **1984**, *37*, 649.

(21) (a) Dessy, G.; Fares, V. *Acta Crystallogr., Sect. C: Cryst. Struct. Commun.* **1979**, *8*, 101. (b) Park, K.-H.; Marshall, W. J. *J. Am. Chem. Soc.* **2005**, *127*, 9330. (c) Morozova, N. B.; Stabnikov, P. A.; Baidina, I. A.; Semyannikov, P. P.; Trubin, S. V.; Igumenov, I. K. *J. Struct. Chem.* **2007**, *48*, 889. (d) Marsh, R. E. *Acta Crystallogr., Sect.B : Struct. Sci.* **2009**, *65*, 782.

(22) Whitehorne, T. J. J.; Vabre, B.; Schaper, F. *Inorg. Chem.* **2013**, *submitted, ic-2013-020866*.

(23) Singh, J. V.; Baranwal, B. P.; Mehrotra, R. C. *Z. Anorg. Allg. Chem.* **1981**, *477*, 235.

(24) Clegg, W.; Cope, E. K.; Edwards, A. J.; Mair, F. S. *Inorg. Chem.* **1998**, *37*, 2317.

(25) Carey, D. T.; Cope-Eatough, E. K.; Vilaplana-Mafe, E.; Mair, F. S.; Pritchard, R. G.; Warren, J. E.; Woods, R. J. *Dalton Trans.* **2003**, 1083.

(26) Monillas, W.; Bazzoli, T.; Yap, G.; Theopold, K. *J. Chem. Crystallogr.* **2010**, *40*, 67.

(27) El-Zoghbi, I.; Ased, A.; Oguadinma, P. O.; Tchirioua, E.; Schaper, F. *Can. J. Chem.* **2010**, *88*, 1040.

(28) Save, M.; Schappacher, M.; Soum, A. *Macromol. Chem. Phys.* **2002**, *203*, 889.

(29) *APEX2*, Release 2.1-0; Bruker AXS Inc.: Madison, USA, 2006.

(30) *SAINT*, Release 7.34A; Bruker AXS Inc.: Madison, USA, 2006.

(31) Sheldrick, G. M. *SADABS*, Bruker AXS Inc.: Madison, USA, 1996 & 2004.

(32) Sheldrick, G. M. *Acta Crystallogr.* **2008**, *A64*, 112.

4. Supporting Information

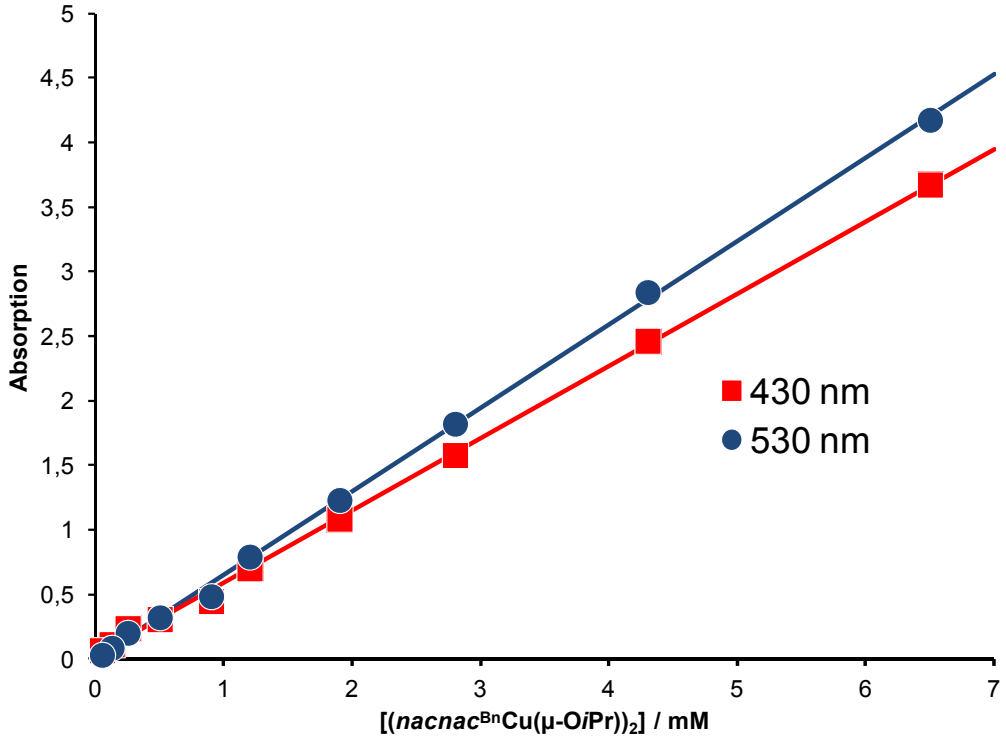

Figure S4.1. Absorption-concentration dependence for **4.4d** in toluene at different concentrations ($5.0 \cdot 10^{-5}$ M – $6.5 \cdot 10^{-3}$).

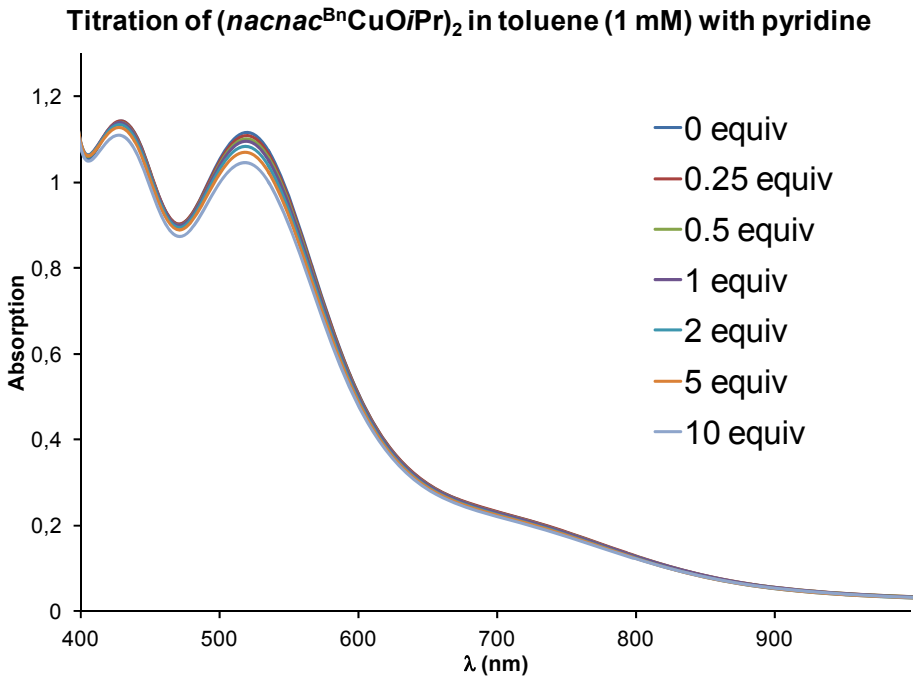

Figure S4.2. UV/vis spectra of **4.4d** in toluene, titrated with pyridine.

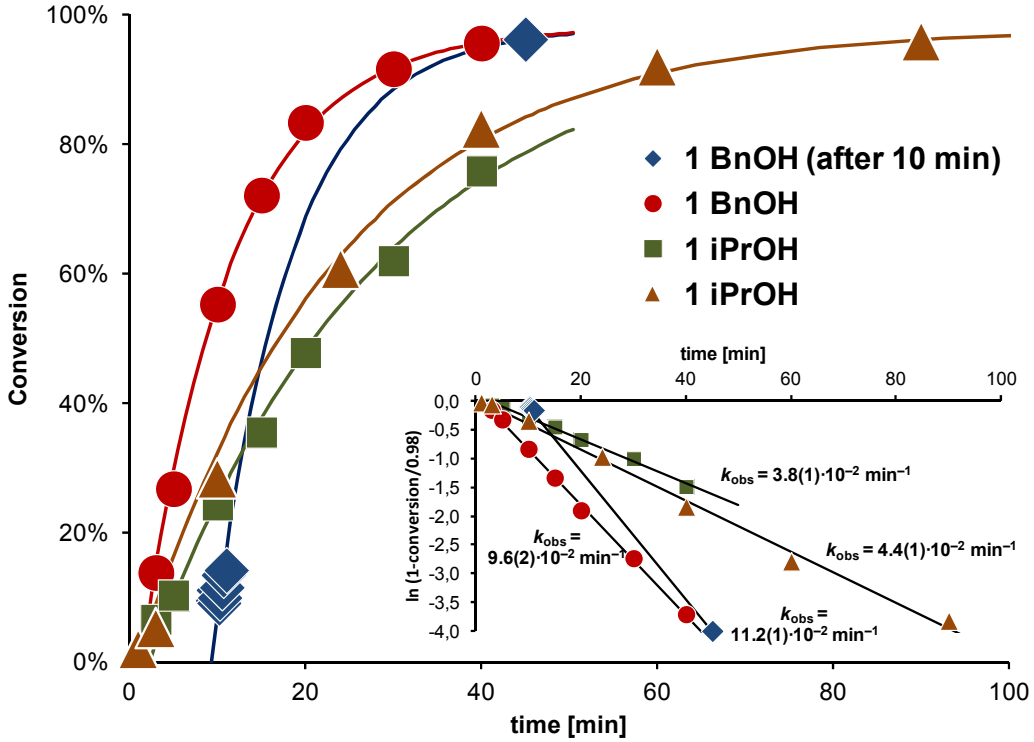

Figure S4.3. Conversion vs. time plots for rac-lactide polymerization with **4.5d**/BnOH (diamonds: alcohol added after 10 min; circles: alcohol added immediately) and **4.5d**/*i*PrOH (squares, triangles).

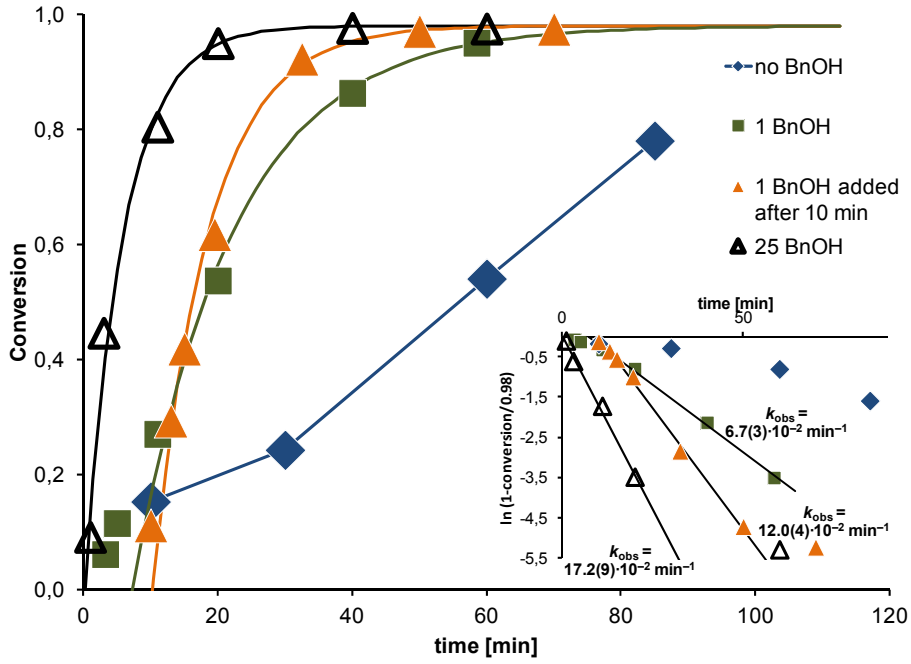

Figure S4.4. Conversion vs. time plots for rac-lactide polymerization with **4.5b** (diamonds), **4.5b**/BnOH.

5. Lactide, β-butyrolactone, δ-valerolactone and ε-caprolactone polymerization with copper diketiminate complexes

Canadian Journal of Chemistry,
Published on the web 5 December **2013**,
10.1139/cjc-2013-0392

*Todd J. J. Whitehorne, Frank Schaper**

Département de chimie, Université de Montréal, 2900 Boul. E.-Montpetit, Montréal, QC, H3T-1J4, Canada

Abstract

Pseudo-first-order rate constants for the polymerization of *rac*-lactide with dimeric (*nacnac*^{Bn}Cu(μ-O*i*Pr))$_2$ (*nacnac*^{Bn} = deprotonated *N*,*N*'-dibenzyl-2-amino-4-imino-pent-2-ene), **5.1**, in acetonitrile, THF, dichloromethane and toluene are k_{obs} = 2.4(1), 5.3(5), 3.6-4.4 and 10(1) min^{-1}, respectively (25 °C, 1.0 mM **5.1**). A bimodal polymer molecular weight distribution is obtained in toluene, narrow polydispersities of 1.1 for THF and acetonitrile. Under the same conditions (25 °C, 1.0 mM **5.1**, CH_2Cl_2), **5.1** polymerizes β-butyrolactone (BL), ε-caprolactone (CL) and δ-valerolactone (VL) with rate constants of k_{obs} = 3.0(1)·10^{-2}, 1.2–2.7·10^{-2}, and 0.11(1) min^{-1}, respectively. Homopolymers showed narrow polydispersities of appr. 1.1. Sequential addition polymerizations showed evidence for transesterification if BL or CL are introduced after a lactide block.

KEYWORDS: polymerization, beta-butyrolactone, epsilon-caprolactone, delta-valerolactone, rac-lactide, copper, catalysis

Introduction

The limited availability of fossil fuels as a carbon source and growing concerns about the accumulation of plastic debris in the environment have combined to generate interest in polylactic acid (PLA), the condensation polymer of lactic acid.[1-4] Due to the problems step-growth polymerizations pose in obtaining high molecular weight polymers of a defined nature, PLA is produced industrially by ring-opening polymerization of lactide (LA), the dimeric anhydride of lactic acid (Scheme 5.1), with metal catalysts, most often tin(II) octoate.[4] Although in practical use, $Sn(Oct)_2$ is far from being an optimal catalyst. Consequently, a lot of interest focussed in recent years on the development of new catalysts/initiators for lactone polymerization in general and lactide polymerization in particular.[5-17] We recently presented copper(II) diketiminate complexes as candidates for lactide polymerization, in particular (*nacnac*^{Bn}Cu(μ-OiPr))$_2$, **5.1**.[18-19] Although **5.1** does not show any stereoselectivity in the polymerization of *rac*-lactide, it is among the most active catalysts reported (>90% conversion in < 1 min at 25 °C), but does not catalyze polymer epimerization, shows no noticeable transesterification of the polymer and does not undergo (unwanted) chain-transfer reactions, avoiding thus the most often encountered side reactions in lactide polymerization.[19] The catalyst is stable in the presence of excess alcohol and polymerizations under immortal conditions[20] are possible. Here we present the application of **5.1** for the polymerization of other cyclic esters, in particular β-butyrolactone (BL), ε-caprolactone (CL) and δ-valerolactone (VL). To the best of our knowledge, Cu(II) based catalysts have not been used in the polymerization of BL or VL. Two cases of CL polymerization are reported for Cu(II), using either $Cu(OTf)_2$[21] or (N^N)$Cu(OAc)_2$[22] at elevated temperatures (N^N = pyrazolylmethyl-pyridine).

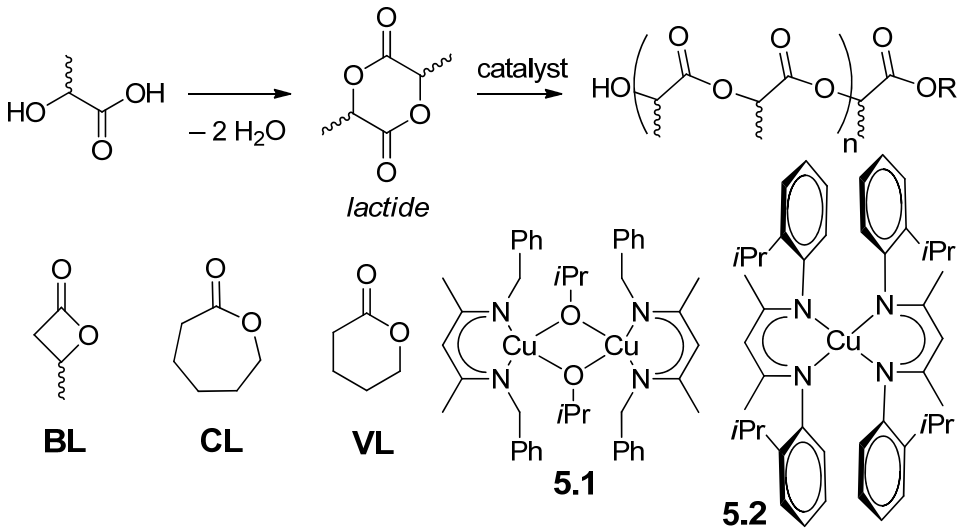

Scheme 5.1

Results and Discussion

General catalyst stability. While **5.1** shows remarkable stability under polymerization conditions, the compound is nevertheless sensitive to air and moisture. To investigate the impact lack of chemical robustness has on polymerization performance, Figure 5.1 compares the obtained vs. expected molecular weight for polymerizations of *rac*-lactide with **5.1** at different catalyst concentrations and monomer : catalyst ratios (Table S5.1).

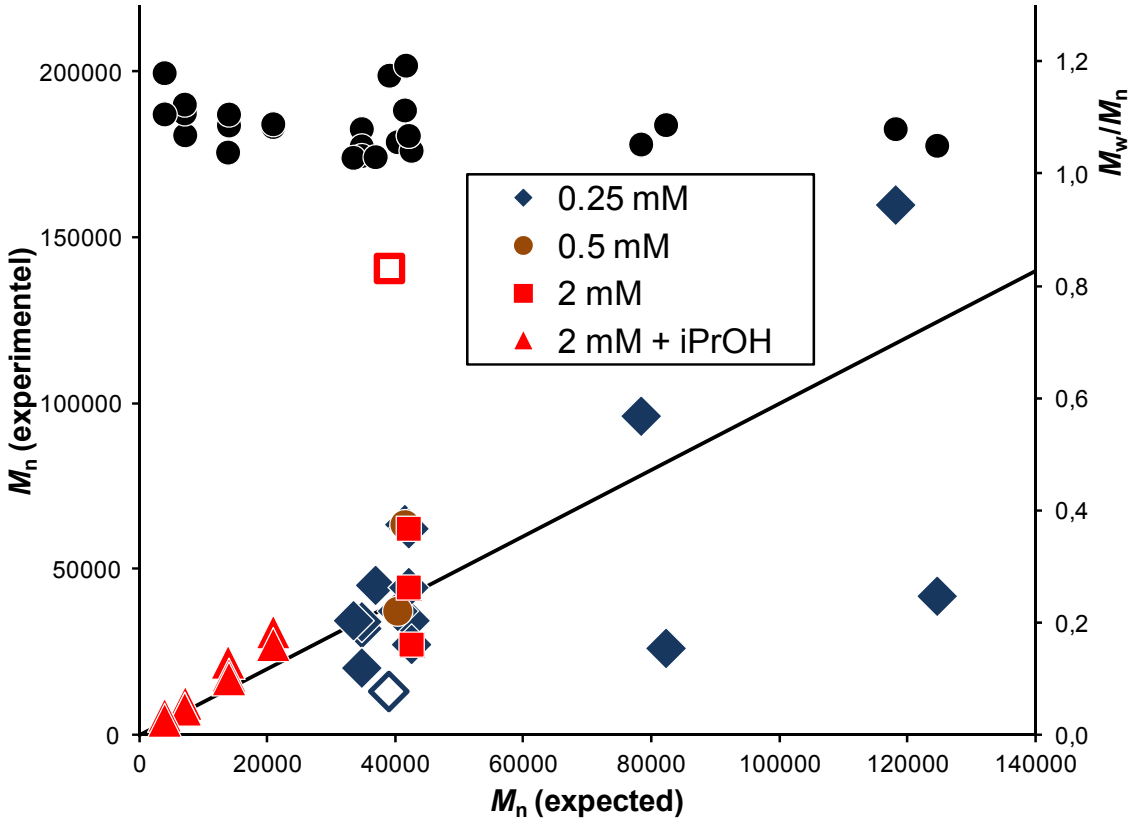

Figure 5.1. Comparison of expected vs. obtained polymer molecular weight for polymerizations of *rac*-lactide (CH_2Cl_2, 25 °C) at different catalyst concentrations and monomer : catalyst ratios (Table S5.1). "Immortal" polymerizations in the presence of 1-10 equiv of isopropanol are included as red triangles. Polydispersities of all experiments are represented by black discs (right axis).

With only two exceptions, polydispersities in all polymerization experiments were below 1.2, indicative of the stability of **5.1** against side reactions under polymerization conditions. However, significant differences between predicted and obtained polymer molecular weight are observed in several polymerizations. There is no evident correlation between catalyst concentration and these deviations, but higher lactide:catalyst ratios seem to lead to increased discrepancies, despite three-fold recrystallization of the monomer. In two cases, a strong deviation is accompanied by slightly broadened polydispersities, indicating an experimental problem (Fig. 5.1, open markers). For

others, narrow polydispersities are observed even with significant deviation from the expected polymer molecular weight. A certain spread can be attributed to weighing errors, but for the most part they point towards catalyst decomposition prior to the onset of polymerization, in particular when the polymer molecular weight is higher than expected. Polymerizations under immortal conditions, i. e. in the presence of excess alcohol as a chain transfer reagent, are significantly more reproducible and show very small deviations between obtained and expected polymer molecular weight (Fig. 5.1, red triangles). Polymer weight in immortal polymerizations depends on the ratio monomer : (catalyst + chain transfer reagent). While decomposition of the catalyst still effects activity in immortal polymerizations, the actual number of catalyst centres becomes of increasingly less importance, as far as polymer molecular weight control is concerned, when alcohol is present as chain transfer agent. Immortal polymerizations thus offer a convenient way of assuring polymer molecular weight control in polymerizations with compounds sensitive to air and moisture, such as **5.1**.

To further address stability of **5.1**, several polymerizations were conducted using unpurified *rac*-lactide as received (Table 5.1). Activities in dichloromethane were identical (if anything, slightly higher) than for purified lactide (Table 5.1). Polydispersities are identical to purified monomer and expected and obtained molecular weight agree nicely. Despite the lack of chemical robustness in **5.1**, extensive purification of monomer does not seem to be required.

Influence of the solvent. To test the compatibility of **5.1** with different solvents, *rac*-lactide polymerizations were carried out in toluene, dichloromethane, THF and acetonitrile (Table 5.1, Fig. 5.2). A very similar, high activity was observed in all solvents, with activities in polar solvents slightly lower, most likely due to competing solvent coordination to **5.1**. UV/vis studies of **5.1** indicate that polar solvents, such as THF or pyridine, coordinate to **5.1** under dissociation of the

dimer.[18] Polymerizations in toluene had to be conducted at lower lactide concentration due to the limited solubility of the monomer in toluene. In addition, polymerization in toluene led to a polymer with a bimodal polymer molecular weight distribution, in contrast to the generally high polymer molecular weight control of **5.1** in dichloromethane. Polymerizations in THF and acetonitrile showed polydispersities of 1.1 and below. Polymer molecular weights for polymerization in THF are surprisingly small, despite the narrow polydispersity. All obtained polymers are atactic with a slight heterotactic bias and the solvent has no influence on polymerization stereocontrol.

Table 5.1. *rac*-Lactide polymerizations with **5.1** in different solvents.

Solvent	k_{obs} · **min**	P_r	M_n **(calc.) /** M_n	M_n	M_w/M_n
CH_2Cl_2 [a]	7.2(1)–8.2(1)	n.d.	1.2–1.4	30 500-36 500	1.04–1.07
CH_2Cl_2 [b]	3.6(4)–4.4(5)	0.56–0.57	0.7–1.5	27 500–62 500	1.04–1.07
Toluene	10(1)	0.53	0.9 & 0.4	11 500 & 28 500	bimodal
THF	5.3(5)	0.56	3.1	13 000	1.11
acetonitrile	2.4(1)	0.54–0.56	1.2–1.5	23 500–25 000	1.06–1.07

Conditions: 25 °C, 1.0 mM **5.1** (= 2.0 mM [Cu]), [lactide] = 0.60 M (0.15 M for toluene). M_n and M_w obtained by GPC vs. polystyrene standards with a Mark-Houwink correction factor of 0.58. Expected polymer molecular weight, M_n(exp.), calculated from [lactide]/[Cu]·final conversion·144.14 g/mol + 60 g/mol. P_r determined from decoupled ^{1}H NMR by $P_r = 2 \cdot I_1/(I_1+I_2)$, with I_1 = 5.20 – 5.25 ppm (*rmr, mmr/rmm*), I_2 = 5.13 – 5.20 ppm (*mmr/rmm, mmm, mrm*). [a] With unpurified lactide, no recrystallization or drying. [b] Data taken from ref. [18]

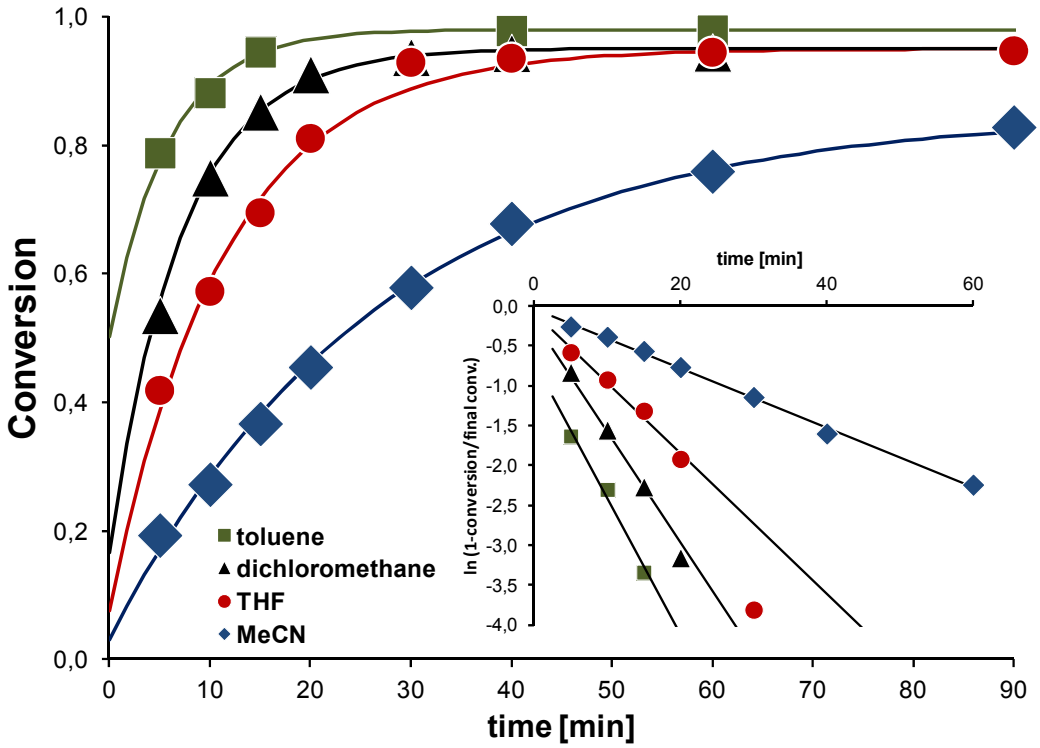

Figure 5.2. Kinetic traces for the polymerization of *rac*-lactide in different solvents. Lines represent best fits obtained from regression analysis yielding the rate constants in Table 5.1.

Butyrolactone polymerizations. Catalyst **5.1** was tested for the polymerization of β-butyrolactone (BL) using the same conditions as for *rac*-lactide (Scheme 5.2). **5.1** was active for polymerization at 25 °C and kinetic investigations found the expected first-order dependency on monomer concentration with apparent rate constants of 2.9(1)–3.1(1)·10^{-2} min^{-1} (Table 5.2, Fig. 5.3, Fig. S5.1). Activity towards BL is thus two orders of magnitude lower than for *rac*-lactide polymerization,[18-19] despite the higher ring strain in BL. This is in line with relative activities in lactide and butyrolactone polymerizations reported for other catalysts (Table 5.3). It is argued that the unfavourable syn-periplanar orientation of the oxygen lone pair with the double bond and steric encumbrance by the ring substituents are less severe in puckered lactones with larger ring-sizes.[23] BL polymerizations with **5.1** showed the same high control of the polymer molecular weight

observed for lactide polymerizations. The polydispersity was below 1.1 and observed and expected polymer molecular weight deviated only slightly. Similar to lactide polymerization with **5.1**, an atactic polymer with slight bias towards alternating enantiomer insertion ($P_r = 0.61$) is obtained.

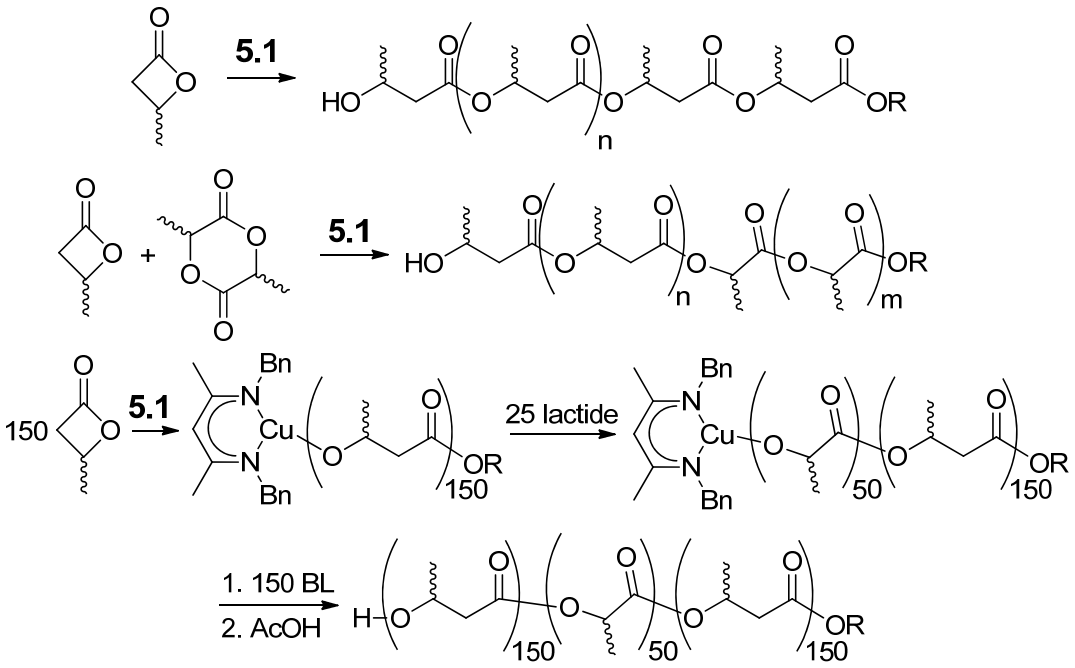

Scheme 5.2

Table 5.2. β-Butyrolactone polymerization catalyzed by **5.1**.

Monomer (equiv/Cu)	Conversion	Time	k_{obs} · min	M_n (calc.)	M_n	M_w/M_n
BL (300)	98%	120 min	$3.1(1)\cdot10^{-2}$, $P_r = 0.61$	25 000	23 500	1.03
BL (300)	90%	90 min	$2.9(1)\cdot10^{-2}$			
BL (150) + LA (150) [a]	100% (LA), 70% (BL)	100 min	1.6(1) (LA), $3.6(5)\cdot10^{-2}$ (BL, < 15 min), $9.5(5)\cdot10^{-3}$ (BL, > 30 min)	31 000	40 500	1.58
1. BL (150), [b]	75%,	100 min,		10 000,	10 500,	1.03,
2. LA (25),	100%,	2 min,		13 500,	13 500,	1.04,
3. BL (150)	85%	100 min		25 500	24 000	1.28

Conditions: 25 °C, 1.0 mM **5.1** (= 2.0 mM [Cu]) in CH_2Cl_2, [BL] = 0.60 M. M_n and M_w obtained by GPC vs. polystyrene standards. Molecular weights are uncorrected. Expected M_n calculated from [BL]/[Cu]·final conversion·86.09 g/mol + 60 g/mol. P_r determined from ^{13}C NMR.[24-25] [a] Random copolymerization, [BL] = [*rac*-lactide] = 0.30 M. [b] Sequential monomer addition: $[BL]_1 = [BL]_2 = 0.30$ M. [lactide] = 50 mM.

Table 5.3. Comparison of second order rate constants k·M·min for the coordination-insertion polymerization of lactide, β-butyrolactone, ε-caprolactone, and δ-valerolactone with different metal catalysts.

	T	lactide	β-butyrolactone	ε-caprolactone	δ-valerolactone
$(\mathbf{5.1})_{0.5}$ [a]	25 °C	2000	15 [b]	6–13 [b]	60 [b]
5.2 + 10 $PhCH_2OH$	25 °C	100	5 [b]	0.6 [b]	
$Al(OiPr)_3$ [23]	80 °C	$3\cdot10^{-1}$	$2\cdot10^{-3}$	0.5 (20°C)	
(Salen)AlOR [26]	100 °C	4.0	0.2	44	
(Salen)AlOR [26]	100 °C	38	13	>900	
(Salan)AlMe/ROH [27]	70 °C	0.03 [c]	0.4 [c]	0.3 [c]	
$La(OiPr)_3$ [28]	21 °C	10–35 [c]	0.1–0.2 [c]	300	100
$\{(N\text{^}O)ZnEt\}_2$ [29]	50 °C	3 [c]	0.3 [c]		
$(N\text{^}O_3)Y(OiPr)(THF)$ [30-31]	20 °C	40 [c]	300 [c]		
$LY(CH_2SiMe_3)_2$ [32]	25 °C	13 [b]	0.05 (50 °C) [c]	3600 [b]	2 [b]

[a] Rate constants based on [catalyst] = [Cu] = 2·[**5.1**]. [b] Assuming a first-order dependence on catalyst concentration. [c] Estimated from time and conversion.

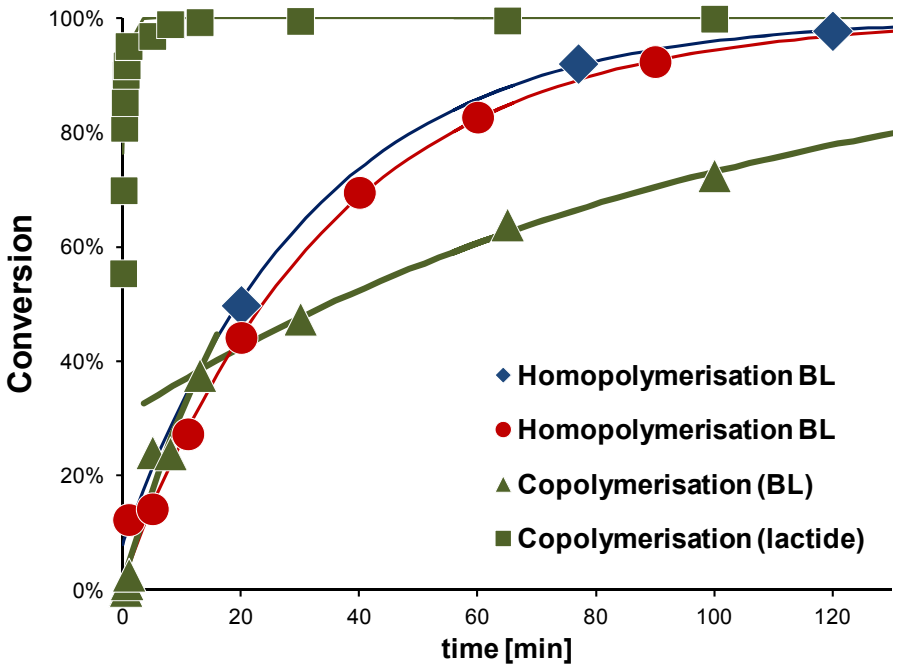

Figure 5.3. Conversion – time plots for the polymerization of β-butyrolactone with **5.1**. Conditions: CH_2Cl_2, 1.0 mM **5.1** = 2.0 mM Cu, 25 °C, [BL] = 0.60 M (homopolymerization), [BL] = [lactide] = 0.30 (copolymerization). Solid lines correspond to best fits from regression analysis yielding the rate constants in Table 5.2.

Copolymerization of *rac*-lactide (LA) and β-butyrolactone (BL) showed the formation of a block copolymer with complete conversion of *rac*-lactide before any incorporation of BL was observed (Scheme 5.2, Fig. 5.3). The observed apparent rate constant of 2 min^{-1} for lactide polymerization agrees reasonably well with the rate constant for homopolymerization at these conditions (4 min^{-1}). In difference to homopolymerization, lactide conversion reaches 100% since BL insertion prevents lactide deinsertion and no lactide monomer can be detected after 15 min polymerization by ^{1}H NMR. BL consumption over time does not follow the pseudo-first-order kinetics expected from the homopolymerization. Instead, polymerization proceeds with a rate close to the homopolymerization rate until 15 min (40% BL conversion). After this point the polymerization rate drops to 1/3 of the homopolymerization rate. We can exclude delayed deactivation by

monomer impurities, since this behaviour was not observed in homopolymerization. Rate constants in copolymerization may differ from those in homopolymerization in the case of competing monomer coordination to the catalyst centre, but a decreased polymerization rate which recovers once all lactide is consumed should have been observed in this case. To the contrary, the reaction rate drops at 15 min, approximately the same time when no lactide monomer is detected anymore in ^{1}H NMR spectra of reaction samples. A similar behaviour is observed with ε-caprolactone as monomer (*vide infra*).

A three-block copolymer was obtained by sequential monomer addition of 150 equiv BL, 25 equiv lactide and 150 equiv BL (Scheme 5.2). The obtained polymer molecular weights (Table 5.3) are in close agreement with the conversion determined by NMR, indicating the absence of chain transfer. Polydispersities are below 1.1, even after the addition of the second monomer block, but increase to 1.3 for the second BL addition. Broadening of the polymer molecular weight distribution thus seems to be associated with a previously introduced polylactide block in the polymer.

Caprolactone polymerizations. Complex **5.1** is active in the homopolymerization of ε-Caprolactone (CL), but observed activities are much lower than expected (Table 5.4, Fig. 5.7). Compared to lactide, CL is typically one or more orders of magnitude more reactive (Table 5.3). In the case of **5.1**, however, CL polymerization activity is three orders of magnitude *smaller* than that of lactide and even smaller than BL. Despite this unusual low reactivity in comparison to lactide, the activity of **5.1** compares very favourably to previous reports on Cu(II)-catalyzed CL polymerization: 10 mM $Cu(OTf)_2$ afforded 85% conversion at 60 °C in 24 h with $M_w/M_n = 2$,[21] while ≈50 mM (N^N)$Cu(OAc)_2$ at 110 °C showed 80% conversion after 48 h with $M_w/M_n = 3–4$ (N^N = pyrazolylmethyl-pyridine).[22] Copolymerizations of lactide and CL consequently showed

the production of a block copolymer with consumption of lactide in < 1 min with rate constants comparable to homopolymerizations. This is then followed by slow CL polymerization. As already observed for the copolymerization of lactide with BL, the copolymerization rate of CL is smaller by a factor of 2–4 than homopolymerization, although lactide has been completely consumed. Again, we observe in copolymerizations that initial activities are close to the homopolymerization rate before the drop to a lower level. The same reduced rate constant for CL is observed in sequential copolymerization if *rac*-lactide is polymerized first (Table 5.4). CL polymerizations with **5.1** show relatively poor polymer molecular weight control. In homopolymerizations, the polydispersity remains narrow, but obtained polymer molecular weights are either too low or too high. In copolymerizations, expected and obtained polymer molecular weights are in better agreement, but polydispersities are above 1.4, an usual broad distribution for polymerizations with **5.1** (*vide infra*).

Table 5.4. ε-Caprolactone polymerization catalyzed by **5.1**.

	Monomer (equiv/Cu)	Conversion	Time	k_{obs} · min	M_n (calc.)	M_n	M_w/M_n
1	CL (300)	98%	130 min	$2.7(1)\cdot10^{-2}$	33 500	3500	1.15
2	CL (300)	76%	80 min	$1.2(1)\cdot10^{-2}$	26 000	49 500	1.04
3	CL (150) + LA (150) [a,b]	96%, 42%	100 min	6.6(2) (LA), $3.9(1)\cdot10^{-3}$ (CL)	21 500	19 500	1.43
4	CL (150) + LA (150) [a,b]	100%, 46%	100 min	6.4(6) (LA), $5.6(1)\cdot10^{-3}$ (CL)	29 500	23 500	1.59
5	1. LA (150), 2. Cl (150) [b,c]	>95%, 50%	2 min, 2.5 h	n. d., $4.1(1)\cdot10^{-3}$ (CL)	20 500, 30 000	18 500, 28 500	1.07, 1.48
6	1. CL (150), 2. LA (25), 3. CL (150) [c,d]	90%, 100%, 79%	100 min, 2 min, 100 min	$2.6(3)\cdot10^{-2}$, n. d., $1.6(1)\cdot10^{-2}$	15 500, 19 000, 30 500	16 500, 18 000, 29 500	1.08, 1.09, 1.20
7	1. CL (150), 2. lactide (150), 3. CL (150) [c,e]	97%, 100%, 60%	180 min, 2 min, 90 min	$2.6(1)\cdot10^{-2}$, 9(4) $7.2(1)\cdot10^{-3}$	16 500, 37 000, 48 000	13 000, 21 000, 30 500	1.11, 1.19, 1.32

Conditions: 25 °C, 1.0 mM **5.1** (= 2.0 mM [Cu]) in CH_2Cl_2, [CL] = 0.60 M. M_n and M_w obtained by GPC vs. polystyrene standards with a Mark-Houwink correction factor of 0.56. Expected M_n calculated from [monomer]/[Cu]·final conversion·$M_{monomer}$ + 60 g/mol. [a] Random Copolymerization. [b] [CL] = [LA] = 0.30 M. [c] Sequential monomer addition. [d] $[CL]_1 = [CL]_2$ = 0.30 M, [LA] = 50 mM. [e] $[CL]_1 = [CL]_2 = [LA]$ = 0.30 M.

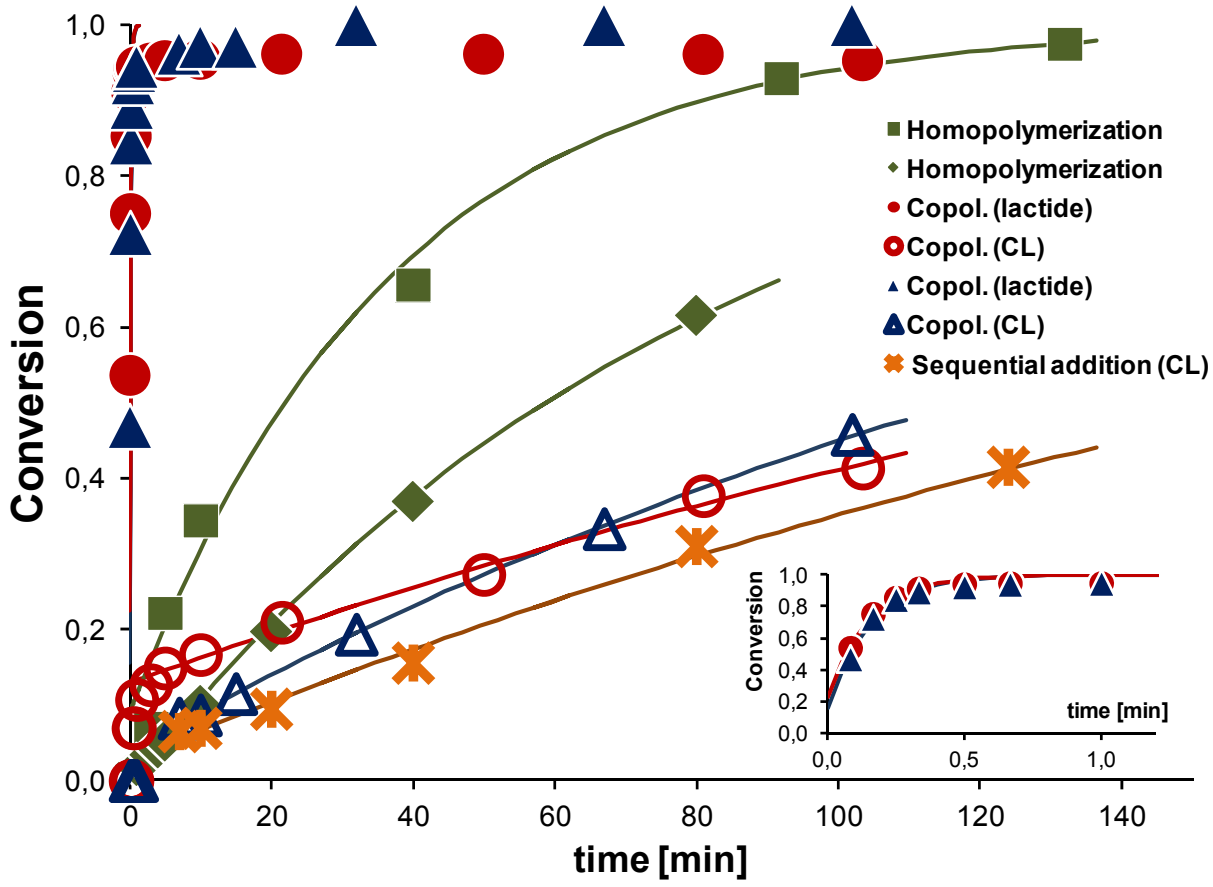

Figure 5.4. Kinetic traces for the homopolymerization of ε-caprolactone and its copolymerization with *rac*-lactide (lactide:CL = 1:1).

In an alternative copolymerization experiment, 150 equiv (per copper atom) of CL were polymerized with **5.1** for 100 min, followed by addition of 25 equiv lactide and a second addition of 150 equiv CL (Fig. 5.5). The polymerization rate of the first fraction of CL is, as expected, identical to those observed in homopolymerizations. Lactide polymerization as well is undisturbed by the presence of polyCL and full monomer consumption was observed in <2 min, well in line with the observed homopolymerization activities. The second fraction of CL is polymerized with slightly smaller activity than that of the first fraction (Table 5.4, Fig. 5.5 & S2). When the length of the lactide block is increased to 150 equiv per Cu, the activity of the second block is depressed

significantly (Table 5.4, Fig. 5.5). Increases in the observed molecular weights for each monomer addition agree with the expected values calculated from conversion. There is thus no notable chain transfer or decomposition. For the second CL addition, following the introduction of the lactide block, polydispersities broaden noticeably in both cases.

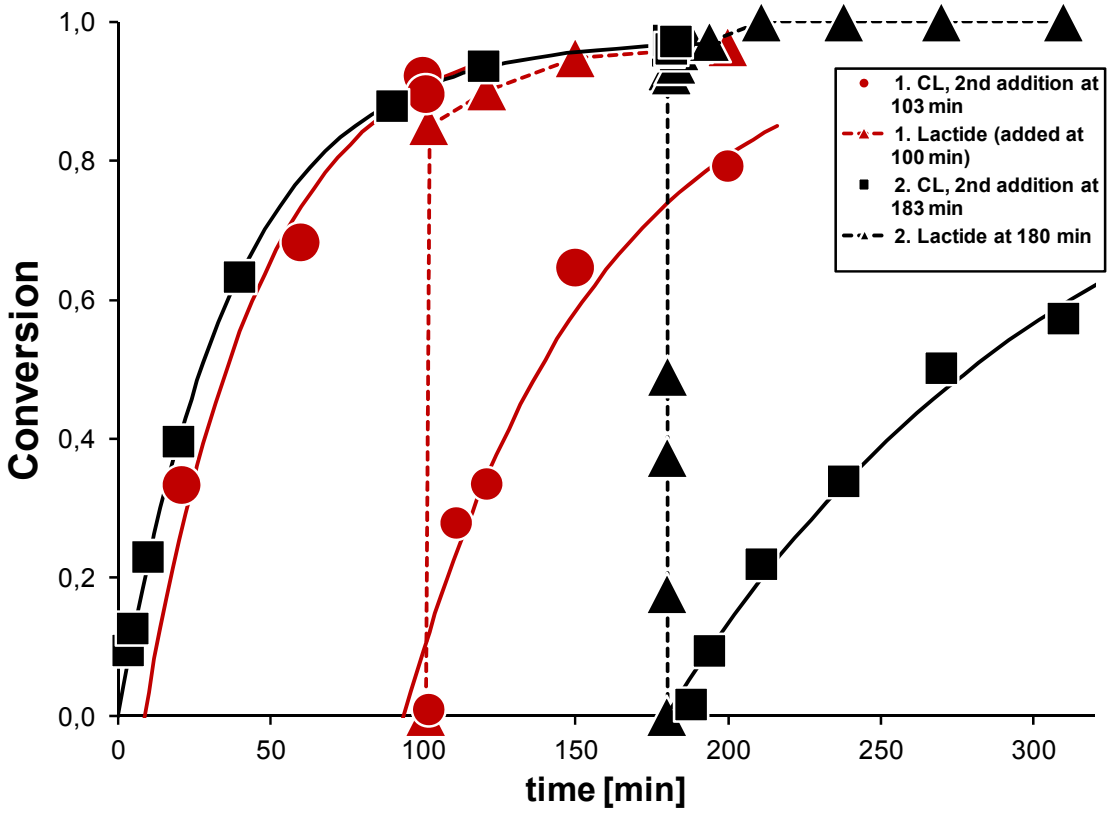

Figure 5.5. Sequential copolymerization of ε-caprolactone. Red circles: 0.30 M CL, 0.050 M lactide (not shown), 0.30 M CL. Black squares: 0.30 M CL, 0.30 M lactide (not shown), 0.30 M CL. Conditions: CH_2Cl_2, 1.0 mM **5.1** = 2.0 mM Cu, 25 °C. Best fit lines for CL correspond to the rate constants obtained by linear regression, which are listed in Table 5.4.

In CL as well as in BL copolymerizations with lactide, depression of CL (or of BL) activity was observed even after all lactide monomer seem to have been consumed according to proton NMR. In CL/lactide/CL sequential addition experiments, the depression of activity correlates with the length of the lactide block. In addition, poly(CL-block-LA) and poly(BL-block-LA) show narrow

polydispersities if BL (or CL) is polymerized first (M_w/M_n = 1.04–1.19, Table 5.3&4), but increased polydispersities if the first monomer is lactide (M_w/M_n = 1.20–1.48). A similar observation was reported without explanation for a lactide/BL copolymerization with a hafnium catalyst which produces poly(CL-block-LA) with M_w/M_n = 1.09 if BL is polymerized first, but with M_w/M_n = 1.33 if BL is polymerized after lactide.[33] A closer look at the proton spectra of the 150 CL/150 LA/150 CL sequential addition experiment (Table 5.4) revealed that only polyCL peaks were observed after first CL addition. After lactide addition, only polyCL and PLA resonances were present, indicative of poly(CL-block-LA). During the second CL addition, however, peaks were observed in the ^{1}H NMR which are indicative for CL-LA linkages (Fig. 5.6),[34] in higher percentage than possible from the remaining lactide monomer, and resembling the results of a random copolymer. The ^{13}C NMR spectrum of poly(CL-LA-CL) shows a higher amount of CL units neighbouring lactide than possible from sequential addition (>36%, more than half of the second fraction added, Fig. 5.6). Even more significant is the presence of "clc" triads, i. e. an isolated *lactic acid* unit. Since insertion of lactide always generates "ll" dyads, a "clc" triad cannot originate from insertion. NMR spectra of poly(BL-LA-BL) sequential additions showed the same trend: Additional peaks were observed during the second BL addition in the ^{1}H NMR. The ^{13}C NMR spectrum showed an increase in the number of (strongly overlapping) resonances, but the spectrum was too complicated to be evaluated. Based on these findings, we propose that transesterification (normally absent in homopolymerization as indicated by narrow polydispersities), takes place with **5.1** when (i) a lactide block is present and (ii) a monomer different from lactide is added. Transesterification preferentially with the PLA blocks of other polymers would lead to lactide-terminated chains, which would explain broadened polydispersities as well as reduced activities (if CL (or BL) insertion into a lactide-terminated chain is slow). Also

in line with this are colour changes of the catalyst during polymerization. In a CL/LA/CL sequential addition experiment, the reaction mixture turned golden-orange after addition of CL. Once lactide was introduced, the typical purple-red colour observed in lactide polymerizations was obtained. This colour persisted throughout the reaction, even after the second fraction of CL was added.

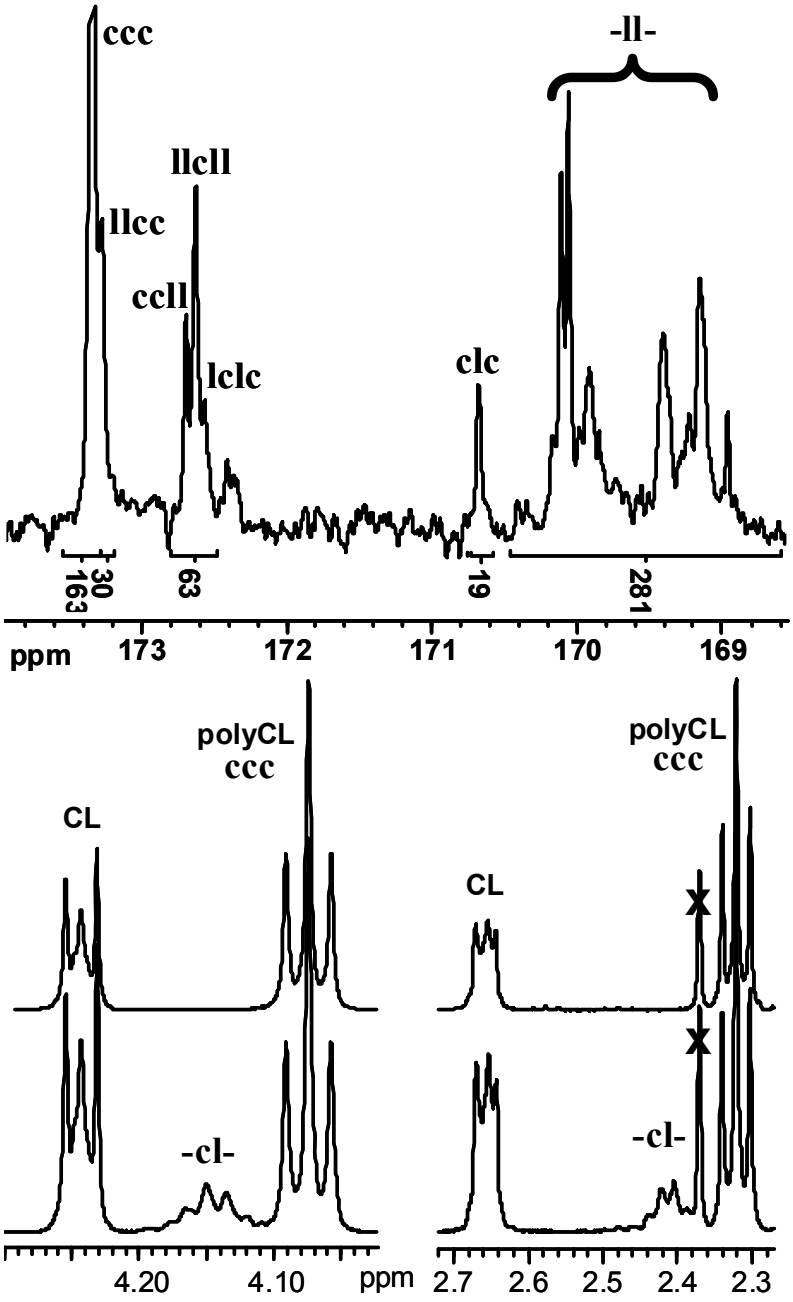

Figure 5.6. Top: ^{13}C NMR spectrum of poly(CL-LA-CL) obtained from sequential addition of monomers. Assignment according to literature.[35] "c" signifies an ε-caprolactone unit, "l" a lactic acid unit, i. e. one lactide is "ll". Bottom: ^{1}H NMR spectra of poly(CL-LA-CL) before (top trace) and after (bottom trace) addition of the second CL fraction. "-cl-" signifies an ε-caprolactone unit neighbouring a lactide unit.[34]

δ-Valerolactone polymerization. δ-Valerolactone (VL) was polymerized using **5.1** under conditions identical to those described above (25 °C, CH_2Cl_2, 1.0 mM **5.1**, $[VL]_0$ = 0.60 M). The obtained pseudo-first order rate constant (k_{obs} = 0.11(1) min^{-1}, Table 5.5) shows an activity towards VL which lies between that of lactide and BL, a result in agreement with typical literature observations (Table 5.3). Contrary to other monomers and due to its small ring strain, VL polymerization did not reach completion but plateaued at 50% conversion under the experimental conditions applied (CH_2Cl_2, 25 °C, $[VL]_0$ = 0.60 M, Fig. 5.7). The observed conversion (50%, [VL] = 0.30 M) agrees well with the equilibrium monomer concentration in pure monomer (0.39 M).[36] A multiaddition experiment showed that incomplete conversion was indeed due to the polymer-monomer equilibrium and not due to catalyst decomposition. At [**5.1**] = 1.0 mM, equilibrium monomer concentration is reached at 150 equiv VL. Consequently, no polymer is obtained after the first addition of 100 equiv VL ($[VL]_{total}$ = 0.20 < $[VL]_{eq}$). Of the second 100 equiv VL added, only half, the portion above $[VL]_{eq}$, are polymerized (P_n = 45, Table 5.5). Since equilibrium monomer concentration is now reached, all of the third 100 equiv VL are polymerized (P_n = 125, Table 5.5) to yield a polymer identical to the one obtained by direct addition of 300 equiv VL. Polydispersities were slightly higher than usually observed for **5.1** (1.2–1.4) and might be a consequence of the fast depolymerization reaction with VL as a monomer.

Table 5.5. δ-Valerolactone polymerization catalyzed by **5.1**.

Monomer (equiv/Cu)	**Conversion**	**Time**	k_{obs} · **min**	M_n **(calc.)**	M_n	P_n [a]	M_w/M_n
VL (300)	50%	30 min	0.11(1)	15 000	12 000	120	1.21
1. VL (100),	n. d.			0 [c]	no polymer		
2. VL (100),				5000 [c]	4500	45	1.39
3. VL (100)[b]				15 000 [c]	12 500	125	1.16
VL (150) + CL (150)	70% (VL), 90% (CL)	120 min	0.042(1) (VL), 0.022(1) (CL)	26 000	24 500		1.13

Conditions: 25 °C, 1.0 mM **5.1** (= 2.0 mM [Cu]) in CH_2Cl_2, [VL] = 0.60 M. M_n and M_w obtained by GPC vs. polystyrene standards with a Mark-Houwink correction factor of 0.57. [a] Polymerization degree. [b] Multiaddition experiment [VL] = 0.20 M in each addition ([VL]:[Cu] = 100). [c] M_n calculated from ([monomer] – 0.30 M)/[Cu]·$M_{monomer}$ + 60 g/mol.

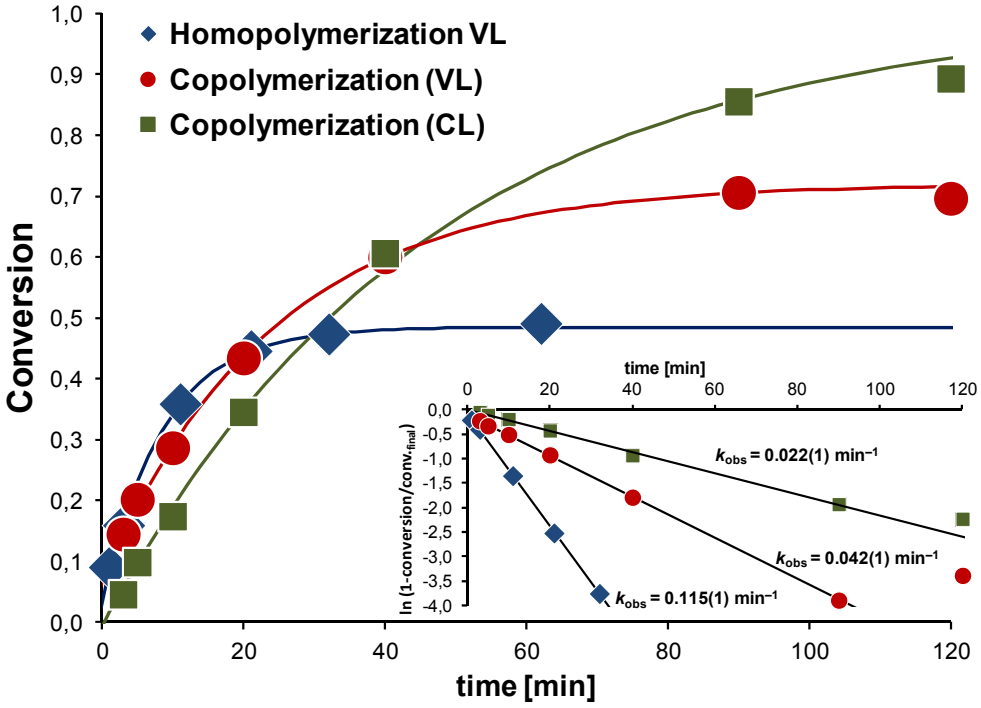

Figure 5.7. Conversion-time plot for polymerization of δ-valerolactone with **5.1** (CH_2Cl_2, 25 °C, **[5.1]** = 1.0 mM, [VL] = 0.60 M).

We were interested to combine thermodynamically unfavourable VL insertion with kinetically unfavourable CL insertion under equilibrium polymerization conditions. Random copolymers of CL and VL have been obtained previously with either metal alkoxide catalysts[37] or enzymes.[38] Polymerization of 0.30 M CL with 0.30 M VL, i. e. the equilibrium monomer concentration for VL by 1.0 mM [**5.1**], proceeded to near completion with a rate constant for CL consumption of 0.02 min^{-1}, in close agreement with the rate constant in homopolymerization of CL (Fig. 5.7, Table 5.5). VL consumption plateaus at 70% ([VL] = 0.1 M) with an apparent rate constant of 0.04 min^{-1}. Inspection of the ^{13}C NMR spectra of the obtained copolymer showed an approximately equal distribution of all CL/VL triads (Fig. 5.8), with slight overrepresentation of CL-CL to the cost of VL-VL, as expected given the higher amount of CL consumed. A tentative triad assignment of the carbonyl region is provided in Fig. S5.3. Calculated intensities using a terminal model and obtained intensities agree well, indicating that a random copolymer with relatively homogenous microstructure was obtained.

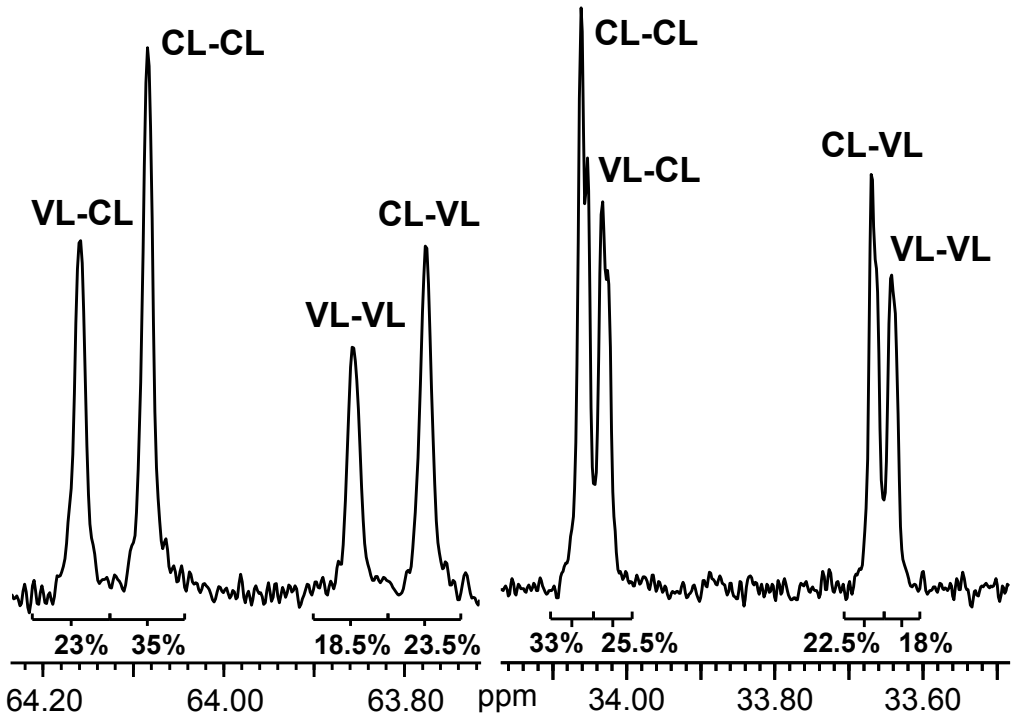

Figure 5.8. Expanded ^{13}C NMR spectrum of poly(VL-co-CL) with dyad assignments according to literature.[38-39] For a tentative assignment of triads in the carbonyl region, see Figure S5.3 and Table S5.2.

Alternative copper catalysts. Next to heteroleptic complexes, such as **5.1** and its related 3-chlorosubstituted analog, homoleptic bisdiketiminate complexes, *nacnac*$^{R}_{2}$Cu, were also active in *rac*-lactide polymerization, but required benzyl alcohol as a co-catalyst.[18] To verify the influence of ligand substitution on relative activities towards cyclic esters, *rac*-lactide, ε-caprolactone and δ-valerolactone were polymerized with **5.2** carrying a *N*-isopropylphenyl substituent (Scheme 5.1, Table 5.6, Fig. 5.9). With ratios of **5.2**:alcohol:monomer = 1:10:1000, **5.2** polymerized *rac*-lactide in 20 min, while CL and VL polymerizations did not reach completion after 5 h polymerization time. Due to slow initiation of polymerization,[18] rate constants in Table 5.6 are only (lower) estimates for CL and VL, but it is evident that **5.2** shows less discrimination between *rac*-lactide and ε-caprolactone than **5.1**. Polymerizations with **5.2**/$PhCH_2OH$ show excellent polymer weight

control with narrow polydispersities and a close agreement of calculated and observed polymer molecular weight, although the concentration of active catalyst is not constant during polymerization. In fact, linearised ln(conversion) vs. time plots show a strong negative curvature, indicating constantly increasing catalyst concentrations and that initiation was not complete even after 5 h. Since **5.2** does not contain an initiating group, the active species is formed only upon reversible protonation of a diketiminate ligand by alcohol. Polymer molecular weights thus depend on the ratio monomer:alcohol only and are independent from the concentration of **5.2** or of the actual active species *nacnac*CuOR, demonstrating the enhanced polymer molecular weight control possible in immortal polymerizations.

Table 5.6. Lactone polymerization catalyzed by **5.2** + 10 equiv benzyl alcohol.

Monomer	**Conversion**	**Time**	k_{obs} **· min**	M_n **(calc.)**	M_n	M_w/M_n
rac-lactide	99%	20 min	$2.6(1)\cdot10^{-1}$	14 500	11 500	1.18
CL	86%	5 h	$1\cdot10^{-2}$	10 000	8000	1.09
VL	22%	5 h	$1\cdot10^{-3}$	2300	1800	1.11

Conditions: 25 °C, 2.0 mM **5.2** in CH_2Cl_2. [**5.2**]:[$PhCH_2OH$]:[monomer] = 1:10:1000. M_n and M_w obtained by GPC vs. polystyrene standards with a Mark-Houwink correction factor (see Exp. Section).

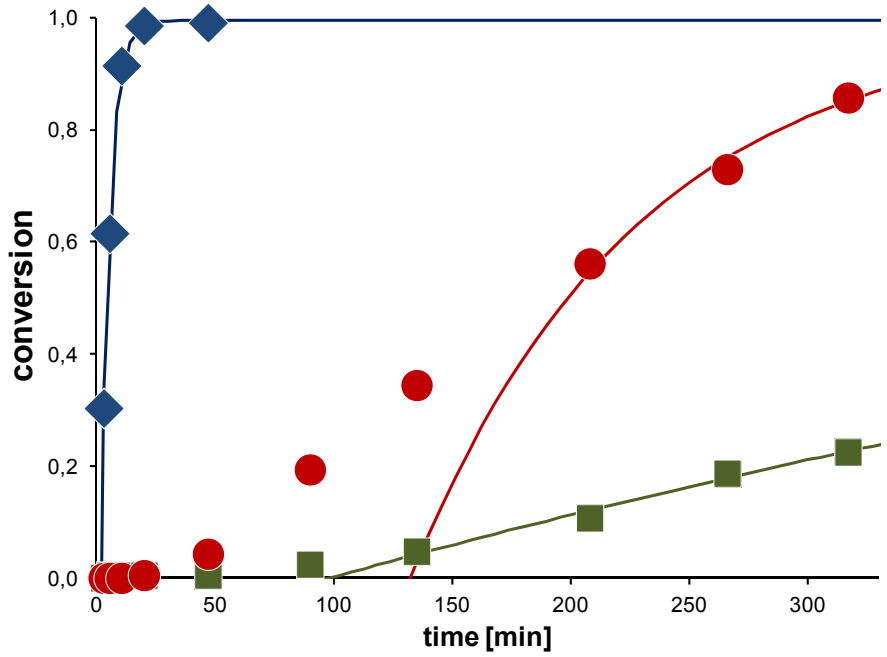

Figure 5.9. Conversion-time plots for the polymerization of *rac*-lactide (diamonds), ε-caprolactone (circles) and δ-valerolactone (squares) with **5.2**. Conditions: CH_2Cl_2, 25 °C, [**5.2**] = 2 mM, [$PhCH_2OH$] = 20 mM, [monomer] = 2 M). Solid lines represent the rate constants in Table 5.6.

Conclusions

Copper complex **5.1** is active for the room temperature polymerization of β-butyrolactone, δ-valerolactone, and ε-caprolactone. For the first two monomers, these are the first reports of Cu-catalyzed polymerization, while activities are orders of magnitude above previous Cu(II)-catalyzed polymerizations of ε-caprolactone.[21-22] In homopolymerizations the excellent polymer weight control of **5.1** is retained and polydispersities are consistently below 1.2. **5.1** is thus a reliable catalyst for the polymerization of a variety of lactones, albeit without the extreme activity observed for lactide. Although **5.1** does not catalyze transesterification in homopolymerizations, severe transesterification side reactions are observed in copolymerizations of other monomers with lactide, which severely limits possible applications of **5.1** in copolymerizations. The problem seems to be limited to lactide as a monomer, since poly(VL-CL) was obtained with narrow

polydispersities. Polymerization under immortal polymerization conditions using **5.2**/ROH showed excellent stereocontrol, albeit lower activities. Since **5.2**/ROH shows a less pronounced preference for lactide over other monomers, future studies will verify if **5.2** avoids the transesterification into the PLA block of copolymers shown by **5.1**.

Experimental Section

General considerations. All reactions were carried out using Schlenk or glove box techniques under nitrogen atmosphere. Complex **5.1** and **5.2** were prepared as described elsewhere.[18-19] Solvents were dried by passage through activated aluminum oxide (MBraun SPS), de-oxygenated by repeated extraction with nitrogen, and stored over molecular sieves. *rac*-Lactide (98%) was purchased from Sigma–Aldrich, purified by 3x recrystallization from dry ethyl acetate and kept at –30 °C. Other monomers were dried by stirring over Na_2CaCO_3 for at least 12h, vacuum transferred and stored over molecular sieves at –30 °C. ^{1}H and ^{13}C NMR spectra were acquired on a Bruker AVX 400 spectrometer. Molecular weight analyses were performed on a Waters 1525 gel permeation chromatograph equipped with three Phenomenex columns and a refractive index detector at 35 °C. THF was used as the eluent at a flow rate of 1.0 $mL \cdot min^{-1}$ and polystyrene standards (Sigma–Aldrich, 1.5 $mg \cdot mL^{-1}$, prepared and filtered (0.2.0 mM) directly prior to injection) were used for calibration. Obtained molecular weights were corrected by a Mark-Houwink factor of 0.58 (polylactide), 0.57 (poly-δ-valerolactone), and 0.54 (poly-ε-caprolactone).[28] Although similar correction factors for poly-β-butyrolactone have been reported, a close agreement of uncorrected M_n, M_n calculated from end group analysis by NMR and expected M_n was reported in several cases. Polymer molecular weights for poly-β-butyrolactone were thus not corrected.

General polymerization procedure. In a glove box a stock solution of **5.1** or **5.2** (100 μL, $5.0 \cdot 10^{-2}$ M in CH_2Cl_2, 5.0 μmol) was added to a solution of the monomer in dichloromethane (2.5 mL). Samples for kinetic investigations were taken at the desired intervals and added to vials already containing a dichloromethane solution of acetic acid (5 mM). Reaction mixtures were quenched at the desired polymerization time by addition of a dichloromethane solution of acetic acid (5 mM). For samples as well as the bulk reaction, volatiles were immediately evaporated under vacuum. For polymerizations with β-butyrolactone, dichloromethane was allowed to evaporate at ambient pressure. Solid polymer samples were stored at –80 °C. Conversion was determined from ^{1}H NMR in $CDCl_3$ by comparison to remaining monomer. P_r values were determined from homodecoupled ^{1}H NMR spectra (lactide) or ^{13}C NMR (β-butyrolactone).

Acknowledgments. This work was supported by the Natural Sciences and Engineering Research Council of Canada (NSERC) and the Centre in Green Chemistry and Catalysis (CGCC). We thank Pierre Ménard-Tremblay and Dr. R. E. Prud'homme for access to GPC.

Supporting information. Figure S5.1-S5.3, Table S5.1, S5.2.

References

(1) Ahmed, J.; Varshney, S. K. *International Journal of Food Properties* **2011**, *14*, 37.
(2) Vijayakumar, J.; Aravindan, R.; Viruthagiri, T. *Chem. Biochem. Eng. Q.* **2008**, *22*, 245.
(3) Tokiwa, Y.; Calabia, B. P. *Can. J. Chem.* **2008**, *86*, 548.
(4) Vink, E. T. H.; Rábago, K. R.; Glassner, D. A.; Springs, B.; O'Connor, R. P.; Kolstad, J.; Gruber, P. R. *Macromolecular Bioscience* **2004**, *4*, 551.
(5) Sauer, A.; Kapelski, A.; Fliedel, C.; Dagorne, S.; Kol, M.; Okuda, J. *Dalton Trans.* **2013**, *42*, 9007.
(6) Dagorne, S.; Normand, M.; Kirillov, E.; Carpentier, J.-F. *Coord. Chem. Rev.* **2013**, *257*, 1869.
(7) Wheaton, C. A.; Hayes, P. G. *Comments on Inorganic Chemistry* **2011**, *32*, 127.
(8) Dutta, S.; Hung, W.-C.; Huang, B.-H.; Lin, C.-C. In *Synthetic Biodegradable Polymers*, Rieger, B.; Künkel, A.; Coates, G. W.; Reichardt, R.; Dinjus, E.; Zevaco, T. A., Eds. Springer-Verlag: Berlin, 2011; Vol. pp 219.
(9) Dijkstra, P. J.; Du, H.; Feijen, J. *Polym. Chem.* **2011**, *2*, 520.
(10) Jones, M. D. In *Heterogenized Homogeneous Catalysts for Fine Chemicals Production*, Barbaro, P.; Liguori, F., Eds. Springer Netherlands: 2010; Vol. 33, pp 385.
(11) Carpentier, J.-F. *Macromol. Rapid Comm.* **2010**, *31*, 1696.
(12) Ajellal, N.; Carpentier, J.-F.; Guillaume, C.; Guillaume, S. M.; Helou, M.; Poirier, V.; Sarazin, Y.; Trifonov, A. *Dalton Trans.* **2010**, *39*, 8363.
(13) Wheaton, C. A.; Hayes, P. G.; Ireland, B. J. *Dalton Trans.* **2009**, 4832
(14) Williams, C. K.; Hillmyer, M. A. *Polym. Rev.* **2008**, *48*, 1.
(15) Platel, R. H.; Hodgson, L. M.; Williams, C. K. *Polym. Rev.* **2008**, *48*, 11
(16) Dechy-Cabaret, O.; Martin-Vaca, B.; Bourissou, D. *Chem. Rev.* **2004**, *104*, 6147.
(17) Chisholm, M. H.; Zhou, Z. *J. Mater. Chem.* **2004**, *14*, 3081.
(18) Whitehorne, T. J. J.; Schaper, F. *Inorg. Chem.* **2013**, *submitted (ic-2013-02133c).*
(19) Whitehorne, T. J. J.; Schaper, F. *Chem. Commun.* **2012**, *48*, 10334.
(20) Inoue, S. *J. Polym. Sci., Part A: Polym. Chem.* **2000**, *38*, 2861.
(21) Wang, Y.; Kunioka, M. *Macromolecular Symposia* **2005**, *224*, 193.
(22) Ojwach, S. O.; Okemwa, T. T.; Attandoh, N. W.; Omondi, B. *Dalton Trans.* **2013**, *42*, 10735.
(23) Duda, A.; Kowalski, A.; Libiszowski, J.; Penczek, S. *Macromolecular Symposia* **2005**, *224*, 71.
(24) Jedliński, Z.; Kowalczuk, M.; Kurcok, P.; Adamus, G.; Matuszowicz, A.; Sikorska, W.; Gross, R. A.; Xu, J.; Lenz, R. W. *Macromolecules* **1996**, *29*, 3773.
(25) Ajellal, N.; Bouyahyi, M.; Amgoune, A.; Thomas, C. M.; Bondon, A.; Pillin, I.; Grohens, Y.; Carpentier, J.-F. o. *Macromolecules* **2009**, *42*, 987.
(26) Pepels, M. P. F.; Bouyahyi, M.; Heise, A.; Duchateau, R. *Macromolecules* **2013**, *46*, 4324.
(27) Cross, E. D.; Allan, L. E. N.; Decken, A.; Shaver, M. P. *J. Polym. Sci., Part A: Polym. Chem.* **2013**, *51*, 1137.
(28) Save, M.; Schappacher, M.; Soum, A. *Macromol. Chem. Phys.* **2002**, *203*, 889.
(29) Grunova, E.; Roisnel, T.; Carpentier, J.-F. *Dalton Trans.* **2009**, 9010.
(30) Amgoune, A.; Thomas, C. M.; Roisnel, T.; Carpentier, J.-F. *Chem. Eur. J.* **2006**, *12*, 169.
(31) Amgoune, A.; Thomas, C. M.; Ilinca, S.; Roisnel, T.; Carpentier, J.-F. *Angew. Chem., Int. Ed.* **2006**, *45*, 2782.

(32) D'Auria, I.; Mazzeo, M.; Pappalardo, D.; Lamberti, M.; Pellecchia, C. *J. Polym. Sci., Part A: Polym. Chem.* **2011**, *49*, 403.
(33) Jeffery, B. J.; Whitelaw, E. L.; Garcia-Vivo, D.; Stewart, J. A.; Mahon, M. F.; Davidson, M. G.; Jones, M. D. *Chem. Commun. (Cambridge, U. K.)* **2011**, *47*, 12328.
(34) Nomura, N.; Akita, A.; Ishii, R.; Mizuno, M. *J. Am. Chem. Soc.* **2010**, *132*, 1750.
(35) Bero, M.; Kasperczyk, J.; Adamus, G. *Die Makromolekulare Chemie* **1993**, *194*, 907.
(36) Duda, A.; Kowalski, A. In *Handbook of Ring-Opening Polymerization*, Wiley-VCH Verlag GmbH & Co. KGaA: 2009; Vol. pp 1.
(37) Storey, R. F.; Hoffman, D. C. *Makromolekulare Chemie. Macromolecular Symposia* **1991**, *42-43*, 185.
(38) Hunley, M. T.; Sari, N.; Beers, K. L. *ACS Macro Letters* **2013**, *2*, 375.
(39) Shin, E. J.; Brown, H. A.; Gonzalez, S.; Jeong, W.; Hedrick, J. L.; Waymouth, R. M. *Angew. Chem., Int. Ed.* **2011**, *50*, 6388.

5. Supporting Information

Table S5.1. Polymerization of *rac*-lactide in CH_2Cl_2.

Catalyst/lactide / *i*PrOH	**[Cu] / (mmol·L^{-1})**	**Conversion** [a]	**$M_{n,calc}$ [c] / (g·mol^{-1})**	**M_n [d] / (g·mol^{-1})**	**M_w/M_n [d]**
1/300 [e]	2.0	97%	42 000	44 500	1.07
1/300	2.0	97%	42 000	44 500	1.07
1/300	2.0	98%	42 500	27 500	1.04
1/300	2.0	90%	39 000	141 000	1.18
1/300 [e]	0.50	93%	40 500	37 500	1.06
1/300	0.50	95%	41 500	63 500	1.11
1/300	0.25	85%	37 000	45 500	1.03
1/300 [e]	0.25	80%	34 500	34 500	1.03
1/300	0.25	80%	34 500	20 500	1.05
1/300	0.25	80%	34 500	32 000	1.08
1/300	0.25	97%	42 000	34 500	1.05
1/300	0.25	77%	33 500	34 500	1.03
1/300	0.25	90%	39 000	13 000	1.18
1/600	0.25	95%	82 000	26 500	1.09
1/600	0.25	91%	78 500	96 500	1.05
1/900	0.25	96%	124 500	42 000	1.05
1/900	0.25	91%	118 000	160 000	1.08
1/300/1	2.0	96%	21 000	31 000	1.08
1/300/1	2.0	96%	21 000	27 500	1.09
1/300/2	2.0	95%	14 000	22 000	1.04
1/300/2	2.0	96%	14 000	18 000	1.09
1/300/2	2.0	96%	14 000	17 000	1.11
1/300/5	2.0	97%	7000	9500	1.07
1/300/5	2.0	96%	7000	8000	1.11
1/300/5	2.0	96%	7000	8000	1.12
1/300/10	2.0	96%	4000	6000	1.11
1/300/10	2.0	96%	4000	4500	1.18

[a] Calculated from ^{1}H NMR spectra. [b] PLA precipitates at 80% conversion, final conversion estimated. [c] Calculated from ([lactide]$_0$/[*i*PrOH]$_0$+[Cu])·conversion·144 + 60. [d] Determined by size exclusion chromatography *vs.* polystyrene

standards, corrected by a Mark-Houwink factor of 0.58.[1] [e] Data taken from Whitehorne, T. J. J.; Schaper, F. *Chem. Commun.* **2012**, *48*, 10334.

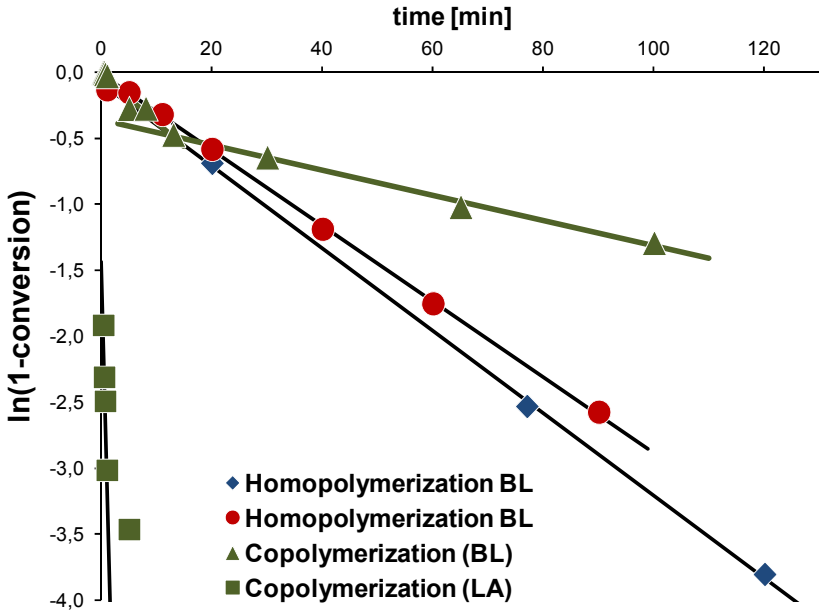

Figure S5.1. Linearized first-order conversion – time plots for the polymerization of β-butyrolactone with **1**. Conditions: CH_2Cl_2, 1.0 mM |**5.1**| = 2.0 mM Cu, 25 °C, [BL] = 0.60 M (homopolymerization), [BL] = [lactide] = 0.30 (copolymerization). Solid lines correspond to best fits from regression analysis yielding the rate constants in Table 5.2.

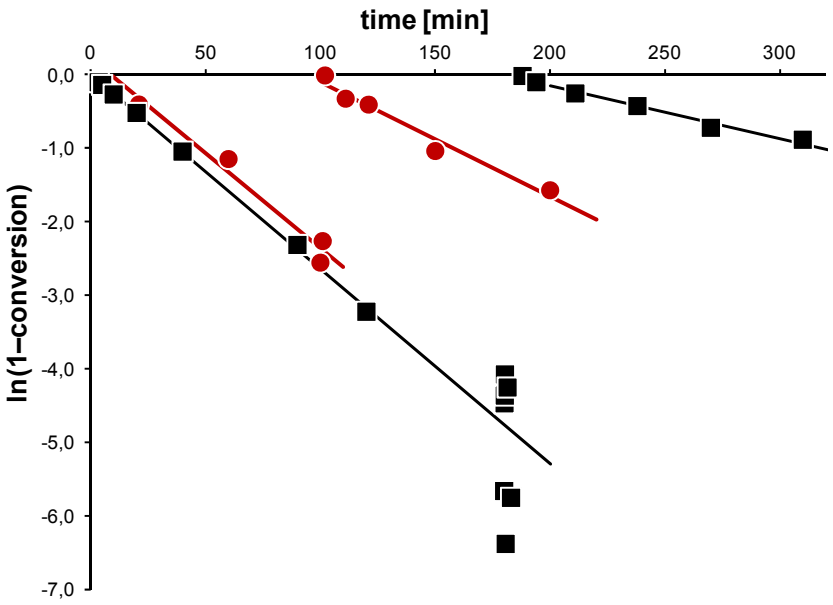

Figure S5.2. Linearized first-order conversion – time plots for sequential monomer addition experiments: Red circles: 0.30 M CL, 0.050 M lactide (not shown), 0.30 M CL. Black squares: 0.30 M CL, 0.30 M lactide (not shown), 0.30 M CL. Conditions: CH_2Cl_2, 1.0 mM 5.**1** = 2.0 mM Cu, 25 °C. Solid lines correspond to best fits from regression analysis yielding the rate constants in Table 5.4.

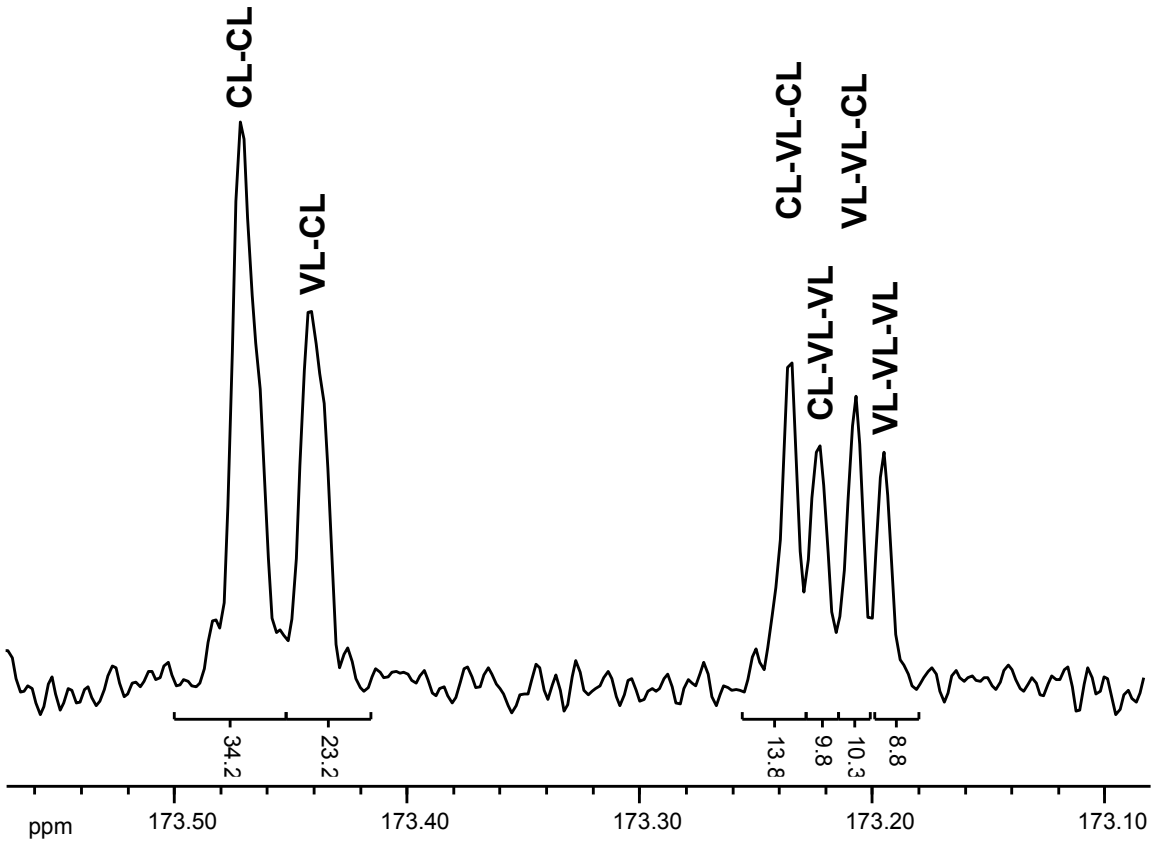

Figure S5.3. Tentative assignment of the carbonyl region of poly(CL-co-VL).

Table S5.2.

ppm	Assignment	Observed intensity	Calculated from $I_{XX\text{-}YY} \cdot P_{YY\text{-}ZZ}$
173.47	CL-CL	34.2	34.0
173.44	VL-CL	23.2	23.1
173.23	CL-VL-CL	13.8	13.1
173.22	CL-VL-VL	9.8	9.9
173.21	VL-VL-CL	10.3	10.4
173.19	VL-VL-VL	8.8	7.8

$P_{YY\text{-}ZZ}$ calculated from the intensities cited in the text. Probability of CL insertion after CL: $P_{CL\text{-}CL} = I_{CL\text{-}CL} / (I_{CL\text{-}CL} + I_{CL\text{-}VL}) = 0.596$. Likewise, $P_{VL\text{-}CL} = 0.571$

6. Conclusions & Perspectives

The synthesis of the zinc diketiminate complexes in Chapter 2 was straightforward via protonation of zinc bis(trimethylsilylamide) by one equivalent of diketimine, followed by the addition of alcohol, thus forming the desired heteroleptic complex. The selective catalytic performance of *nacnac*^{An}ZnO*i*Pr proved to be very poor for production of isotactic polymer (P_r = 0.88 – 0.93). Focus then turned to Mg: reaction of Mg(TMSA)$_2$ (TMSA = trimethylsilylamide) with Cl*nacnac*^{Bn}H, *nacnac*^{Bn}H or *nacnac*^{Mes}H yielded *nacnac*Mg(TMSA). However, addition of isopropanol failed to result in the desired catalyst. *tert*-Butanol was used successfully, but the resulting complexes showed slow initiation in polymerization, requiring the addition of benzyl alcohol as a cocatalyst. With complexes *nacnac*^{An}Mg(TMSA) and Cl*nacnac*^{An}Mg(TMSA), an active catalyst containing a M-O bond was in-isolable, as protonation of the diketimine occurred before isolation of the heteroleptic *nacnac*^{An}MgOtBu complex. Thus lactide polymerization with these catalysts required *in-situ* activation with benzyl alcohol. Although polymerizations were poorly behaved with high polydispersities and a non-living behaviour, these catalysts were highly active. With Cl*nacnac*^{Bn}MgO*t*Bu an increase in isotactic preference (P_r = 0.43) in comparison to previous work[1]was found at low temperatures.

The Cu(II) complexes found in Chapters 3 & 4 were synthesized via a novel protonation pathway, utilizing Cu(O*i*Pr)$_2$ as the starting material. Addition of one equivalent of β-diketimine yielded heteroleptic complexes when the less sterically demanding benzyl ligands Cl*nacnac*^{Bn}H, or *nacnac*^{Bn}H were used. With sterically more demanding alkyl ligands, such as the chiral *nacnac*$^{CMe(H)Ph}$H, *nacnac*^{An}H, and *nacnac*^{Mes}H, no reaction was seen. The highly sterically demanding *nacnac*^{dipp}H ligand led to decomposition presumably via a β-hydrogen elimination pathway. With Cu(O*t*Bu)$_2$ no reaction took place. In keeping with the target of C_2-symmetric chiral

catalysts, non-symmetric aryl ligands (*nacnac*^{ipp}H and *nacnac*^{Naph}H) were reacted with Cu(O*i*Pr)$_2$. Unfortunately the result was always the homoleptic bis(diketiminate) complex.

Heteroleptic Cu(II) complexes discussed within this thesis (Chapters 3 & 4) proved to be extremely active catalysts. The second order rate constant of *nacnac*^{Bn}CuO*i*Pr (k_2 = 32(2) $s^{-1} \cdot M^{-1}$) is of the same order of magnitude as the most active catalysts reported. The homoleptic complexes proved inactive towards lactide polymerization without addition of benzyl alcohol as an activator. With all copper complexes, polymer molecular weight could be controlled by addition of benzyl alcohol or isopropanol. These complexes are thus excellent immortal polymerization catalysts while retaining low polydispersities, and showing excellent stability in the presence of excess alcohol. A negative aspect is their lack of selectivity (P_r = 0.53 - 0.60). In chapter 5 these catalysts were applied to the polymerization of other cyclic lactones. In lactone/lactide copolymerization significant transesterification was present, something not seen in the homopolymerization of lactide in chapter 4.

Perspectives

As this work continues to grow and develop, some choices will have to be made. For instance, which metal centre should receive the most attention for further investigation considering the findings herein? Should this ligand system and strategy of C_2-symmetric rotamers be investigated further or should β-diketimines be abandoned in favour of a system that allows for ease of synthesis and functionalization?

In comparison to Zn(II), Mg(II) shows the greater promise as a catalytic centre for isoselectivity and activity with this class of ligand. However, Mg complexes are much more sensitive to impurities, in monomer and solvent, will most likely prove unsuitable for living polymerization[2]. Thus, polymer molecular weight control and polydispersities may suffer using

Mg(II). Zn(II) shows less sensitivity, but coupled with a lack of isoselectivity and poor kinetic performance, it is not an ideal candidate as a catalytic centre for this ligand architecture. This discussion will thus focus on Mg(II) and Cu(II), which both have their advantages.

Mg(II) has shown to be sensitive to polymerization conditions, and fails to result in living and or even immortal polymerizations. Cu(II) diketiminate complexes have been shown to be stable in the presence of excess alcohol, allowing for immortal polymerizations. However Cu(II) has yet to show selectivity in polymerization. As Cu(II) catalysts are less easily synthetically accessible (*vide supra*), Cu catalysts are less present in literature. Continuation of this work should thus follow the design of novel ligands for Cu(II) with a secondary application of these ligands to Mg(II).

In terms of ligand design, the approach taken in this work was a valid one. Large bulky N-alkyl β-diketimines could still be applied to Cu(II) and Mg(II). The implementation of planar 9-anthrylmethyl, and mesitylmethyl *N*-substituents, may have been the wrong approach as they can result in intramolecular attractive π- π interactions pushing the equilibrium towards the *syn* conformation and away from the desired chiral rotomer forms (Figure 1.10) which would result in increased atactic enchainment. This *syn* conformation was seen in crystal structures of monomeric *nacnac*Mg(TMSA) (Fig. 2.3, 2.5). Some proposed examples of promising N-alkyl substituents are shown in Figure 6.1.

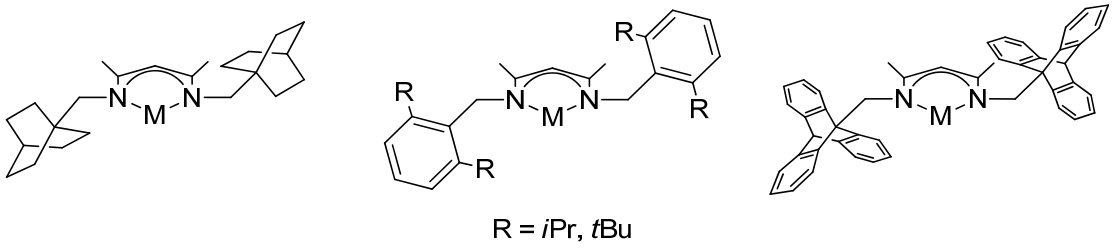

Figure 6.1 – Proposed future β-diketimine ligands for ROP

These proposed ligand designs could even be further enhanced by the addition of fluorination to either the methyl backbone groups of the metallocycle or directly to the N-substituents. However, due to the increasing difficulties in the synthesis of novel bulky N-alkyl β-diketimines, the failed attempts of which have not been discussed in this document, it is more advantageous to switch to a ligand system that has an ability for functionalization and ease of synthesis.

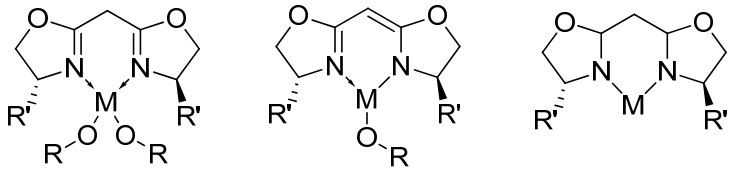

Figure 6.2 –Possible M(II) bisoxazoline conformations as catalysts

For this reason bisoxazolines (Fig. 6.2) are a framework that on paper look like the perfect ligand for continued research into selective polymerization of *rac*-lactide. They offer a rigid frame that force the formation of chiral rotamers when using a racemic mixture of ligand. The functionalizable R substituents point down directly into the polymerization site pocket for maximum selectivity of the incoming unit. A positive and negative aspect of these systems is the lack of literature evidence. With respect to Cu(II), the neutral ligand was used to form a complex of Cu(II) triflate.[3] The neutral ligand could be built upon and would be very interesting if an analogous catalyst containing $Cu(O\textit{i}Pr)_2$ could be formed since $Cu(O\textit{i}Pr)_2$ is inactive for polymerization due to insolubility. The neutral ligand has also been used in Zn(II) and Mg(II) triflates [4] and tested for asymmetric catalysis, in particular asymmetric cyclopropanation. The electronics of the ligands can also be changed by incorporation of boron into the bridge of the bisoxazolate[5]. However the most interesting aspect of these ligands is that they can be neutral,

monoanionic, and dianionic allowing for development into a rich new area of novel selective *rac*-lactide polymerization catalysts.

References

1. Drouin, F.; Whitehorne, T. J. J.; Schaper, F., *Dalton Transactions* **2011,** *40*, 1396-1400.
2. Chamberlain, B. M.; Cheng, M.; Moore, D. R.; Ovitt, T. M.; Lobkovsky, E. B.; Coates, G. W., *Journal of the American Chemical Society* **2001,** *123*, 3229-3238.
3. Bigot, A.; Williamson, A. E.; Gaunt, M. J., *Journal of the American Chemical Society* **2011,** *133*, 13778-13781.
4. Takacs, J. M.; Lawson, E. C.; Michael Reno, J.; Youngman, M. A.; Quincy, D. A., *Tetrahedron: Asymmetry* **1997,** *8*, 3073-3078.
5. Mazet, C.; Köhler, V.; Pfaltz, A., *Angew. Chem. Int. Ed.* **2005,** *44*, 4888-4891.